The Dissertation Committee for Pengfei Guo Certifies that this is the approved version of the following dissertation:

Characterization of genes involved in the synthesis of $\beta(1\rightarrow3)$ glucan, and investigation of genetic interactions among three Rho-type GTPase genes in the polymorphic fungus *Wangiella* (*Exophiala*) *dematitidis*

Committee:

Paul J. Szaniszlo, Supervisor

Scott W. Stevens

Terry O'Halloran

Philip Tucker

Ming Tian

Characterization of genes involved in the synthesis of $\beta(1\rightarrow3)$ glucan, and investigation of genetic interactions among three Rho-type GTPase genes in the polymorphic fungus *Wangiella* (*Exophiala*) *dematitidis*

by

Pengfei Guo, B.S.; M.S.

Dissertation

Presented to the Faculty of the Graduate School of

The University of Texas at Austin

in Partial Fulfillment

of the Requirements

for the Degree of

Doctor of Philosophy

The University of Texas at Austin

August 2010

Dedication

To my parents, my wife and my two lovely kids for their love and encouragement.

Acknowledgements

I am sure that no words can express my appreciation to my supervisor Dr. Paul J. Szaniszlo for his consistently supports and guidance during my research. Also he is the guider who have led me discovering my inside desire for the knowledge, which will change my life forever. I also say thank you to my co-advisor Dr. Makkuni Jayaram, who provides valuable comments and supports during my research life as a graduate student. I would like to thank my committee members: Dr. Philip Tucker, Dr. Terry O'Halloran, Dr. Scott Stevens and Dr. Ming Tian for their valuable suggestions and revision on my dissertation. I thank all my lab members: Dr. Hongbo Liu, Dr Dariusz Abramczyk, Dr Qin Wang, and Dr Changwon Park for the best experience of working together. I thank Dr. Qingfeng Wang for the help with PCR overlapping technique and Dr. John Mendenhall for the assistance with microscopy. I'm grateful to members from Shelly Payne's lab: Dr. Elizabeth Wyckoff, Dr. Alexandra Mey, Emily Helton, Ma Li, for theirs kindness help with the real time RT-PCR and encouragement. Also, I thank the department of Microbiology and the Graduate school of University of Texas at Austin for the top education experience, which has become the best memory of my life. Last but not least, thank my family for their endless love and forever support.

Characterization of genes involved in the synthesis of β(1→3) glucan, and investigation of genetic interactions among three Rho-type GTPase genes in the polymorphic fungus *Wangiella* (*Exophiala*) *dematitidis*

Publication No._____

Pengfei Guo, Ph.D.

The University of Texas at Austin, 2010

Supervisor: Paul J. Szaniszlo

Morphological transitions in *Wangiella dermatitidis,* a causative agent of human phaeohyphomycosis, influence virulence processes in this polymorphic fungus. My project first involved the cloning and characterizion of the β(1→3) glucan synthase gene *WdFKS1*, which encodes the enzyme's catalytic subunit, followed by cloning and characterizing the *WdRHO1* gene, which encodes its regulatory subunit. To better understand the Rho-type GTPase-mediated regulation of cell polarity and its role in fungal morphological transitions, a homologue of *WdRAC1* from a *W. dermatitidis* was subsequently identified by degenerate PCR and gene walking. Gene deletions of *WdFKS1* and *WdRHO1* in haploid *W. dermatitidis* were lethal, whereas the deletion of *WdRAC1* was not. RNA interference on *WdFKS1* mRNA expression resulted in incomplete septa

and damaged cell wall integrity, as well as slow growth rate in *W. dermatitidis*. Overexpression studies, after site-specific integrations of *WdRHO1 and WdRAC1* alleles under control of the *glaA* promoter into the nonessential *WdPKS1* locus, showed the different alleles had different effects on the cell morphological development. For example, whereas overexpression of the *wdrho1*$^{+}$ allele did not affect the growth rate of *W. dermatitidis*, the overexpression of *wdrho1*^{G14V}, a constitutively active mutation, slowed growth and repressed true filamentous hyphal growth by promoting pseudohyphal growth. While the deletion of *WdRAC1* did not affect growth, its loss retarded polarized hyphal growth in a hyphal-inducing minimal medium. Moreover, three new phenotypes of a previously derived *WdCDC42* deletion mutant were discovered during this study: in the first, the *wdcdc42*Δ mutant displayed cell lysis when incubated in YPMaltose medium at 37ºC; in the second, a dark budding neck abnormality was found after Calcoflour staining; and in the third, the *wdcdc42*Δ mutant displayed no branching during true hyphal growth. Interestingly, the overexpression of *wdrac1*^{G16V} complemented the second and the third phenotypes caused by the *WdCDC42* deletion. In addition, the *wdcdc42*Δ*/wdrac1*^{G16V} double mutant unexpectedly displayed an interrupted carotenogenesis pathway. These results support that in *W. dermatitidis*, Rho-type GTPases play essential roles in growth rate determination and cellular morphogenesis, especially while producing polarized hyphal growth during its many morphological transitions.

Table of Content

Chapter 4

List of Tables

List of Figures

Chapter 1 General introduction

1.1 The fungal cell wall.

The fungal cell wall is the outermost boundary of a fungal cell and is essential for fungal survival because of its protective qualities. Its major components have been proven to protect the fungal protoplast from lysis due to life in hypotonic environments and to help a fungus avoid immune responses when infecting humans. Basically, the cell wall plays an essential role in osmotic protection, vegetative or reproductive growth, sporulation, and cellular macromolecule transportation (Perfect, 1996). In general, fungal cell walls are composed of complexes of proteins, polycarbohydrates such as chitin, mannan, glucan and frequently pigments, such as various melanins.

An important component of each cell wall type is the glucose polymer β-1,3-glucan. β-1,3-Glucan synthase (UDP-glucose:1,3-β-D-glucan 3-β-D-glucosyltransferase; EC 2.4.1.34) is a membrane enzyme activated by GTP, which has been fractionated into soluble (GTP-binding) and membrane-bound (catalytic) components (Kang and Cabib, 1986; Mol, et al., 1994). Members of the echinocandin family of antifungal agents can inhibit β-1,3-glucan synthase (Douglas, et al., 1994; El-Sherbeini and Clemas, 1995).

Mannoproteins of various types are another major cell wall component. Mannoproteins can be classified into two groups: enzymes located in the cell wall or in the periplasmic space and structural mannoproteins that form integral components of the cell wall. Although mannoproteins are considered to be a filling material in the glucan structural network, the actual protein part of a cell wall mannoprotein functions as an acceptor for crosslinks with other sugar chains (Cabib, et al., 1988).

A third type of cell wall polycarbohydrate is chitin. Chitin is a linear homopolymer of β-(1,4)-linked-N-acetylglucosamine (GlcNAc), which is an essential component of almost all fungal cell walls because it is essential for cell wall integrity and viability (Muzzarelli, et al., 1985). It also plays an important role in fungal morphogenesis. Inhibition of chitin synthesis in the absence of osmotic stabilization usually results in cell death. Chitin synthases [UDP-N-acetyl-D-glucosamine: chitin 4-β-N-acetylglucosamine transferase, EC (2.4.1.16)], which are membrane bound proteins, are responsible for the synthesis and deposition of the chitin (Muzzarelli, et al., 1986; Munro, et al., 2001). Chitin synthases, which are located in the plasma membrane and deposit chitin to the cell wall, have a conserved chitin synthase domain and cross-membrane motifs.

Melanin is a major characteristic component of the cell walls of many fungi. It has been proven to be a virulence factor in numerous fungal pathogens of plants and

animals (Langfelder, et al., 2003). Several different types of melanin have been reported in fungi, but the two most important types are dihydroxyphenylalanie (DOPA)-melanin and dihydroxynaphthalene (DHN)-melanin. In general, melanins are macromolecules formed by oxidative polymerization of phenolic or indolic compounds which often result in brown or black in color (Langfelder et al., 2003). Melanin is thought to protect cells against oxidative stresses. Unmelanized "albino" strains have less virulence and are more easily killed by neutrophils during the infection of mice (Dixon et al, 1997; Cooper and Szaniszlo, 1998; Feng et al., 2001). Recently, it was reported that melanized fungi show enhanced growth when exposed to ionizing radiation, indicating that melanin may play a role in energy capture and utilization (Dadachova, et al., 2007)

1.2 The model fungal system: *Wangiella dermatitidis*.

Wangiella dermatididis is a polymorphic pathogenic fungus, which can cause cutaneous, subcutaneous and central nervous system infection. Systemic pheohyphomycosis caused by *W. dermatitidis* includes respiratory, intestinal, cardiac, and cerebral infections (de Hoog et al., 2005; Mukaino et al., 2006; Tseng et al., 2005). Because chitin in the cell wall has been shown to have relevance to these morphological transitions and both melanin and chitin are essential for the full virulence of this fungus, the polymorphic feature of *W. dematitidis* makes it an excellent model to discover cell-

Fig. 1.2. Polymorphogenic development in *W. dermatitidis*. (modified from Szaniszlo, 2006).

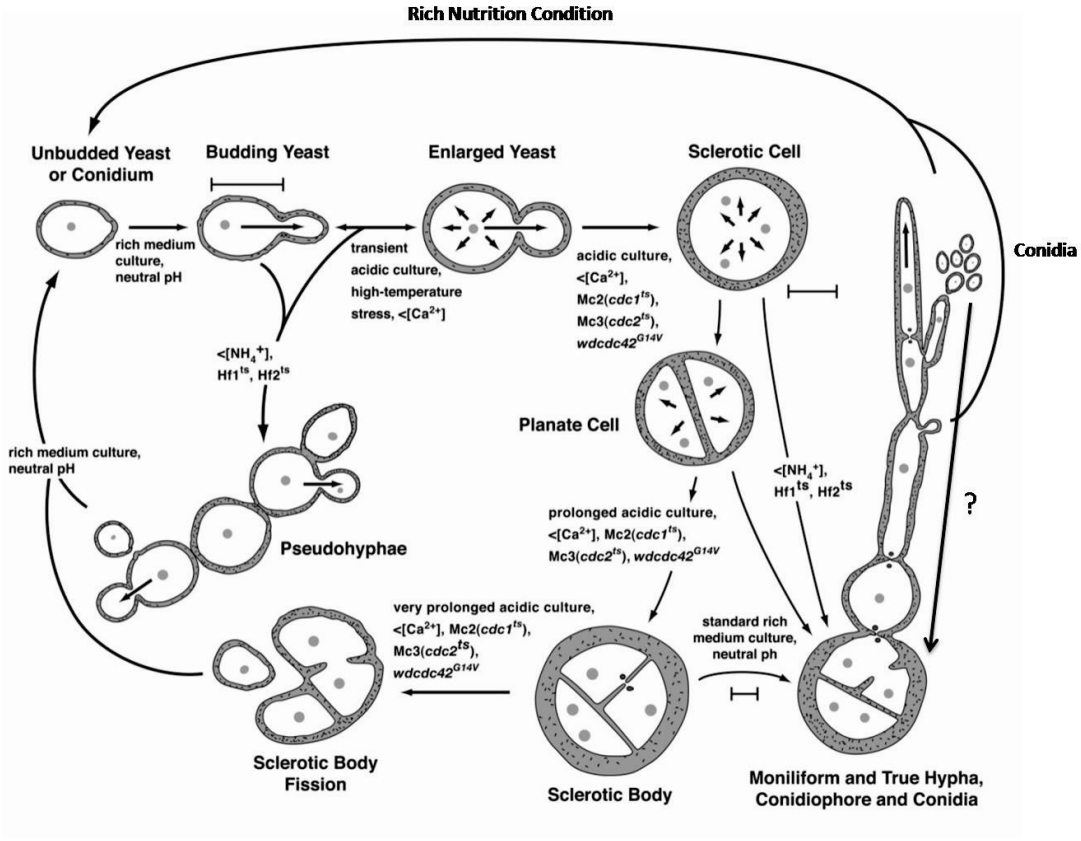

wall related virulence factors among the more than 100 other black pathogenic fungi known to cause human disease (Szaniszlo et al., 1993; Szaniszlo 2002, 2006).

1.2.1 Polymorphic transitions in *W. dermatitidis*.

The polymorphism of *W. dematitidis* is expressed in three well-defined vegetative growth modes; blastic, apical, and isotropic [Fig. 1.2]. Of these, the blastic mode is most common, producing growth predominantly as budding yeast forms in rich nutrient environments. But *W. dematitidis* can also be induced to undergo dramatic morphological changes that involve transitions to either sclerotic (isotropic) or hyphal (apical) growth (Kwon-Chung and Bennet, 1992; Matsumoto, et al., 1994; Szaniszlo, 2006), depending on various environmental conditions [Fig. 1.2], such as low Ca^{2+} or NH^{4+} concentrations, or low pH (Copper and Szaniszlo, 1993). Furthermore, temperature-sensitive mutants of two types, Mc3 and Hf1, which produce multicellular forms and hyphal forms respectively from yeast cells at the restrictive temperature, have been derived (Roberts and Szaniszlo, 1978; Mcintosh, et al., 1995).

1.2.2 The cell wall composition of *W. dermatitidis*.

In *W. dermatitis*, two major cell wall components: chitin and 1, 8-dihydroxylnaphthalen (DHN) melanin have been investigated in considerable depth

(reviewed by Szaniszlo, 2002; Szaniszlo, 2006). Chitin is not uniformly deposited in the cell walls of *W. dermatitidis*, but is instead localized mostly to more specific regions. These regions include the side walls and septa of hyphae and sclerotic forms and mother and daughter cell junctions in yeast cells, as well as in yeast birth scars. Melanin deposition in the cell wall is more uniform, but increases when *W. dermatitidis* is subjected to temperature stress or during the yeast-to-sclerotic body transition (Szaniszlo, et al., 1983; Copper et al., 1984). Non-melanized *W. dermatitidis* strains, such as *wdpks1*have less virulence than melanized strains in mouse model systems (Dixon, et al., 1992; Feng, et al., 2001). However, compared to its melanin and chitin, the most prominent of the cell wall components in *W. dermatitidis*, its *β*-1,3-glucan has not been investigated to nearly the same extent (Szaniszlo, et al., 1983; Montijn, et al., 1997).

Chapter 2 General Materials and Methods

2.1 Media and growth conditions.

The well described *Wangiella dermatitidis* strain 8656 (ATCC34100) was the wild-type strain used in this work (refs). Routine culture of *W. dermatitidis* was on YPD agar (YPDA; 1% yeast extract, 2% peptone, 2% dextrose, 2% agar) and in YPD broth (YPDB) at 25^{o}C as described previously (Liu et al., 2004). For the transformations of *W. dermatitidis*, YPDA containing 50 μg/ml hygromycin B (Invitrogen, Carlsbad, CA) was used to select resistant transformants that contained the hygromycin phosphotransferase gene (*hph*, GenBank accession number AF013601), or minimal medium (SD) agar (0.17% yeast nitrogen base w/o amino acids, 0.5% ammonium sulfate, 2% dextrose, 2% agar) that contained 20 μg/ml chlorimuron ethyl (Fisher, Pittsburgh, PA) was used to select the resistant transformants that contained the acetolactate synthase gene [*sur* (sulfonylurea resistant), GenBank accession number AY142483], respectively. To detect or induce filamentous growth, potato dextrose agar (PDA; Difco Scientific, Detroit, Mich.) was used. For storage, *W. dermatitidis* stationary-phase cells (0.5 ml) were mixed with 0.15 ml 65% glycerol to reach 15% final concentration and stored at -80°C.

E. coli strain XL1-blue (*recA1 endA1 gyrA96 thi-1 hsdR17 supE44 relA1 lac* [F′ *proAB lacI*qZΔ*M15* Tn*10* (Tetr)]; Stratagene, La Jolla, CA) and *E. coli* strain DH10B (F-*mcr*A Δ(*mrr-hsd*RMS-*mcr*BC) φ80*lac*ZΔM15 Δ*lac*X74 *rec*A1 *end*A1 *ara*D139Δ(*ara, leu*)7697 *gal*U *gal*K λ- *rps*L *nup*G; Invitrogen) were used for cloning and plasmid preparation. *E. coli* was grown in Luria-Bertani medium (LB; 1% tryptone, 1% NaCl, 0.5% yeast extract) at 37°C. LB containing 100 μg/ml ampicilline or LB containing 20 μg/ml chloramphenicol was used when the plasmid was introduced into the *E. coli* cells. For storage, *E. coli* stationary-phase cells (0.5 ml) were mixed with 0.5 ml 65% glycerol to reach the final concentration of ~30% and stored at -80°C.

2.2 Reagents and equipment.

Primers were synthesized by Invitrogen (Carlsbad, Calif.). Restriction enzymes were usually purchased from New England BioLabs (NEB, Beverly, MA) and Promega (Madison, WI). The T4 DNA ligase was purchase from Invitrogen (USA). The QIAprep miniprep kit (Qiagen, Chatsworth, CA) was used for the preparation of plasmid DNA. The QIAquick gel extraction kit (Qiagen) and the MinElute PCR purification kit (Qiagen) were used to purify DNA. The RNeasy Mini kit (Qiagen) was for the isolation of total RNA. The pGEM-T easy vector kit (Promega) was used for the ligation of PCR products. The DECAprime II random priming DNA labeling kit (Ambion, Austin, TX) was used to label probes. Isotopes were purchased from Dupont NEN (Boston, MA).

Nytran N nylon membranes were from Schleicher & Schuell (Keene, NH). PCR amplifications were carried out with a 2720 thermal cycler (Applied Biosystems, Foster City, CA). A pulser transformation apparatus (Bio-Rad, Hercules, CA) was used for electroporation. UV crosslinking was performed in CL-100 Ultraviolet Crosslinker (Ultra-Violet Products, San Gabriel, CA). Hybridization was carried out in a Personal Hyb Techne hybridizer HB-2D (Stratagene). Reagents were usually purchased from Sigma (Saint Louis, MO) and Fisher (Pittsburg, PA).

2.3 Extraction of genomic DNA.

To obtain genomic DNA, stationary-phase cells of *W. dermatitidis* cultured in YPDB at 25°C (5 ml) were collected by centrifugation, washed with deionized water and resuspended in 200 µl breaking buffer (2% Trition X-100, 1% SDS, 100 mM NaCl, 10 mM Tris-Cl, 1 mM EDTA, pH 8.0), to which 200 µl glass beads (0.5 mm glass beads, Biospect Products, Bartelsville, Okla.) and 200 µl phenol/chloroform (Ambion) were added. The mixture was then vortexed with a Multi-Tube Vortexer (VWR) at highest speed for 5 min, after which 200 µl TE (pH 8.0) was added. Following centrifugation, the supernatant was precipitated with 1/10 volume of 3M NaOAc (pH 5.2) and 2 volumes of 100% ethanol. Finally, the DNA pellet was washed with 70% ethanol, dried and dissolved in 30 µl Tris-Cl pH 8.0 (~5 µg genomic DNA), and treated with 7.5 µl of 1 mg/ml DNase-free RNase A to remove co-precipitated RNA.

2.4 Preparation of ^{32}P-DNA probes by a random priming method.

The DECA prime II DNA labeling kit (Ambion) was used to label probes. Approximately 20 ng of gel-purified DNA fragments (QIAquick Gel Extraction Kit)were used in 2.5 µl 10x Decamer solution (contains random decamer oligos). After being denatured at 100°C for 3-5 min and then chilled on ice for 2 min, 5 µl of 5x buffer (-dATP), 1 µl of exonuclease-free Klenow and 3 µl α-^{32}P dATP (3000Ci/mmol, 10 mCi/ml, Dupont NEN) were added and the resulting mixture incubated at 37°C for 30 min. After the reaction was stopped by adding 75 µl of 30 mM EDTA, the labeled probe was separated from the incorporated nucleotides by spinning in a Sephadex G50 column (Sigma).

2.5 Screens of the *W. dermatitidis* cosmid genomic library.

For titrating a cosmid genomic library of *W. dermatitidis* (Feng et al., 2001), dilutions were plated on LB agar containing 20 µg/ml chloramphenicol. Next, 10^4 cells were spread on the LB agar contained in these 15 cm large Petri plates and incubated at 37°C for 12 h. Nylon membranes were then placed over the colonies that developed, their positions were marked with a needle, and the colonies were transferred to Whatman 3MM filter paper that was saturated subsequently first with 0.5 M NaOH for 7 min, followed by two washes with 1 M Tris-Cl pH 7.4 for 2 min, then with 0.5 M

Tris-Cl pH 7.4 and 1 M NaCl for 4 min, and finally with 2x SSC for 4 min. The procedures for the UV crosslinking, prehybridization, hybridization, washing, exposure and radioactive signal detection were subsequently carried out similarly to those used for the Southern analysis.

2.6 Southern analysis.

Prior to Southern analysis, the *W. dermatitidis* genomic DNA (1 μg) was digested overnight (around 8 hours) with restriction endonucleases and then subjected to electrophoresis in a 0.8% agarose gel. After the DNA was denatured by soaking with moderate shaking the gel in 0.25 M HCl, thrn neutralizing with a 0.5 M NaOH/ 1.5 M NaCl for 1 h and rinsing several times in dH_2O, the agarose gel was neutralized by soaking and moderately shaking in 1 M Tris-Cl pH 7.4, 1.5 M NaCl for 20 min twice. Using upward capillary transfer with 10x SSC (1.5 M NaCl, 0.15 M sodium citrate), the DNA in the gel was transferred overnight to a Nytran N nylon membrane (Schleicher & Schuell). After the transfer, the nylon membrane was rinsed in 2x SSC, air dried on a Whatman 3MM filter paper and then UV crosslinked (CL-100 Ultraviolet Crosslinker). The DNA-bound membrane was then prehybridized in PerfectHyb Plus hybridization buffer (Sigma) in a hybridization oven (Personal Hyb Techne hybridizer HB-2D, Stratagene) for 30 min at 68°C. After the probe was heated to 100°C for 10 min, it was immediately placed on ice for 5 min, and then added to the hybridization tube to

hybridize for 3 h at 68°C. After the hybridization, the membrane was washed in low stringency wash buffer (2x SSC, 0.1% SDS) for 5 min at room temperature, and then high stringency wash buffer (0.5x SSC, 0.1% SDS) for 20 min at 68°C twice, followed by exposure to a phosphorimager screen. The radioactive signals were finally detected by exposing with X-OMAT film (Kodak).

2.7 Northern analysis.

Total RNA was isolated with the RNeasy kit (Qiagen). After the *W. dermatitidis* cells (about 10^8 cells) were ground thoroughly in liquid nitrogen with a mortar and pestle to break cells, the frozen fine powder was transferred to guanidine isothiocyanate-containing buffer RLT, Included in the Qiagen kit. The resulting lysate was then spun through a QIAshredder to remove cell debris and to homogenize the lysate. Next the supernatant was mixed with ethanol, then applied to an RNeasy spin column, which was subsequently washed with RW1 and RPE and eluted with RNase-free H_2O. The final concentration of RNA was determined using a NanoDrop ND-1000 Spectrophotometer (NanoDrop Technologies, Wilmington, Del.). The quality of RNA was estimated by electrophoresis of 2 μg RNA in an RNA gel. For the Northern blotting itself, 10 μg of the RNA was mixed in 50% formamide, 1x MOPS running buffer [20 mM MOPS (3-(N-morpholino)-propanesulfonic acid), 5 mM sodium acetate and 1 mM EDTA, adjusted to pH 7 with 10 M NaOH], 2 M formaldehyde, 0.1% bromophenol

blue and 0.05 mg/ml ethidium bromide, after which the mixture was incubated at 65°C for 5 min, followed by fast chilling on ice for 2 min. Electrophoresis of the samples was at ~5V/cm in a 1% agarose gel containing 2 M formaldehyde, with 1x MOPS running buffer. A 0.24-9.5 kb RNA ladder (Invitrogen) was run simultaneously to provide size markers. After electrophoresis, the RNA gel was rinsed with deionized water, photographed, and then soaked in 10x SSC for 10 min. The procedures for membrane transfer, UV crosslinking, prehybridization, hybridization, washing, exposure and radioactive signal detection were similar to those used for the Southern analysis.

2.8 PCR amplifications.

PCR was usually carried out with 2.5 µl of 10x PCR buffer (15 mM Mg^{2+}, 500 mM KCl, 100 mM Tris-HCl, pH 9), 0.5 µl of 10mM dNTP, 1 µl of 10 µM primers, 0.2 µl of Taq DNA polymerase (5U/µl, Fisher) and template DNA mixed in a final volume of 25 µl. The PCR reaction conditions were as follows: 5 min at 94°C for premelting; 30 cycles of 30 sec at 94°C for denaturation, 30 sec at 55°C for annealing, and 1 min at 72°C for extension; 7 min at 72°C for completion of the extension. The product of a PCR amplification was detected after agarose gel electrophoresis.

2.9 RT-PCR.

Total RNA was treated with RQ1 RNase-Free DNase (Promega). RT-PCR was carried out with the One-step RT-PCR kit (Qiagen). RT-PCR was performed with 5 µl of 5x PCR buffer (provided by Qiagen kit), 1 µl of HotStarTaq® DNA Polymerase) and 1 µg total RNA mixed in a final volume of 25 µl. The RT-PCR reaction conditions were as follows: 30 min at 50°C for reverse transcription and 15 min at 95°C for initial PCR activation; 35 cycles of 30 sec at 94°C for denaturation, 30 sec at 55°C for annealing, and 1 min at 72°C for extension; 10 min at 72°C for completion of the extension. The product of a RT-PCR amplification was detected after agarose gel electrophoresis.

2.10 Real time RT-PCR.

In order to quantitatively measure the expression of the *WdFKS1, WdCDC42, WdRHO1, and WdRAC1* genes, amplification of an endogenous control gene (one involved in "housekeeping") was performed simultaneously, and the relative expression level between the target genes and the endogenous control gene was assessed. The *WdACT* (Genbank reference AY071826.1) was used as the housekeeping gene in these assays. The primer/probe combinations were designed by Applied Biosystems (Foster City, CA) through their Assays-by-Design^{SM} service. Probes were synthesized using 6-carboxy-tetramethyl-rhodamine [TaqMan TAMRA] labels at the 5′ and 3′ ends, respectively. The primer/probe combinations are shown in

Biosystem 7700 Real Time PCR apparatus (Foster City, CA) was used to perform the quantitative expression study. Each sample consisted of 18 µL from the cDNA reaction described above, 20 µL 2× Taqman® Universal PCR Master Mix and 2 µL of 20× primer/probe mixture. The reaction protocol consisted of one cycle at 50 °C for 2 min, followed by one cycle at 95 °C for 5 min, followed by 40 cycles of a 15-s denaturation step at 95 °C followed by a 1-min annealing/extension step at 60 °C. Each amplification reaction was setup in triplicate. The following three negative control reactions were carried out with each set of samples analyzed: (1) no RNA-template but reverse transcriptase and polymerase provided; (2) RNA and polymerase provided but no reverse transcriptase; and (3) RNA and reverse transcriptase provided but no polymerase.

Table 2.1 Primer/probe combinations used for real time RT-PCR assay.

Description	Sequence
WdACT forward primer sequence	5′- CCGTCCTTGGTCTCGAA -3′
WdACT reverse primer sequence	5′- ACACTTCATGATGGAGTTG-3′
WdACT probe	5′- CGGCGGTATCCATGTTACCACC -3′
WdFKS1 forward primer sequence	5′-CGTTTGGCCCCATTGCT-3′
WdFKS1 reverse primer sequence	5′-AGCAAGCCATGCCGAACA-3′
WdFKS1 probe	5′-TGCTGGTGTGCTTGCCGG-3′
WdRHO1 forward primer sequence	5′- ACGTCGCCGATGTCGAA -3′
WdRHO1 reverse primer sequence	5′- GCCTGCCGTATCCCATAGG-3′
WdRHO1 probe	5′- TCGATGGAAAACACGTTGAACTCG-3′
WdRAC1 forward primer sequence	5′- CGGTGTGCCCATCATCCT -3′
WdRAC1 reverse primer sequence	5′- CGGCCGTGGCTTTATCG-3′
WdRAC1 probe	5′- TCGGAACCAAACTGGATTTGA-3′
WdCDC42 forward primer sequence	5′- GACCCACAAGTCCGTGAGAAAC -3′
WdCDC42 reverse primer sequence	5′- TTCTTTCACCATCCTCCTTACGA-3′
WdCDC42 probe	5′- CGCCAAACAGAAGATGCAACCCG-3′

2.11 Sequencing and computer analysis.

DNA sequencing was performed by the Core Facility of Institute of Cellular and Molecular Biology, The University of Texas at Austin, using Big Dye technology (Applied Biosystems). NCBI databases were searched with BLAST programs (www.ncbi.nlm.nih.gov/BLAST/). Protein structure was analyzed using ExPASy tools (expasy.org/tools/). Multiple alignments and phylogram constructions were done using ClustalW (www.ebi.ac.uk/clustalw/).

2.12 Transformations of *E. coli* and *W. dermatitidis.*

To make *E. coli* cells competent for transformations, cells from an overnight culture (8 ml) were inoculated to 200-ml LB broth, shaken vigorously at 37°C for ~1.5 to 2.5 h until the OD595 reached ~0.5, and then pelleted by centrifugation. After the supernatant was discarded, the pellet was then vortexed in 30 ml ice cold, filter sterilized TFBI buffer (30 mM KOAc, 100mM RbCl, 10 mM $CaCl_2$, 50 mM $MnCl_2$, and 15% glycerol, pH 5.8) to resuspend the pellet. This mixture was then placed on ice for 2 h, centrifuged, after which the supernatant was again discarded. Once the pellet was carefully resuspended in 5 ml ice cold filter-sterilized TFBII buffer (10 mM MOPS, 75 mM $CaCl_2$, 10 mM RbCl and 15% glycerol, pH 6.5), the resulting mixture was placed on ice for 15 min, and then aliquoted (100 μl per Eppendorf tube) and

immediately frozen on dry ice and stored at -70°C. For the transformation itself, the competent cells were first mixed with DNA and incubated on ice for 20 min, next heat-shocked for 1 min in a 42°C water bath and then immediately chilled on ice for 1 min prior to adding 1 ml LB broth. The resulting transformation culture was finally incubated at 37°C with moderate shaking for 45 min, before being spread on LB agar selection medium for incubation at 37°C overnight.

Transformation-competent yeast cells of *W. dermatitidis* were prepared from mid-log-phase cultures washed with cold 10% glycerol. Purified plasmid DNA was added to the cell suspensions at a ratio of about 1 μg of DNA per 10^7 cells. Electroporation was carried out with a Gene Pulser electroporation system (Bio-Rad) at a setting of 1.45 kV, 25 μF, and 200 Ω. Transformants were grown in YPD medium containing 30 μg of hygromycin (Sigma)/ml at 25°C.

2.13 Methylbenzimidazole-2-yl-carbonate (MCB)-induced haploidization.

Diploid *W. dermatitidis* cells were grown in CDY broth at 37°C until mid-log phase. Samples were then resuspended to a final concentration of approximately $2x10^5$ CFU/ml in 10 ml of prewarmed CDY medium containing 100μg/ml of MCB (Cooper and Szaniszlo 1993) and further incubated at 37℃ with gently shaking after cell samples were collected at 24 and 48 h, followed by serial dilution in saline, aliquots

were spread onto CDY agar medium. After incubation at 25°C for 7 days, albino colonies were selectively streaked on new CDY agar medium.

2.14 Microscopy.

For staining of the cell wall with Calcofluor (Sigma) or staining of nuclei with DAPI (4′,6′-diamidine-2-phenylindole) (Accurate Chemical, Westbury, N.Y.), fungal cells were fixed for 3 h in 5% formaldehyde and then washed twice with 1x PBS buffer at room temperature. After staining for 5-10 min, the samples were repeatedly washed with saline and were finally examined and photographed by using a Zeiss Axio Imager A1 microscope system (Zeiss, Germany). For documentation of colony morphology, cell culture plate media were photographed directly with the same photomicroscope immediately after removal from incubation.

Chapter 3: WdFks1p, the catalytic subunit of *β*-1, 3-glucan synthase, is essential for cell wall integrity in *W. dermatitidis.*

3.1 INTRODUCTION

3.1.1 *β*-1, 3-glucan: an important cell wall component.

β-1, 3-Glucans, the main structural polysaccharides in fungal call walls, belong to the so-called hollow helix family of proteins because they have a shape comparable to a flexible wire spring that can exist in various states of extension (Rees, et al., 1982). Among the cell wall polysaccharides of fungi, the *β*-1, 3-glucans, which can be specifically stained with aniline blue, contribute most of the mechanical strength and elasticity to the cell wall (Yong and Jacobs, 1998; Beauvais, et al., 2001). In stationary phase cells of *Saccharomyces cerevisiae*, *β*-1, 3-glucan molecules consist of about 1500 glucose monomers (Fleet, 1991). The glucose monomers are joined by *β*-1, 3 covalent bonds to form the polymers (Fig. 3.1). In the lateral walls of *S. cerevisiae*, the *β*-1, 3-glucan is reported to be only slightly crystalline (Kreger and Kopecka, 1975). However, this may have been a misinterpretation of data resulting from the partial hydrolysis of glucan chains during the extraction procedure. Considerably higher degrees of polymerization have been reported, but this was achieved only after more careful selection of the type of acid used for extraction (Müller, et al., 1997). Environmental

conditions also can affect the degree of glucan synthesis. For example budding yeast uses two *β*-1, 3-glucan synthase complexes, the functions of which depend on growth phase and carbon source (Cabib, et al., 1998). In addition, the degree of branching of *β*-1, 3-glucan may depend on growth conditions. In their mature form, the *β*-1, 3-glucan chains of stationary-phase cells may also contain *β*-1, 6-linked glucose residues at concentrations of 3-4%, which are moderately branched (Manners et al., 1973). Krainer and co-workers have found that a portion of the *β*-1, 3-glucan indeed assumes a helical structure (Krainer, et al., 1994). It is still unknown whether growing *β*-1, 3-glucan chains in *S. cerevisiae* are extended at the reducing or non-reducing end. In its mature form, *β*-1, 6-glucan is a highly branched, water-soluble polymer that consists on average of about 130 glucose monomers (Manners, et al., 1973). Generally the *β*-1, 6-glucan functions in the cell wall to connect GPI-dependent cell wall proteins to the *β*-1, 3-glucan network. It may also function as an acceptor site for chitin, particularly in cases of cell wall stress (Kollar, et al., 1997; Montijn, et al., 1997).

3.1.2 Genes encoding the *β*-1, 3-glucan synthase catalytic subunit: *FKS.*

In *S. cerevisiae,* *β*-1, 3-glucan synthase, the enzyme required for the polymerization of *β*-1, 3-glucan requires at least two subunits for full activity, as demonstrated by the separation of the enzyme activity into soluble (GTP-binding) and membrane (catalytic) fractions (Inoue et al., 1995). Several lines of evidence show that the *FKS* genes of this yeast species encode subunits essential for catalytic activity of the

Fig. 3.1 Structure of a *β*-1, 3-glucan polymer and the *β*-1, 3 covalent bond between two glucose monomers.

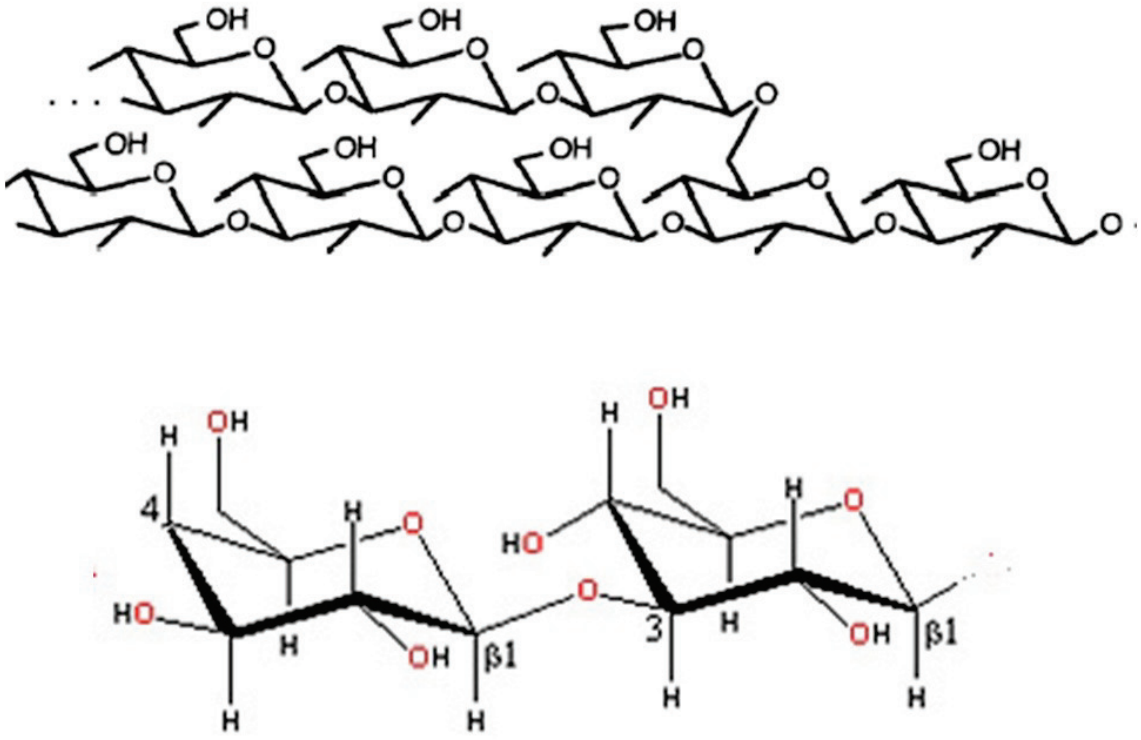

membrane fraction of glucan synthase. The two subunits, ScFks1p and ScFks2p, are both integral membrane proteins that are only associated with the membrane fraction of cells. Yeast *ScFKS1* encodes a 215-kDa integral membrane protein (ScFks1p), which mediates sensitivity to the echinocandin class of antifungal glucan synthase inhibitors, and is a subunit of this enzyme. Yeast *ScFKS2* encodes a predicted protein (ScFks2p) of 1,895 amino acids with a molecular mass of 217 kDa, which is also a subunit of the enzyme. The amino acid (aa) sequence of ScFks2p is 88% identical to that of ScFks1p and 19 amino acids longer at the N terminus. Most of the aa residues (1,743) of the two proteins are much the same (91% identity, with no gaps), except in the N-terminal domains (aa 1 to 133 of ScFks1p and 1 to 152 of ScFks2p) where they diverge significantly (48% identity, with several gaps in the alignment). Although the sequences of the N terminal domains differ, they have a similar and unusual aa compositions. Overall the region is more acidic (pI of 2.71 for ScFks1p and 2.62 for ScFks2p) compared with the C-terminal domains (pI of 8.14 for ScFks1p and 8.06 for ScFks2p). In vitro, the levels of glucan synthase activity correlate with the levels of ScFks1p and ScFks2p.

Disruption of Sc*FKS1* reduces glucan synthase activity. However, this reduction can be remedied by the presence of Ca^{2+} in the growth medium, which results in an elevated level of ScFks2p (Mazur et al., 1995). The enzyme containing ScFks2p is more sensitive to echinocandin than that containing ScFks1p. Since ScFks1p and ScFks2p

seem to be alternative subunits with similar functions, their regulation often appears to be opposite: when the level of one is high, then that of the other is low. Growth in the presence of Ca^{2+} increases echinocandin sensitivity of the enzyme in the wild type, reflecting the increase in the level of ScFks2p and decreased ScFks1p level under these conditions. Disruption of *ScFKS1* results in mutants exhibiting poor growth compared with that of the wild type, but it is not lethal. Thus, *ScFKS2* only partially compensates for the lack of *ScFKS1*. This growth defect is at least partly due to low levels of expression of *ScFKS2* under these conditions. While the addition of Ca^{2+} to the growth medium can recover the growth defect, it greatly correlates with the increased level of expression of *ScFKS2*. Thus, when ScFks2p is expressed at a high enough level, it appears to be fully able to substitute for ScFks1p (Mazur et al., 1995). On the other hand, although disruption of *ScFKS2* does not affect growth, this disruption does result in a sporulation defect, which could not be complemented by *ScFKS1*. This may not be surprising, because the spore wall of *S. cerevisiae* has been reported to contain considerable glucan (Kane et al., 1974). Thus, *ScFKS2* seems to be important for the formation of this apparently essential spore wall polymer, whereas *ScFKS1* is likely to be poorly expressed on sporulation medium, which contains acetate as the sole source of carbon. It is important to note that there is increased expression of *ScFKS2* in the absence of glucose during vegetative growth. Expression of *ScFKS2* is Ca^{2+}/calcineurin dependent. In the absence of *ScFKS1*, the growth of cells is completely dependent on the expression of *ScFKS2*. Therefore, the cell has two distinct forms of *β*-1,3-glucan

synthase, one containing ScFks1p and the other containing ScFks2p, and these two forms have different functions within the cell. Interestingly, a third *FKS* homolog in *S. cerevisiae* was recently discovered as a result of the genome sequencing effort, which is dispensable (Ram, 1995).

3.1.3 *FKS* homologs among fungi.

In *Candida albicans*, three genes (*FKS1/GSC1*, *GSL1*, and *GSL2*) are homologous to *Saccharomyces* and *Aspergillus FKS* genes by sequence (Mio, et al., 1997). However, in *C. albicans* only *CaFKS1* and *CaGSL1* mRNA expression has been demonstrated. Only one of the *Candida* genes, *CaFKS1*, is indispensable, which suggests that CaFks1p may predominate in *C. albicans* and implies that CaGsl1p is either dispensable or possesses a different function (Douglas, et al., 1997). In *Aspergillus fumigatus*, so far, only a single glucan synthase gene has been cloned, disruptions of which proved it to be an essential gene (Beauvais, et al., 2001). In addition, *FKS* genes have been demonstrated to be essential single-copy genes in *Cryptococcus neoformans*, *Coccidioides posadasii, Fusarium solani* and *Yarrowia lipolytica* (Douglas, et al., 1997; Beauvais, et al., 2001; Pereira, et al, 2000; Ha, et al., 2006; Thompson, et al., 1999).

Although chitin in the cell wall of *W. dematitidis* has been shown to have relevance to its polymophic morphological transitions and both melanin and chitin are essential for the full virulence of this filamentous and conidiogenous fungus, the roles of glucan in those rles are still unknown. The aim of the work that I present here was to investigate the possible putative *FKS* homologs present in *W. dematitidis* so as to increase our knowledge about cell wall biosynthesis in this organism.

3.2 MATERIALS AND METHODS

3.21 Strains, culture conditions.

The *W. dermatitidis* strains used in this research are listed in Table 3.1. Routine culture of *W. dermatitidis* was on YPD agar (YPDA) and in YPD broth (YPDB) as described previously (Liu et al., 2004). For the detection of filamentous growth, *W. dermatitidis* was grown on starch agar (Difco Scientific, Detroit, Mich.).

3.22 Degenerate PCR, library screening and cloning.

The catalytic subunit of a fungal glucan synthase complex has an extremely well conserved catalytic core, which in the case of the *S. cerevisiae* enzyme starts at amino

Table 3.1 Strains used in this research.

Strain	Genotype*a*	Reference(s) or source
3u2m-428	*mcm2/cdc1 mcm3/cdc2 met ura mel3 mel4*	Cooper and Szaniszlo, 1993
W. dermatitidis 8656	Wild type	ATCC 34100
Wdfks1Δ-d12	*wdfks1 wdfks1*::*hph**	This study
wdfksi-6	*wdfks1wdpks1*::pYEX303-*hph- wdfks1*^{RNAi}	This study
*wdfksi-nc**:*	*wdfks1wdpks1*::pYEX303-*hph- wdfks1*^{RNAinc}	This study

hph: hygromycin resistance gene. nc**: negative control strain*

Table 3.2 DNA oligonucleotides used in this study.

Primer	Sequence (5'→ 3')
PFKS3-1	agatctGGTACCGGTATGGGTGAAC
PFKS3-2	TTGCGAACAGCAACATCATC
PFKS3-3	ctgcag GGCGAAACCACGACCAGTA
PFKS3-4	gagctctctagaGGTACCGGTATGGGTGAAC
PFKS3NC-1	ctgcagGGTACCGGTATGGGTGAAC
PFKS3NC-2	gagctctctagaGGCGAAACCACGACCAGTA
PFKS1-1	agatctCGCCTAACCAGGCCTTGT
PFKS1-2	TTCTCTCAATACCCTCAGGG
PFKS1-3	ctg cag TTGCCGTCGATGATCTCGTA
PFKS1-4	gagctctctagaCGCCTAACCAGGCCTTGT
PFKS2-1	agatctTTGCTCCGCGCCTATCCC
PFKS2-2	GATATCTTCGTTGAGGTGAAG
PFKS2-3	ctg cag AATGGAGCTTGCCGCCAAT
PFKS2-4	gagctctctagaTTGCTCCGCGCCTATCCC
PFKS3-1	agatctGGTACCGGTATGGGTGAAC
PFKS3-2	TTGCGAACAGCAACATCATC
PFKS3-3	ctg cagGGCGAAACCACGACCAGTA
PFKS3-4	gagctctctagaGGTACCGGTATGGGTGAAC
PFKS4-1	agatctCCAACCACAGATTCTGCTTG
PFKS4-2	GAAGTGTGACACGAGAGTATG
PFKS4-3	ctg cagGTGAAAGTTGGCATGTTGTC
PFKS4-4	gagctctctagaCCAACCACAGATTCTGCTTG

* Sequences for restriction endonuclease recognition sites are in lower case.

acid 830 and ends with amino acid 1646. Thus, degenerate primers were synthesized with designs based on the conserved catalytic domains of a number of Fks1 proteins. Two of the PCR primers, PFKS1-FR and PFKS1-REV allowed the amplification of a 503-bp PCR product: PFKS1-FR, 5′- CAD ATN CGN AXY AYC TCR TAN CXG TAD YAR -3′; PFKS1-REV, 5′- MAR XAG RCY GCX NAC NCG YMG ATG NGG XRT -3′ (R=A+G, M=A+C, X=A+T+C+G, Y=C+T, D=A+T+G).

PCR amplifications were carried out with 2 μM of the primers, 0.5 mM dNTP, 0.5 μg genomic DNA and 0.5 U/μl Taq polymerase mixed in 1.5 mM Mg++, 50 mM KCl, 10 mM Tris-HCl (pH 9) buffer. The PCR reaction conditions were as follows: 5 min at 94°C for premelting; 50 cycles of 1 min at 94°C for denaturation, 1 min at 55°C for annealing, and 1 min at 72°C for extension; 7 min at 72°C for completion of the extension. The resulting PCR products were then cloned into the pGEM-T easy vector (Promega, Madison, Wis.) and sequenced. The sequencing showed that plasmid pPGFKS1A contained an *FKS1* homolog fragment.

The *WdFKS1* PCR product from plasmid pPGFKS1A was used to screen a *Wangiella* cosmid DNA library (Feng, et al., 2001), which identified a single 46-kb cosmid, pFKSCOS. An 8.4-kb fragment generated by digesting the pFKSCOS with *Sal*I, which can hybridize with the 503-kb PCR product, was cloned into pBSKS, a vector with an ampicillin resistance marker, to generate pFKS001. Three plasmids

pPGFKS002, pPGFKS004, pPGFKS005 were constructed to clone three fragments, which were generated by digesting the 8.4-kb fragment with the *Xho*I restriction enzyme. After sequencing these three plasmids, the full length *WdFKS1* gene sequence was assembled. DNA sequencing of the plasmids was then performed by the Core Facility of Institute of Cellular and Molecular Biology, University of Texas at Austin, using BigDye technology (Applied Biosystems, Foster City, CA). The locations of introns, first predicted in silico by alignments and by identifying consensus splice sequences, were then confirmed by the comparison of the cDNA sequence produced from reverse transcription-PCR (RT-PCR) using the One-Step RT-PCR kit (QIAGEN, Valencia, CA) with the genomic DNA sequence.

3.23 Disruption of the *WdFKS1* gene.

To disrupt the *WdFKS1* gene, a 1.2-kb *Xho*I-end fragment, which belongs to conserved catalytic core region of *WdFKS1* found in pPGFKS001, was cloned into the *Xho*I site of the pCB1004 vector, generating plasmid pCBFKSD. After pCBFKSD DNA was linearized by *Mlu*I digestion, it was used to transform the *W. dematitidis* wild-type strain 8656 and a parasexually derived diploid (strain 3u2m-428). Transformants were then selected by their resitsance to hygromycin B.

3.24 RNA interference vector construction.

To construct the RNAi vector pPG2i, pYEX303 (Ye and Szaniszlo, 2000) was modified. A 583-bp fragment of *WdFKS1* (positions 3349 to 3982) was amplified by primers, PFKS3-1 and PFKS3-2, and then inserted in the *Bgl*II and *EcoR*I site of pYEX303. Next a 501-bp fragment of *WdFKS1* (positions 3349 to 3900) was amplified by primers, PFKS3-3 and PFKS3-4, which was ligated at the *EcoR*I and *Xba*I site to introduce the fragment as an inverted repeat. For construction of the RNAi negative control vector, pPG2iNC, the 501-bp fragment of *WdFKS1* (positions 3349 to 3900) was amplified by primers, PFKS3NC-1 and PFKS3NC-2, and was ligated in the *EcoR*I and *Xba*I site to introduce the 501-bp fragment after the 583-bp fragment.

3.25 Nucleotide sequence accession number.

The sequence of *WdFKS1* was submitted to the GenBank database. The accession number of *WdFKS1* is **EF121814.1**.

3.3 RESULTS

3.31 Cloning, sequencing and characterization of the *W. dermatitidis* β-1, 3-glucan synthase gene: *WdFKS1*.

Functional domains, such as the GTP-binding domain, are often highly conserved among different orthologs of the same protein family. Alignment of the amino acid sequences encoded by members of a family allows for the identification of these highly conserved regions. Degenerate PCR primers with designs based on the conserved regions are then commonly used to amplify related genes from other organisms. The catalytic subunit of a fungal glucan synthase complex has such a well conserved catalytic core, which in the case of the *S. cerevisiae* enzyme starts at amino acid 830 and ends with amino acid 1646. Two PCR primers were designed based on the conserved catalytic core sequences of a number of β-1, 3-glucan synthase (*FKS*) genes of a variety of fungi. My amplifications then allowed the production of a 503-bp PCR product from *W. dermatitidis* genomic DNA, which showed highest homology with derived polypeptides of corresponding β-1, 3-glucan synthases.

To obtain the full length *W. dermatitidis FKS1* gene (*WdFKS1*), a *W. dermatitidis* cosmid DNA library was screened by using the 503-bp PCR product as a probe. The *WdFKS1* PCR product was also used as a probe for Southern blotting. This

approach identified a 46-kb cosmid, pFKSCOS, which was subsequently determined to contain a *WdFKS1* fragment. After digesting the pFKSCOS with different restriction enzymes and screening the fragments by Southern blotting, a 8.4-kb fragment with a *Sal*I end and a 2-kb fragment with an *EcoR*I end were cloned into plasmid pBSKS, a vector with an ampicillin resistance marker, to generate pPGFKS001 and pPGFKSE respectively. The pPGFKSE fragment was then sequenced, analyzed and shown to have highest homology with the glucan synthase gene of *A. fumigatus* (94% identity), which encodes part of the catalytic core. A 12-kb subcloning of pPGFK001 was then carried out after digesting with *Xho*I to generate four small size fragments, three of which were cloned into the *Xho*I site of plasmid pBSKS to create pPGFKS002, pPGFKS004, pPGFKS005. After sequencing, the relevant portions were assembled to obtain the whole 8.4-kb sequence of the *Sal*I fragment. The 2-kb *EcoR*I fragment was finally used to determine the overlapping region of the *Xho*I sub-clones.

3.32 *WdFKS1* has highest homology with *β*-1, 3-glucan synthase genes of other filamentous and conidiogenous Ascomycota.

The *WdFKS1* gene has two putative introns and an open reading frame of 5902 bp that encodes a putative protein of 1939 amino acids (aa). Promoter prediction analysis showed the promoter sequence is from -60 to -10 bp in the upstream region (Fig. 3.3.1A). TAATAT and TATA consensus sequences, which are putative TATA

boxes, are located at the -175 and -140, respectively The first putative intron is located near the 5'-end of the gene at starting position 719, consists of 50 base pairs and has the internal splicing sequences of GTAAGA and CTAAC. The second putative intron is located near the 3'-end at starting position 6072, consists of 35 base pairs and has the internal GTATGT and CTAAC splicing sequences. The predicted molecular weight (MW) of WdFks1p is 222 kDa, and its isoelectric point (PI) is 8.63. The derived protein sequence of *WdFKS1* (WdFks1p) shared highest identities along the whole sequence with those of other conidial Ascomycota, such as CpFksp (83%) of *C. posodasii*, PmFksp (81%) of *P. marneffei*, and AfFksp (80%) of *A. fumigatus* (Fig. 3.3.1B). Considerably lower identities were shared with those of the two yeast Ascomycota species *S. cerevisiae* (ScFks1p, 65%) and *C. albicans* (CaFks2p, 63%). *WdFKS1* also has the highly conserved catalytic core domain characteristic of the glucan synthases of other fungi (Fig. 3.3.1C). A putative UDP-glucose-binding consensus sequence RXTG was also found, which started at amino acid 1570 (Fig. 3.3.1D).

3.33 *WdFKS1* is a single copy essential gene in *W. dermatitidis.*

To determine whether *WdFKS1* is an essential single-copy gene, I did Southern blotting analysis of genomic DNA of *W. dermatitidis* with a 2-kb *WdFKS1* probe. The single band pattern (Fig. 3.3.2A) indicated there is only one copy of the *WdFKS1* homolog in *W. dermatitidis*. To characterize the function of *WdFKS1*, an insertion

Fig.3.3.1. Sequence analysis of WdFks1p. **(A)** Promoter prediction of *WdFKS1* by online software analysis. http://www.fruitfly.org/seq_tools/promoter.html. The transcription start nucleotide is identified with a larger letter. **(B)** Phylogram exhibiting the evolutionary relationships among the Fksp protein sequences. Sequences were generated and aligned using the CLUSTAL W program at http:// www.ebi.ac.uk/clustalw. Wd: *W. dermatitidis*, Pm: *P. marneffei*, Af: *A. fumigatus*. Cp: *C. posadasii*, Ca: *C. albicans*, Sc: *S. cerevisiae*. **(C)** The position of the conserved catalytic domain of WdFks1p. **(D)** The putative UDP-glucose-binding consensus sequence RXTG.

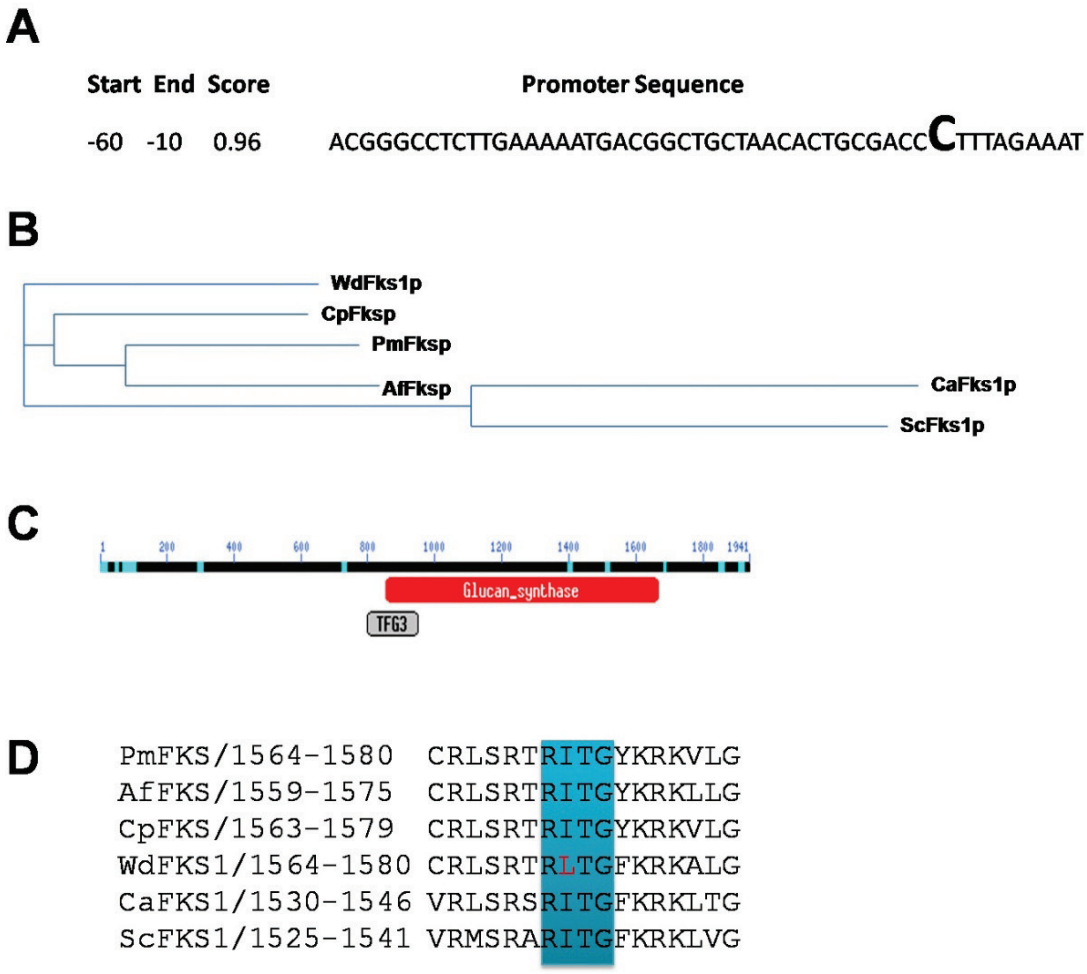

disruption vector was constructed so that a successful insertion would introduce a 5.6-kb plasmid into the *WdFKS1* gene sequence (Fig. 3.3.2B). This plasmid contains a 1.2-kb *Xho*I end-fragment from the conserved catalytic core region that was subcloned from pFKS001 into the *Xho*I site of pCB1004, generating plasmid pCBFKSD, which was linearized by *Mlu*I digestion. The linearized construct was then used to transform the *W. dermatitidis* wild-type strain 8656, which putitively would target to the homologous region of the *WdFKS1* gene in its genome. The intended integration thus would disrupt the catalytic domain of WdFks1p to generate the non-functional protein. Putative *wdfks*Δ disruption mutants were then selected for their resistance to hygromycin B. The gene disruption was carried out in both haploid and diploid cells. The disruption experiments generated four *wdfks*Δ disruption mutants in the diploid strain but none in the haploid strain. The integrative disruption of the diploid mutant *wdfks1*Δ-d12 was confirmed by Southern blotting (Fig. 3.3.2C). However, the haploidization of the diploid *WdFKS1* disruption strains by using methylbenzimidazole-2-yl-carbamate (MBC) (Cooper and Szaniszlo, 1993; Ye and Szaniszlo, 2000), produced no haploid *wdfks1*Δ strains. Thus I suggest that *WdFKS1* disruption mutants cannot be generated in haploid *W. dermatitidis* strains because this gene is essential for its viability.

3.34 *WdFKS1* expression responds differentially to certain stress conditions.

The purpose of the following set of experiments was first to confirm that *WdFKS1* is expressed and second to determine if its level of expression is regulated differentially under various conditions. Among the different stress conditions tested were higher temperature (37°C), nitrogen limitation, osmolarity stress, and an acidic environment condition. Wild-type cells were obtained and cultivated in YPD medium at 25°C until log phase. Then cells were collected, centrifuged, and subcultured in different media. Samples were collected after 40 min and total RNA was extracted and measured. After the total RNA was reverse transcribed into cDNA, the amount of specific *WdFKS1* cDNA was determined by realtime RT-PCR. Each total RNA sample was isolated three times and each cDNA sample was tested in three parallel reactions. The average results were used to determine relative quantity. As shown by Fig.3.3.3, *WdFKS1* mRNA expression is only slightly affected by temperature and osmolarity stresses, but displays significant decrease under nitrogen limitation stress and obvious increase under the acidic condition. A similar effect of temperature has been reported with *Y. lipolytica*, in which the mRNA level of *YlFKS1*remains constant when cells are grown at 23°C or 30°C for 2 h (Maela, et al., 2002). Also it has been reported that *C. albicans GSC1* mRNA levels decline when yeast cells are transferred to RPMI 1640 medium to induce hyphal growth by nitrogen limitation (Mio, et al., 1997), a condition that also induces a yeast cell-to-hyphal switch in *W. dermatitidis*. These results indicate that the *WdFKS1* expression level is negatively regulated during the yeast cell-to-hyphal form switching of this polymorphic fungus. However,in the promoter region of

Fig.3.3.2. Cloning and disruption of the *WdFKS1* gene. **(A)** Southern blotting analysis of genomic DNA of *W. dermatitidis*. DNA of the wild-type strain Wd8656 was digested with *Bam*HI, *Bgl*II, *EcoR*I, *Hind*III, *Kpn*I, *Pst*I, *Sal*I respectively. After separation in a 0.8% agarose gel, the resulting fragments were identified with radiolabled *WdFKS1* probe 1. **(B)** A 1.2-Kb *Xho*I fragment with a *Mlu*I site located in the middle was ligated into pCB1004 to generate the pFKSD. After the pFKSD was linearized by *Mlu*I digestion to target the *WdFKS1* it was used to disrupt the coding sequence for the conserved catalytic region. **(C)** Southern blotting analysis of the diploid *WdFKS1* disruption mutant *wdfks1*Δ-d12. DNA of wild-type strain Wd8656 and the diploid *FKS1* mutant *wdfks1*Δ-d12 were digested with *Sal*I. After separation by electrophoresis in a 0.8% agarose gel, the resulting fragments were identified with the radiolabled *WdFKS1* probe 1

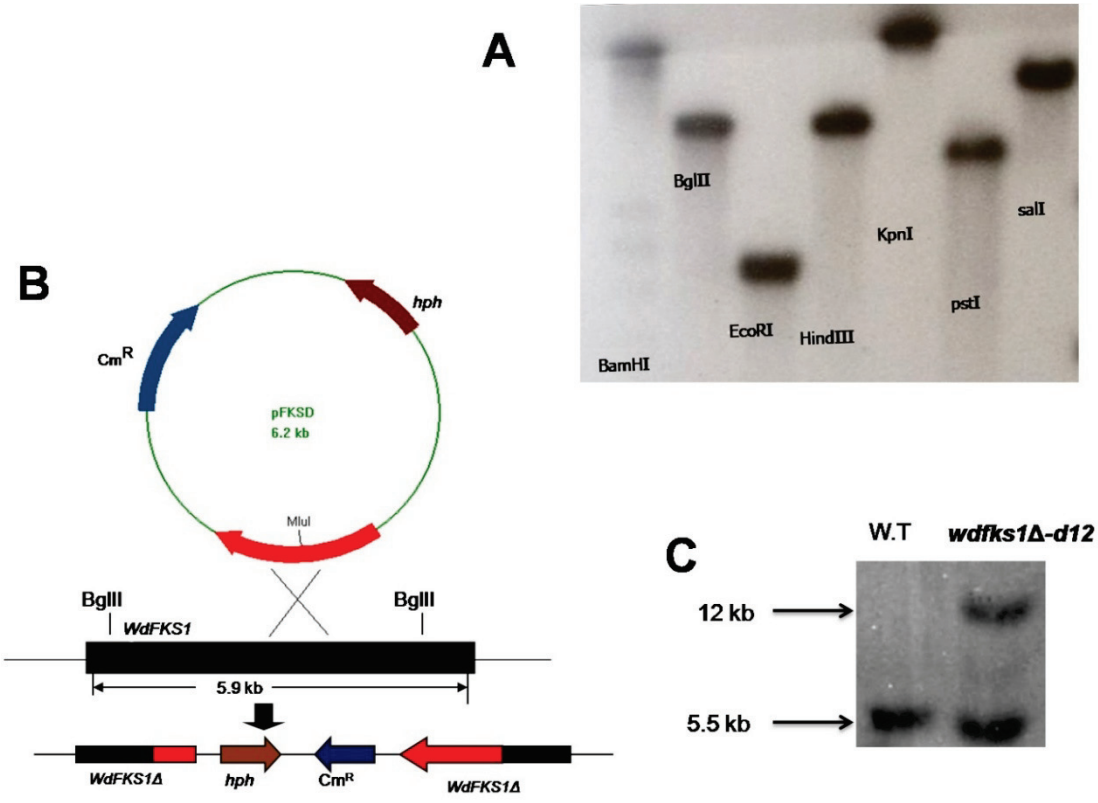

Fig. 3.3.3. The relative abundance of *WdFKS1* mRNA analyzed by realtime PCR. Wild-type cells of *W. dermatitidis* were incubated in YPD broth and grown at 25°C until log phase. Approximately $2x10^7$cells/ml cells were transferred into new media and incubated under different conditions for 40 min. Bar 1: YPD at 25°C; 2: YPD at 37°C; 3: Minimal media at 25°C; 4: YPD broth +1M sorbital at 25°C; 5: MCDB with pH 7.0 at 25°C; 6: MCDB with pH 2.5 at 25°C. Each total RNA sample was isolated three times and converted into cDNA. Each cDNA sample involved three parallel PCR reactions. The average of each data set was then used to determine the relative mRNA abundance.

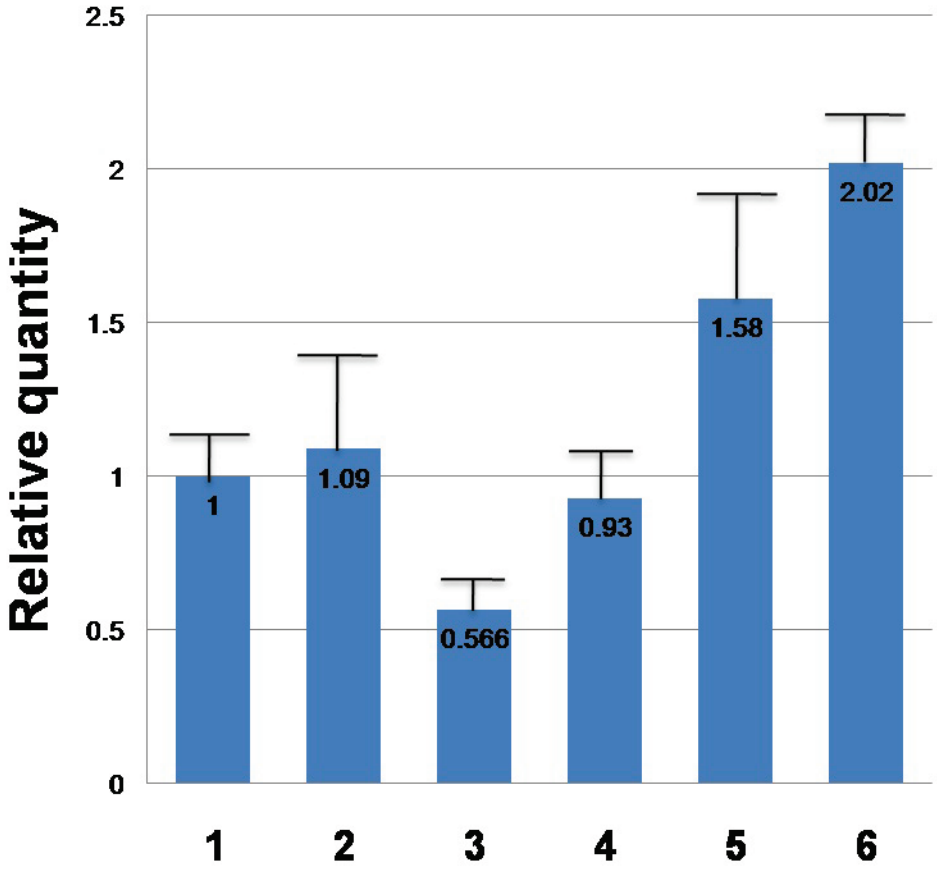

WdFKS1 I did not find the conserved sequence GCCAAG, which mediates pH-dependent gene expression in *A. nidulans* and *P. brasiliensis FKS1* homologs (Tilburn, et al., 1995; Maristela, et al., 2000): most likely this was because I did not obtain enoughupstream region of *WdFKS1*. Nonetheless, my realtime RT-PCR data showed enough up-regulation of the mRNA level after culture under the acidic contition tested, which indicates that the *WdFKS1* is a pH-dependent gene and it mRNA expression level is positively regulated by that stress condition.

3.35 RNA interference of *WdFKS1* mRNA expression retards cell growth and causes cell lysis.

Since my results, which are supported by those of others studying conidiogenous molds, point to the hypothesis that *WdFKS1* is a single copy essential gene, I carried out a functional characterization study by using RNA interference of *WdFKS1* mRNA. This effort was facilitated by the use of a well studied, color-selectable and site-specific integrative transformation system for the ectopic overexpression of genes, which was previously developed specifically for *W. dermatitidis* (Ye, et al., 1999; Ye, and Szaniszlo, 2000; Wang and Szaniszlo, 2007, 2009). The 501-bp *WdFKS1* conserved region (positions 3399 to 3902) was introduced into pYEX303 as an inverted repeat under the regulation of the *glaA* promoter to generate vector pPG2i (Fig. 3.3.4B). Prior to its use, pPG2i was linearized by digestion with *Nar*I and then used to transform *W.*

dermatitidis (Fig. 3.3.4A). After culture, cells of two albino colonies and one brown colony were suncultured and analyzed. Southern blotting then confirmed the site-specific insertion disruption of the *WdPKS1* locus of cells of the albino mutant *wdfksi-6*, but not of that locus of cells from the brown mutant *wdfksi-3* (Fig. 3.3.4D). The albino negative control mutant *wdfksi-nc* also showed the inserted plasmid in the *WdPKS1* locus. The albino mutant *wdfksi-6* was thus selected for a phenotypic analysis. Spot test growth results on YPMaltose agar medium showed that the RNAi interference mutant *wdfksi-6* displayed a slower growth rate compared with the wild type and the empty vector control strain in which the *WdPKS1* gene was disrupted by the pYEX303 vector only (Fig. 3.3.5A). However when I characterized the negative control mutant, it did not display the slow growth phenotype. Since the RNA transcript transcribed under promoter P*glaA* cannot form the stem-loop structure by complementation (Fig. 3.3.4.D), this result provides additional evidence to support my contention that the stem-loop structure of the dsRNA slows cell growth by interfering with *WdFKS1* mRNA synthesis. My growth curve study with YPMaltose broth medium also shows that the *wdfksi-6* mutant grows slower than the control albino strain both at 25°C and 37°C (Fig. 3.3.5B). The growth at 37°C is even slower than at 25°C, possibly due to the fact that the P*glaA* promoter is more active at 37°C than 25°C (Ye, et al., 1999; Ye, and Szaniszlo 2000).

Fig. 3.3.4. RNAi constructs for *WdFKS1* interference. (A) To obtain the RNAi plasmid, a 583-bp fragment was obtained by PCR from the coding sequence of the conserved catalytic region of *WdFKS1* and cloned into plasmid pYEX303 to generate pPG1i. Subsequently a 50-bp fragment lacking 82 nucleotides from the 3′end of the 583-bp fragment was obtained by PCR and cloned into pPG1i in front of the terminator T*glaA* as an inverted repeat sequence to generate the pPG2i. After being linearized by digestion with *Nar*I, the pPG2i plasmid was transformed site-specifically into the nonessential *WdPKS1* locus of the Wd8656 strain. **(B)** The P*glaA* promoter of pPG2i is activated by maltose induction to over-express the 1.1-kb *WdFKS1* fragment. After the transcription of the mRNA fragments, they will form stem-loop structures by self-complementation, which in turn can be recognized by the cell's RNAi machinery to target the *WdFKS1* mRNA. (**C)** To obtain an RNAi negative control plasmid, a 583-bp *WdFKS1* fragment was obtained by PCR from the coding sequence of the conserved catalytic region and cloned into plasmid pYEX303 to generate pPGNC1i. Subsequently a shorter 583-bp fragment lacking 82 nucleotides from the 3′end was obtained by PCR and cloned into pPGNC1i after the 583-bp fragment to generate the pPGNC2i. After being linearized by digestion of *Nar*I, the pPGNC2i plasmid was transformed into Wd8655 in the manner of pPG2i. **(D)** Southern analysis of genomic DNA of RNAi transformants. The genomic DNA of wild-type strain Wd8656 (1), *wdfksi-3* (2), *wdfksi-nc* (3), *wdfksi-6* (4) was isolated and digested by *Hind*III and the resulting fragments separated in a 0.8% agarose gel and probed with the *WdFKS1* probe 1.

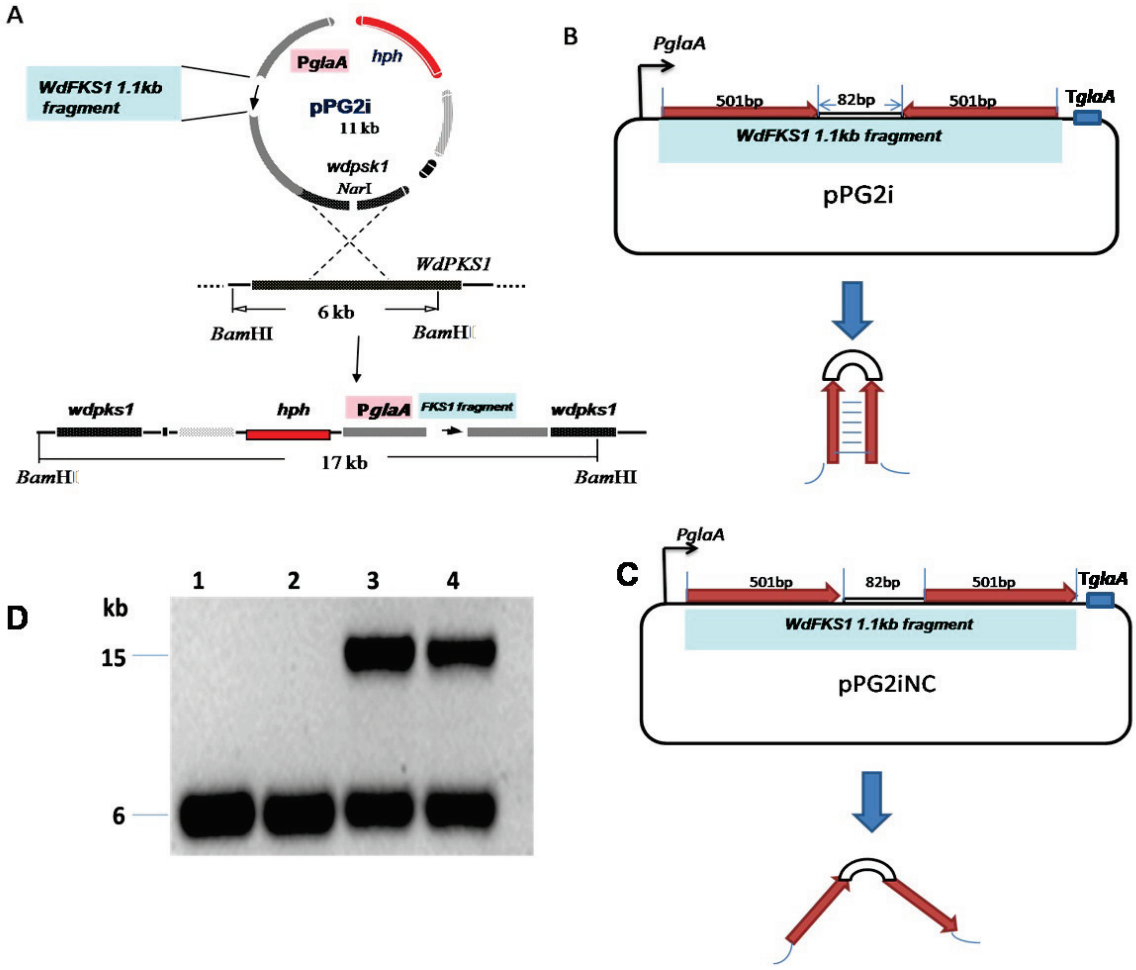
A
WdFKS1 1.1kb fragment
PglaA
hph
pPG2i
11 kb
wdpsk1
NarI
WdPKS1
6 kb
BamHI
BamHI
wdpks1
hph
PglaA
FKS1 fragment
wdpks1
17 kb
BamHI
BamHI
B
PglaA
501bp
82bp
501bp
TglaA
WdFKS1 1.1kb fragment
pPG2i
C
PglaA
501bp
82bp
501bp
TglaA
WdFKS1 1.1kb fragment
pPG2iNC
D
1
2
3
4
kb
15
6

Fig. 3.3.5. Effect of RNAi interference of *WdFKS* expression on growth using YPMaltose induction medium. (A) *Wdpyex303* (1), wild-type 8656 (2), and *wdfksi-6* (3) were spotted with 10^4, 10^3, 10^2 cells on YPMaltose agar medium, and then incubated at 37℃ for 48 h. **(B)** Comparison of the growth rates of *wdfksi-nc* and the *wdfksi-6* grown in YPMaltose liquid medium at 25°C and 37°C and assayed by optical density. The diamonds represent *wdfksi-nc* and the squares represent *wdfksi-6.* The initial inoculation levels for all cultures were ~5x10^5cells/ml. **(C)** The relative abundance of *WdFKS1* mRNA was analyzed by realtime PCR. Cells of *wdfksi-nc* and *wdfksi-6* were incubated in YPD broth at 25°C until log phase. Then ~2x10^7cells/ml cells were transferred into new media and incubated at different conditions in a time course manner. Each total RNA sample was isolated three times and converted into cDNA. Each cDNA sample was assayed in three parallel PCR reactions. The average of the results was used to determine the relative mRNA abundance.

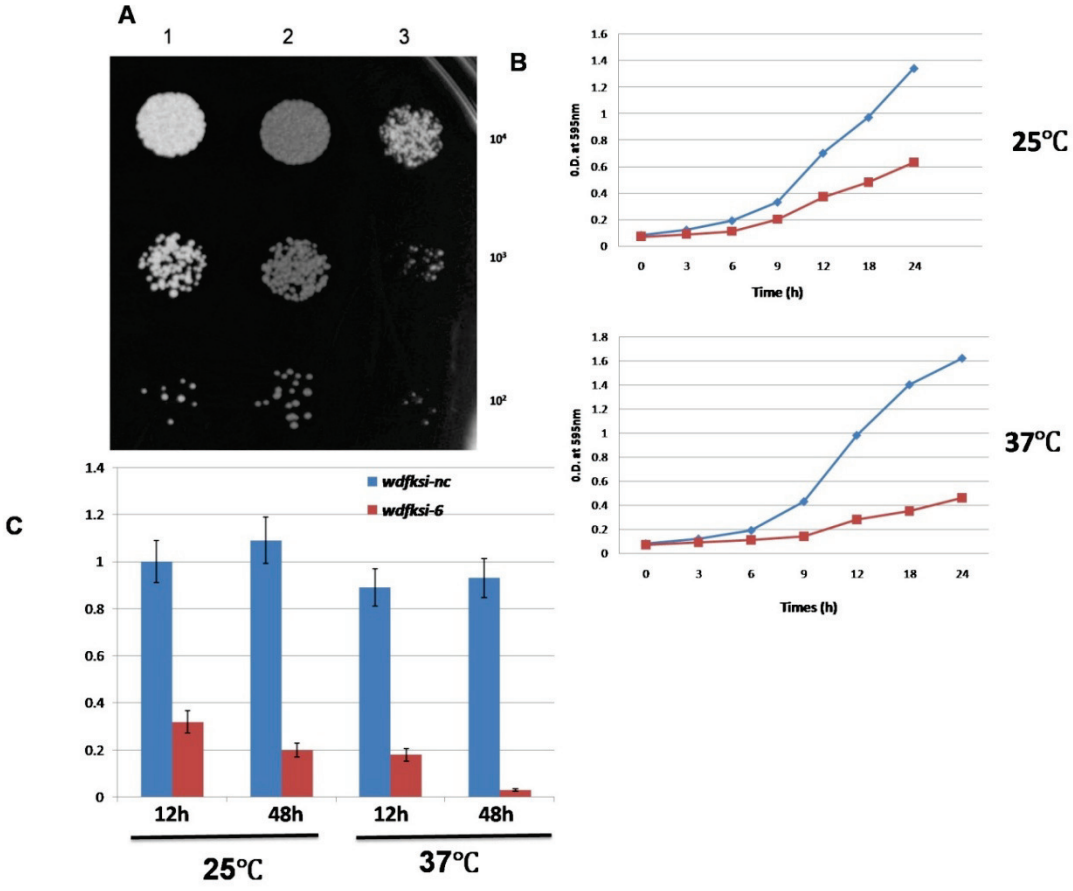

Fig. 3.3.6 Effect of RNAi interference of *WdFKS* expression on cellular morphology using YPMaltose induction medium. **Left:** Cells of *wdfksi-6* and *wdfksi-nc* were cultured in YPMaltose liquid induction medium at 37℃. After 4 days, cells were photographed at the same magnification with a light microscope fitted with a 40 x objective lens in the mode of DIC. Representative cells that have lost integrity are indicated by arrows. The bars in each image represent 20 μm. **Right:** Comparison of the growth rates of *wdfksi-nc* and *wdfksi-6* grown in YPMaltose liquid medium and YPMaltose liquid medium plus 1M sorbital at 37°C. The bars represent the percentage of abnormal cells or cells with abnormal buds in every 100 cells or buds. The light blue bar represents the *wdpyex303* and the deep blue bar represents the *wdfksi-6.* The initial inoculation levels for all cultures were ~5x10^{5}cells/ml.

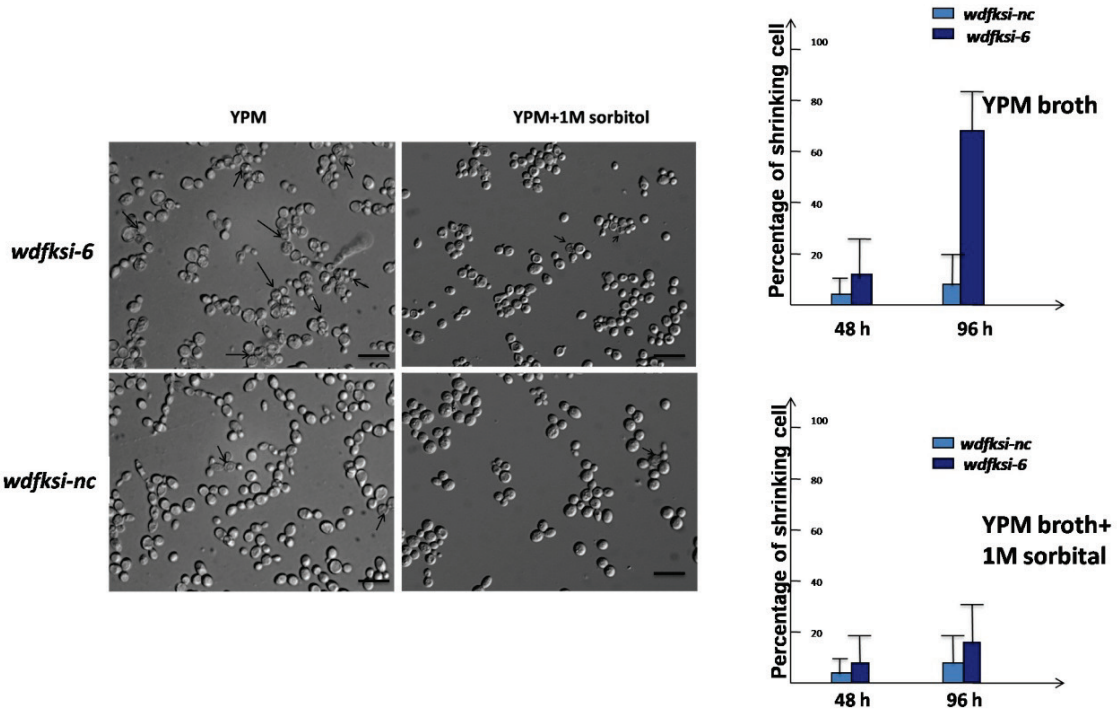

In order to obtain direct evidence showing the reduced mRNA level of WdFKS1in the putative interference strains, realtime RT-PCR was performed to compare the relative quantity of *WdFKS1* mRNA between *wdfksi-nc* and *wdfksi*-6 mutant. From the realtime RT-PCR, I observed an obvious decrease of the *WdFKS1* mRNA expression level in the *wdfksi-6* mutant compared with the *wdfksi-nc* mutant (Fig. 3.3.5.C). These results provide direct evidence that the RNA interference did indeed reduce the *WdFKS1* mRNA levels significantly at both 25°C and 37°C and that the mRNA level reaches a very low level after incubation at 37°C for 48 h. Also, I noticed that the *wdfksi-6* mutant displays a swelling, shrinking, and lysis morphology when incubated at 37°C over 4 days in YPMaltose medium. To find out if this lysis was caused by a change in cell wall integrity, I provided an osmotical support by adding 1M sorbital to the liquid medium. After 96-h incubation at 37°C, the percentage of shrinking cells dropped from 68% to 18% with the help of 1M sorbital (Fig. 3.3.6.). This result indicates that the high percentage of shrinking in cells is cause by damaged cell wall integrity that is due to the reduced incorporation of β-1,3-glucan macromolecules into the *W. dermatitidis* cell walls.

3.36 Reduced *WdFKS1* gene expression leads to altered cellular morphologies.

To characterize the cellular morphology caused by the reduced *WdFKS1* mRNA level, I stained the *wdfksi-6* mutant and *wdfksi-nc* RNAi negative control mutant cells

with calcoflour white. This revealed many incomplete septa associated with the *wdfksi-6* mutant cells when the *wdfksi-6* mutant was incubated in YPMaltose medium for 72 h at 37°C (Fig. 3.3.6A, B): the *wdfksi-6* mutant displayed the incomplete septa in the middle of the cells (see arrows), whereas the negative control mutant *wdfksi-nc* cells (Fig. 3.3.6C, D) did not. It is interesting that it was hard to find similar aberrant septa when the *wdfksi-6* mutant cells were incubated in YPMaltose for 48 h or less. Interestingly, many cells also started to lyse when incubated for over 94 h without the osmotic support (data not shown). However, even in the presence of 1M sorbitol the aberrant septa were not observed after incubation for 96 h or more in YPMaltose broth. When I observed *wdfksi-6* mutant cells stained with Calcoflour white using the microscopeis 100x objective oil lens, the septa showed as ring structures instead of as complete septal plates, because the middle area of the septum did not show fluorescence (Fig. 3.3.7E, F). In *W. dermatitidis*, the septum is mainly composed with chitin, but as with other fungi (Gould and Simanis, 1997; Cabib and Varma, 2001) the *β*-1,3-glucan also probably becomes a component of the division septum, at least during its secondary thickening. However, my results indicate that the incomplete septal structures were caused by the absence of material support from the *β*-1,3-glucan polymer.

Fig. 3.3.7. Effect of RNAi interference of *WdFKS* expression on cell wall and septal staining patterns using YPMaltose medium. Aberrant morphologies and septal ring formation and decreased budding are associated with *wdfksi-6* interference. DIC images of cells of *wdfksi-6* and WT (A, C) stained with Calcoflour white (B, D, E, F); arrows indicate cells that contain a medial septum or a septal ring in unbudded cells. In each case, cells ($1x10^7$ cells/ml) grown at 37℃ were transferred to pre-warmed (37℃) YPMaltose broth and then sampled and observed microscopically in a time-course manner. The cells shown here were sampled after culture for 72 h at 37℃ and photographed at the same magnification with visible light or fluorescent light using a 40x objective lens (A) to (D) or 100X oil lens (E) and (F). The bars in each image represent 5 µm.

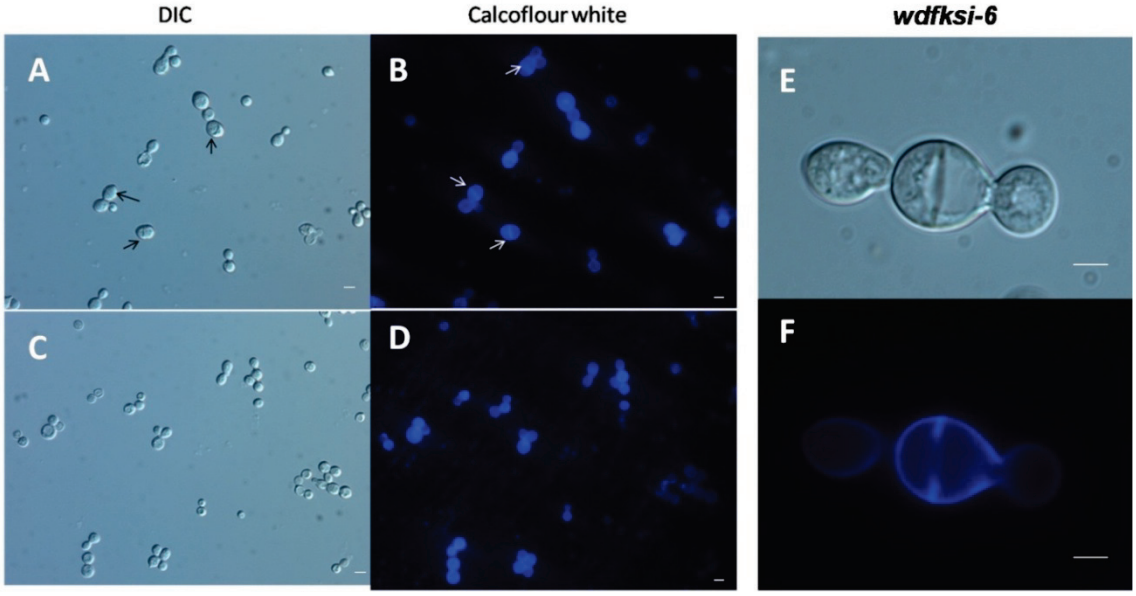

3.4 DISCUSSION

The purpose of my work on the molecular genetics of the *β*-1,3-glucan synthase gene was to increase our present knowledge on cell wall biosynthesis in *W. dermatitidis*. As is well known, the cell wall components chitin and melanin have been intensively studied in *W. dermatitidis* and are both known to contribute to its virulence. (Dixon et al., 1987, 1991, 1992; Feng et al., 2001; Zheng et al., 2006; Wang et al.,2001; Liu et al., 2004). However, the roles of *β*-1,3-glucan and *β*-1,3-glucan synthase have not been investigated in *W. dermatitidis* much beyond its concentration in cell walls and general biochemistry for the former and stimulation by nucleotides and its susceptibility to the echinocandin papulocandin for the latter (Szaniszlo, et al., 1983, 1985; Kang et al., 1986). In this study, I identified and sequenced the *FKS* homolog in *W. dermatitidis*. Two lines of evidence from my work supported the notion that *WdFKS1* is in fact a *FKS* homolog. First, the deduced amino acid sequence is over 63% identical to that of *FKS* genes in *C. albicans* and 83% of *C. posodasii*. Also, the highly conserved domains show homology with the putative UDPG-binding domains of cellulose synthase of *Acetobacter xylinum* (Lin *et al*., 1990; Kelly *et al*., 1996), even though it is a *β*-1,4-glucan glucan synthase. My results also provided two other lines of evidence supporting my conclusion that *WdFKS1* is the only *FKS* homologue in *W. dermatitidis*. These lines of evidence are as follows: (i) degenerate oligonucleotides amplified only a single DNA fragment when genomic DNA from *W. dermatitidis* was used as template; (ii) Southern

analysis of genomic DNA from *W. dermatitidis,* using seven different restriction enzyme digestions, was compatible with only one fragment being generated by each digestion reaction.

The results of my attemptes to disrupt *WdFKS1* have led me to conclude its essentiality. This conclusion is based first in my inability to isolate a single strain in which homologous integration had taken place, despite the fact that cells from a total of over 100 *hph* resistance colonies were screened. Further evidence came from my successful disruption of *WdFKS1* in a synthetic diploid strain. In this case, I was able to isolate several diploid mutants in which the homologous integration of a disruption vector into *WdFKS1* had taken place properly, as confirmed by PCR and by Southern blotting. While not definitive proof, numerous attempts failed to find by MBC-induced haplodization of the diploid a haploid strain in which the *WdFKS1* gene was disrupted by homologous integration. These results all suggest to me that *WdFKS1* is a single copy essential gene in *W. dermatitidis*.

My development of RNAi as a reverse genetic tool for *W. dermatitidis* overcomes many of the difficulties associated with traditional gene disruptions, especially when the gene involved is a single copy essential gene or a multi-copy, dose-sensitive gene. To date, RNAi has been demonstrated in *Histoplasma capsulatum* (Chad, et al., 2004), *Neurospora crassa* (Romano and Macino, 1992) and *Cryptococcus neoformans* (Liu et

al., 2002). The fact that RNAi does not depend on the homologous recombination machinery for silencing makes RNAi a promising alternative for reverse genetics studies in many fungal systems. Although it appears to be missing in some species of Saccharomycetes, such as *C. albicans* and *S. cerevisiae*, many other fungal species seem likely to possess the RNAi machinery.

My study is the first to involve RNAi interference in *W. dermatitidis*, although similar studies have been reported in *A. nidulens*, *H. capsulatum* and *Fusarium solari* (Barton and Prade, 2008; Chad, et al., 2004; Ha, et al., 2006). The RNAi interference construct pPG2i was modified from plasmid pYEX303, which can integrate and disrupt the *WdPKS1* gene through homologous recombination (Ye, et al., 1999; Ye and Szaniszlo, 2000). Four target sequences were selected from a target pool generated from the Ambion online tools (http://www.ambion.com/techlib/misc/siRNA_finder.html). Among these four target sequences, two were located inside the conserved catalytic domain (Fig. 3.4.1.). Of these, only target sequences #2 and #3 showed high RNAi interference efficiency, while target sequences #1 and #4 did not (data not shown), even though target #4 was located inside the conserved catalytic domain. Therefore, I selected for studying the RNAi mutant strain *wdfksi-6*, which overexpresses the RNAi transcript of sequence target #3 (Fig. 3.3.3B). I then designed the negative control construct based on the sequence of target #3 to provide precise negative control evidence (Fig. 3.3.3C). Also, because it was reported with *H. capsulatum* that the ideal

dsRNAs length is at least 500 bp, that the loop size can vary from 25 to 87, but 87-bp loops were the most optimal and the RNAi effects using the 25-bp loop construct exhibited greater variability (Chad A et al., 2004), I introduced 82 nucleotides in the loop structure to try and ensure that the RNAi efficiency would be high.

As expected, the disruption-generated *wdpks1*Δ albino strains, which can be indentified easily from transformant colonies on agar plate medium (Fig. 3.4.2.A), did not show any obvious morphogical changes, beyond the loss of color (Feng, et al., 2001). However, the albino strains all showed significantly slower growth rates. In addition, they also were hygromycin B resistant, and thus were selected by a second selection marker. Among the hygromycin B-resistant albino mutants, 100% of them showed the disrupted *WdPKS1* gene when they were first screened by PCR (data not shown). Southern blotting confirmed the correct integration site (Fig. 3.3.4D). These results support my contention that the double selection greatly increased the site-specific transformation and disruption efficiency. Interestingly, some brown colonies on the hygromycin B-containing YPD agar plates that were picked and tested also showed slow growth, even though they were not albino strains, which suggests that the RNA interference construct missed the *WdPKS1* gene target, but integrated somewhere else in the genome and still ectopically overexpressed the RNAi transcript.

Fig. 3.4.1 Diagram of the four target sequences selected for RNAi interference of *WdFKS1* mRNA. Target sequences are labeled with number and length. The red bar shows the conserved glucan synthase catalytic domain.

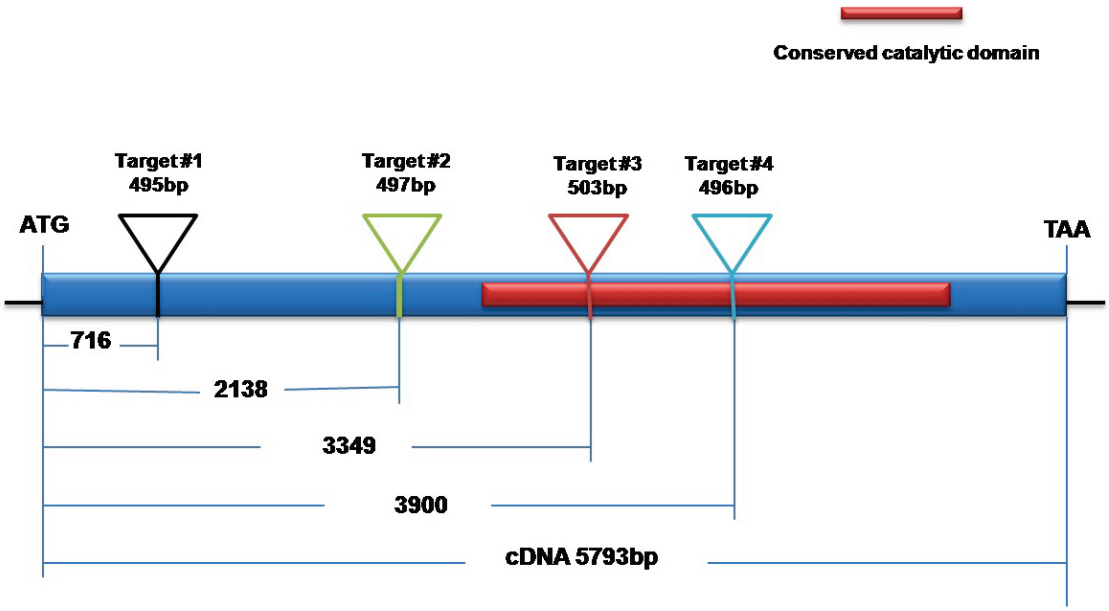

Fig. 3.4.2. **Albino mutant selection and phenotypes**. **(A)** After transformation, cells were spread on YPD agar medium containing hygromycin B (30 μg/ml). The red arrow points to an albino colony. **(B)** Colony morphology comparison between *wdfksi-6* and *wdfksi-nc*. Cells were inoculated onto the Starch agar medium and incubated at 37℃ for 5 days. Then the colonies were observed and compared using a 10x objective lens. The bars indicate 30 μm.

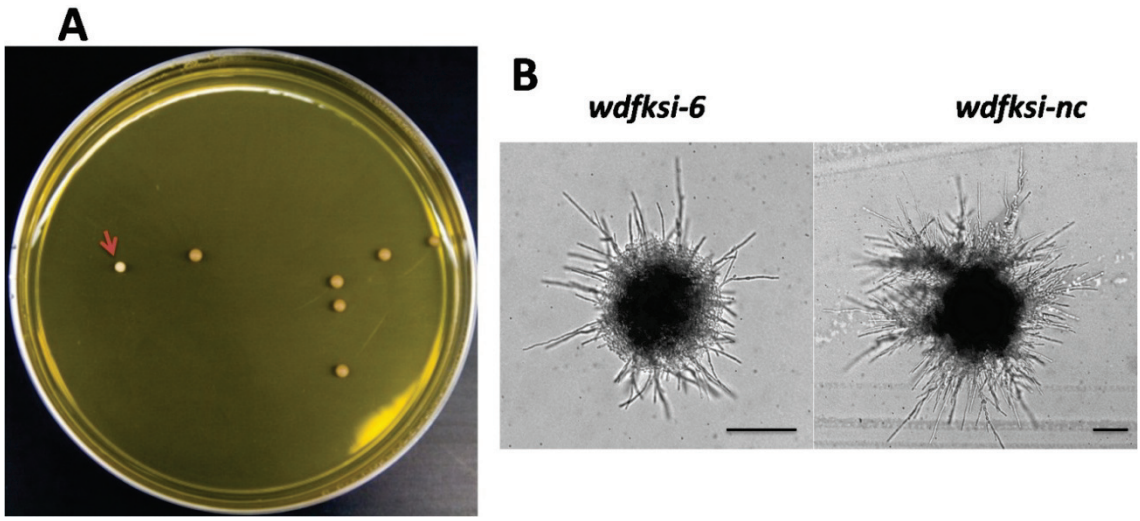

The slower growth of the *wdfksi-6* mutant compared to that of the wild-type strain may be due to the decreased *β*-1, 3-glucan synthase activity in the cell membrane and thus a decrease of *β*-1, 3-glucan polymer into the cell wall. However, the colony morphology of *wdfki-6* on YPMaltose agar is not much different than that of the wild type and negative control strain *wdfksi-nc* (data not shown), except for having a smaller size. In contrast, on the hyphae-inducing starch medium, the *wdfksi-6* mutant displayed mostly shorter hyphae and less intense hyphal growth around the colony (Fig. 3.4.2.B). I suggest that this morphological difference provides evidence that the glucan synthesis rate positively correlates to the rate of hyphal extension and branching. Although the slow growing cells of the *wdfksi-6* mutant did show brighten staining of mother cells, the daughter cells displayed significantly weaker staining compared with mother cells (Fig. 3.3.7F). The poorly staining daughter cells may result from less chitin being deposited into the daughter cell wall caused by there being an incomplete glucan matrix, as the calcoflour white is often used to localize chitin deposition in fungi. It is known that *W. dermatitidis* can be induced to form planate cells and sclerotic bodies with septa inside isotropically enlarged mother cells under certain conditions (Oujezdsky et al., 1978; Roberts and Szaniszlo, 1978; Szaniszlo et al., 1983, Cooper et al., 1984; Cooper and Szaniszlo, 1993; Karuppayil and Szaniszlo, 1997; Abramczyk et al., 2009). In addition, it is clear that septum formation and budding are associated with nuclear division in wild-type cells (Jacobs and Szaniszlo, 1982; Abramczyk et al, 2009). When budding in *W. dermatitidis* is retarded, a yeast or hyphal cell will often isotropically

Fig. 3.4.3. Effect of RNAi interference of *WdFKS* expression on septal ring and nuclear division using YPMaltose induction medium. DIC (A, B, C, G, I) cells of *wdfksi-6* stained with Calcoflour white (C, D, E) or DAPI (G, J) In each case, cells ($1x10^7$ cells/ml) grown at 37℃ were transferred to pre-warmed (37℃) YPMaltose broth and then sampled and observed microscopically in a time-course manner. The cell shown here were sampled after culture for 72 h at 37℃ and photographed at the same magnification with visible light or fluorescent light using a 40x objective lens or 100X oil lens. The bars in each image represent 5 µm, the orange arrows indicate the septum rings and the light blue arrow indicate the nuclei.

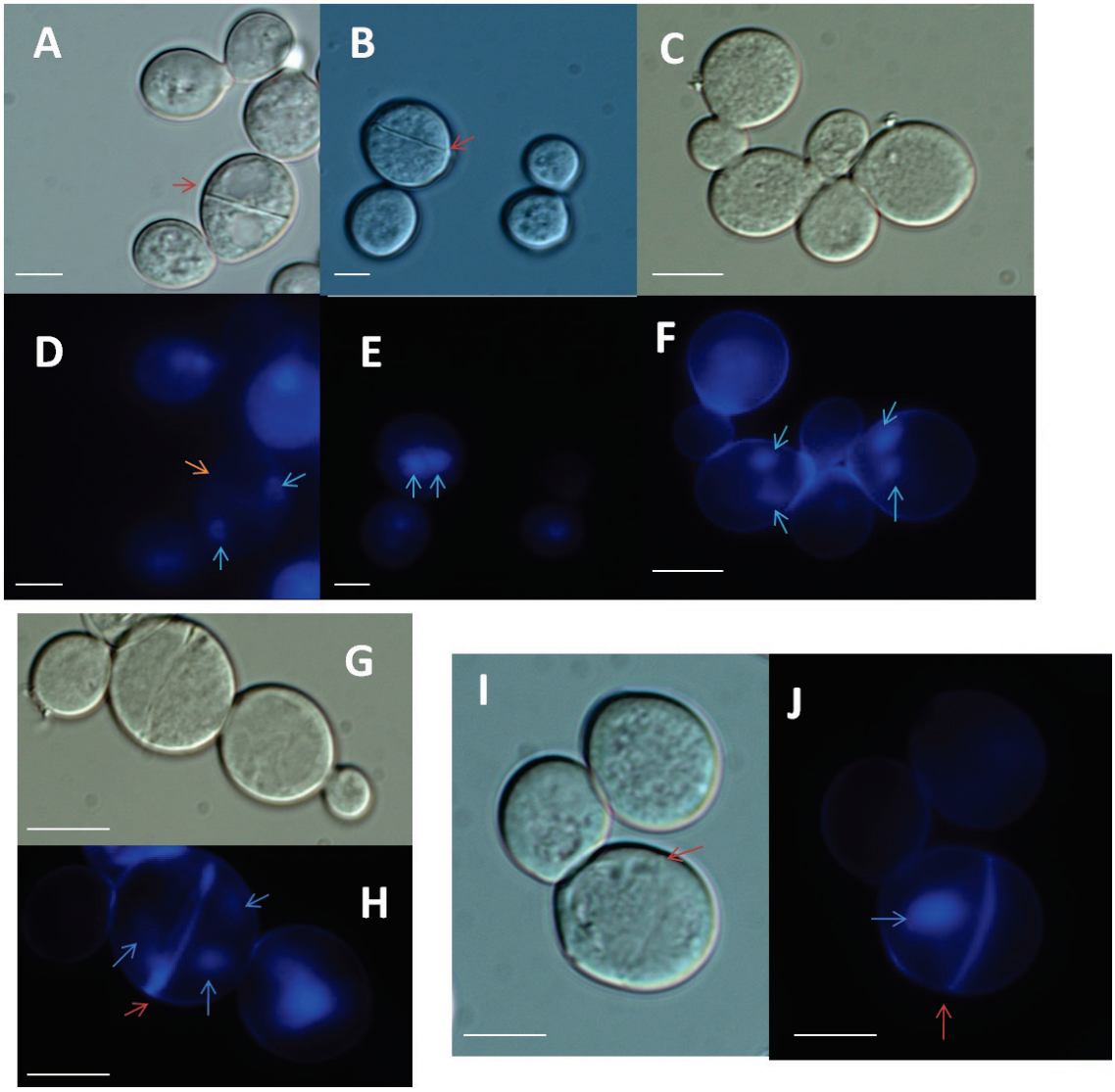

enlarge and turn to slow fission to continue proliferation. In addition, my results suggest that the appearance of a septal ring is a signal for the retardation of budding. Thus as a further check to see if there is a synchronization between septum formation when nuclear division is slowed by reduced mRNA levels of *WdFKS1*, the *wdfksi-6* mutant cells were stained singly with DAPI or doubly with DAPI and calcoflour white. As shown in Fig. 3.4.3A and D, the nuclei are separated by a septum located between them. And as shown in Fig.3.4.4C and F that nucleus had replicated without the appearance of septa. Both cases above can be found in sclerotic cells and in planate cells. On contrast, Fig. 3.4.3B and E show that the nucleus had been replicated, but were not separated by the septum. These results can be interpreted by three possibilities: first, the nuclear division does not synchronize with septum formation because septum formation occurs earlier than the nucleus separates; second, nuclear division does synchronize with septum formation, but the incomplete septum allows the separated nuclei to shuttle between compartments; third nuclear division does not synchronize at all with septum formation and the hollow septum allows the shuttle of nuclei. On this respect, Fig. 3.4.3G and H show a septa ring and three nuclei, results that support the assumption that there has been a disrupted synchronization between nuclear division and septum formation. Additional evidence is provided by Fig. 3.4.3I and J, which show that only one nucleus exists adjacent to a septal ring. These data indicate that the septal ring formation does not synchronize nuclear replication and division not only because the cell proliferation by fission is retarded by the malfunction of septum that is arrested in

the form of a ring structure, but possibly also because of the potential malfunction of a cell cycle check point.

Chapter 4: WdRho1p has distinct roles in morphogenesis and negatively regulates polarized hyphae formation in *Wangiella dermatitidis.*

4.1 INTRODUCTION

4.1.1 The primary function of the Rho-type GTPases.

In 1985, the *RHO* gene was identified, but not until 1993 were the cellular functional roles of Rho GTPases reported. Rho GTPases function as molecular switches that cycle between an active, GTP-bound form and an inactive, GDP-bound form. The cycling between GTP and GDP-bound states is regulated by GDP/GTP exchange factors (GEFs), GTPase activating proteins (GAPs) and guanine nucleotide dissociation inhibitors (GDIs). GEFs stimulate the exchange of GDP with GTP and thereby activate Rho, whereas GAPs bind to the GTP-bound form of Rho and increase its low intrinsic GTPase activity, thereby converting Rho into the GDP-bound inactive form [Fig. 4.1.1].

4.1.2 Functional roles of Rho1p in *Saccharomyces cerevisiae.*

Six Rho-type GTPases, named Rho1 to Rho5 and Cdc42, hace been indentified in *S. cerevisiae*. Rho-type GTPase localize at the plasma membrane and they serve distinct but related roles in cell polarity establishment and maintenance (Schmidt and Hall, 1998). In *S. cerevisiae*, Rho1p has the ability to sense upstream signals that direct cell wall remodeling and cell morphogenesis. Rho1p is localized to the cell periphery and to the septum or the tips of growing buds. Null mutants devoid of Rho1p in both fission and budding yeast are lethal (Nakano, et al., 1997). Rho1p activates the Pkc1-Slt2 cell integrity MAP kinase cascade in response to cell wall stress (Bickle, et al., 1998). In addition, Rho1p has been implicated in the control of bud growth by regulating actin organization and cell wall synthesis (Cabib, et al., 1998, Schmidt, et al., 1997). First, Rho1p in *S. cerevisiae* include reorganization of the actin cytoskeleton via binding to Bni1p (Imamura, et al., 1997; Narumiya, 1996), and specifically activates its effectors in its GTP-bound form (Cabib, et al., 1998). In *S. cerevisiae*, Rho1p regulates glucan synthase at three levels. First, Rho1p regulates the activity of the catalytic subunit directly to control the incorporation rate of UDP-D-glucose. Second: Rho1p regulates the gene expression at the transcriptional level by controlling the promoter activity of the *FKS* genes. Third: Rho1p can regulate the depolarization of Fks1p. Additional roles of Rho1p in *S. cerevisiae* include polarized secretion (Guo, et al., 2001) and endocytosis (Eitzen, et al., 2001).

4.1.3 Functional roles of Rho1p in other fungi

In *S. pombe*, Rho1 is essential for cell viability and cell polarity. The cell wall of cells seem to be loosely organized when expressing the dominant-negative Rho1. In cells, actin patches are delocalized when either a constitutively active Rho1 or a dominant-negative Rho1 were expressed. In addition, both the cell wall and secondary septum are thicker with the expression of constitutively active Rho1. Furthermore, inactivation of Rho1 is required for the separation of daughter cells. Cell fractionation studies suggest that Rho1 is predominantly membrane-bound and Rho1p is observed to localize to the cell periphery as well as the septum. In the dimorphic fungus *C. albicans*, CaRho1p acts in the same manner as in *S. cerevisiae* and plays a role in regulating *β*-1,3-glucan synthesis (Kondoh *et al*., 1997). The depletion of Rho1p from yeast cells results in cell lysis, death and aggregation (Smith, et al., 2002). The *YlRHO1* gene from *Yarrowia lipolytica* is able to complement *rho1* lethality in *S. cerevisiae* but, unlike in *S. cerevisiae,* an *ylrho1* disruptant strain of *Y. lipolytica* is viable (Leon *et al*., 2003). In conidiogenous filamentous fungi, the *RHO1* homologs of *A. fumigatus* and *A. nidulans* have been reported (Beauvais, et al., 2001, Gretel, et al., 2003). In *A. nidulans*, *rhoA,* a *RHO1* homolog, plays a role in emergence both of the primary and secondary germ tubes (Gretel, et al., 2003). An orthologue of Rho1 in *Aspergillus fumigatus* is part of the glucan synthase complex, and acts together with the catalytic glucan synthase Fks1p (Beauvais, et al., 2001). *A. nidulans* strains carrying ectopic copies of a

Fig. 4.1.1 Model of Rho GTPase cycle Rho GTPases are molecular switches that use a simple biochemical strategy to control complex cellular processes. They cycle between two conformational states: one bound to GTP (active state), the other bound to GDP (inactive state), and they hydrolyse GTP to GDP (adapted from Sandrine and Hall, 2002)

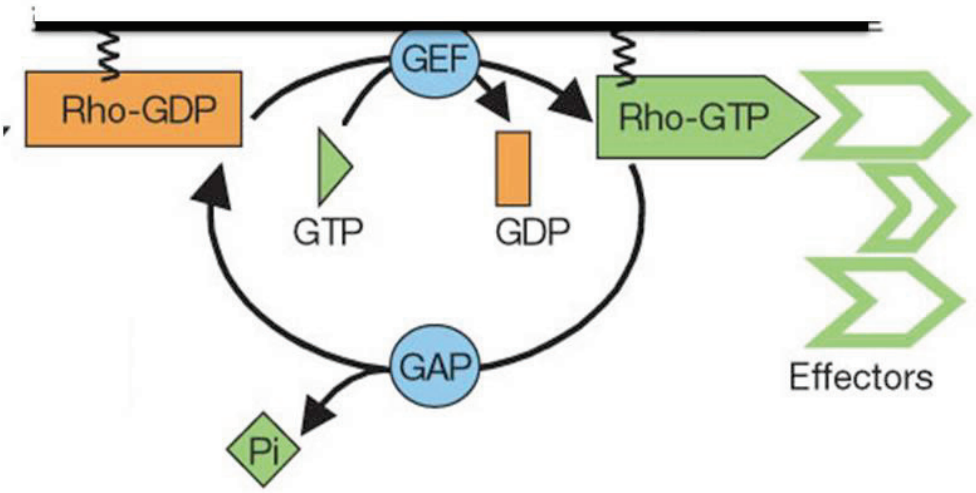

Fig. 4.1.2 Functional roles of Rho1p in *Schizosaccharomyces pombe.* Rho1p is a multifunctional protein and may play several important roles in *Schizosaccharomyces pombe*. First: The activity of Rho1p affects the separation of daughter cells. Second: Rho1p regulates septum formation. Third: Rho1p regulates cell wall synthesis as the regulatory subunit of β-1,3-glucan synthase. Fourth: Rho1p controls cell polarity determination by regulating the localization of actin patches (modified from Nakano, et al., 1997).

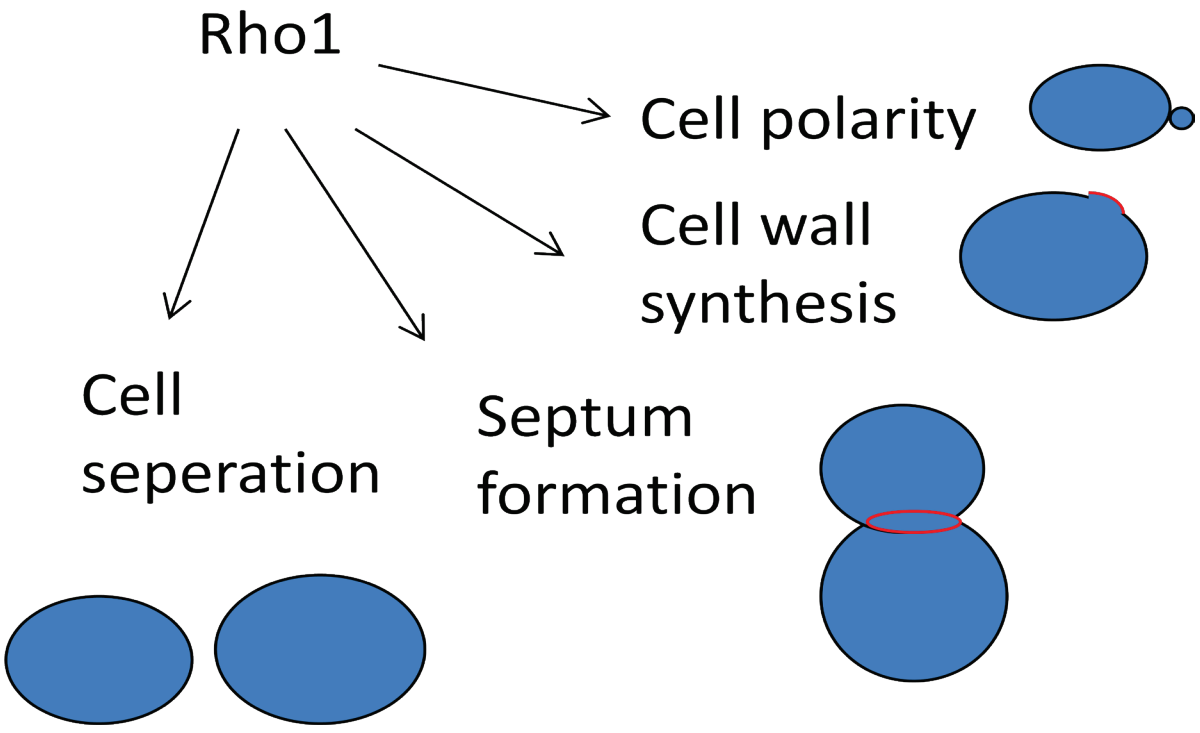

constitutively active *rhoA*^{G14V} allele show restricted growth and an abnormal branching pattern, whereas a strain carrying an ectopic dominant *rhoA*^{E40I} allele exhibite cell lysis and hypersensitivity to calcofluor and caspofungin, suggesting a role of RhoAp in morphogenesis and cell wall biogenesis (Guest, et al., 2004). Targeted deletion of *rho1* has only been successful in one filamentous species, *Ashbya gossypii. Agrho1* null mutants exhibited severely restricted growth, which gave rise to tiny colonies showing cell lysis and colony death after a few days (Wendland and Philippsen, 2001). Collectively, these results indicate that Rho1p is required for the establishment and maintenance of cell polarity, as well as for proper composition and integrity of the fungal cell wall. At present, the roles of Rho1p during fungal infection of plant or animal hosts remain unknown. During the invasion process, pathogenic fungi develop infectious hyphae that are able to penetrate and colonize the underlying tissue. The diseases caused by the hyphal growth require considerable polarized growth in order to breach the host surface. At the same time, maintenance of cell wall integrity is also required to protect against the host defenses. In filamentous fungi, little is known about the roles of Rho1p in polarized hyphal growth, even though polarized hyphal growth is a key element in fungal pathogenicity (Madhani and Fink, 1998). In this study, I focus on the role of WdRho1p on the regulation of polarized hyphal growth and cellular morphology development.

4.2 MATERIALS AND METHODS

4.2.1 Strains, culture conditions.

The *W. dermatitidis* strains used in this research are listed in Table 4.1. Routine culture of *W. dermatitidis* was on YPD agar (YPDA) and in YPD broth (YPDB) as described previously (Liu et al., 2004). For the detection of the filamentous growth, *W. dermatitidis* was grown on starch agar (Difco Scientific, Detriot, Mich.). The restrictive temperature for the ts mutant Hf1 and ts mutant Mc3 was 37°C.

4.2.2 Degenerate PCR, library screening and cloning.

Degenerate primers with designs based on the conserved domains of the Rho1p. Two PCR primers, PFKS1-FR and PFKS1-REV were allowed the amplification of a 503-bp PCR product. WDRHO 5'-GGY GAY GGY GCY TGY GGYAA-3' and WdRHOR 5'-TCY TCY TGG CCG GCN GTR TCC CAN AG-3' (R=A+G, N=A+T+C+G, Y=C+T). PCR amplifications were carried out with 2 μM of the primers, 0.5 mM dNTP, 0.5 μg genomic DNA and 0.5 U/μl Taq polymerase mixed in 1.5 mM Mg++, 50 mM KCl, 10 mM Tris-HCl (pH 9) buffer. The PCR reaction conditions were as follows: 5 min at 94°C for premelting; 50 cycles of 1 min at 94°C for denaturation, 1 min at 55°C for annealing, and 1 min at 72°C for extension; 7 min at 72°C for completion of

Table 4.1. Strains used in this research

Strain	Genotype	Reference(s) or source
3u2m-428	*Mcm2/cdc1 mcm3/cdc2 met ura mel3 mel4*	Cooper and Szaniszlo, 1993
W. dermatitidis 8656	Wild type	ATCC 34100
Hf1	Tempterature-sensitive (ts) hyphal-form mutant	McIntosh, et al., 1995
Mc3	Tempterature-sensitive (ts) *wdcdc2* multicellular form mutant	ATCC 38716
*wdrho1*Δ*-d8*	*wdrho1 wdrho1*::*hph*	This study
wdpyex303	*wdpks1*::pYEX303-*hph*	This study
*wdcdc42*Δ	*wdcdc42*Δ::*sur++*	Ye and Szaniszlo, 2000
wdrho1^{OE}	*wdrho1 wdpks1*::pYEX303-*hph- wdrho1*$^{+}$	This study
wdrho1^{G14V}	*wdrho1 wdpks1*::pYEX303-*hph- wdrho1*^{G14V}	This study
hf1/*rho1*^{G14V}	Hf1 *wdrho1 wdpks1*::pYEX303-*hph- wdrho1*^{G14V}	This study
hf1/wdrho1^{OE}	Hf1 *wdrho1 wdpks1*::pYEX303-*hph- wdrho1*$^{+}$	This study
Mc3/*rho1*^{G14V}	Mc3 *wdrho1 wdpks1*::pYEX303-*hph- wdrho1*^{G14V}	This study
*wdcdc42*Δ/*rho1*^{G14V}	*wdcdc42*Δ::*sur++ wdrho1 wdpks1*::pYEX303-*hph- wdrho1*^{G14V}	This study
*wdcdc42*Δ/*rho1*^{OE}	*wdcdc42*Δ::*sur++ wdrho1 wdpks1*::pYEX303-*hph- wdrho1*$^{+}$	This study

hph: hygromycin resistance gene.* *sur*++: sulfonylurea resistance gene.

^{OE} : Overexpression of wild-type allele

the extension. The resulting PCR products were then cloned into the pGEM-T easy vector (Promega, Madison, Wis.) and sequenced. After sequencing showed that plasmid pPGRHO1A contained an *RHO1* homolog fragment. Gene-walking was carried out in two directions comparison of the cDNA sequence produced from reverse by using DNA walking speedup^{TM} premix kit (Seegene, korea) with two set of primers. 5' upstream direction walking primers: UTSP1, 5'-GCTGACATTCTACCCTCTG-3', UTSP2, 5'-CCCTTTCATCCCCTTCTCTC-3', UTSP3, 5'-AACCCCCTATCATCGACCG-3'; 3' downstream direction walking primers: DTSP1, 5'-TGGACGGTCGATGATAGG-3', DTSP2, 5'-GAGAGAAGGGGATGAAAGGG-3', DTSP3, 5'-CAACAGAGGGTAGAATGTCAGC-3' PCR products by gene walking were cloned in pGEM-T vector and sequenced by by the Core Facility of Institute of Cellular and Molecular Biology, University of Texas at Austin, using BigDye technology (Applied Biosystems, Foster City, CA). The locations of introns, first predicted in silico by alignments and by consensus splice sequences, were then confirmed by the transcription-PCR (RT-PCR) using the One-Step RT-PCR kit (QIAGEN, Valencia, CA) with the genomic DNA sequence. For the RT-PCR, RNA was extracted with hot acidic phenol from cells grown in YPDB for 24 h at 37°C and treated with RQ1 RNase-free DNase (Promega). After the RT-PCR was carried out, the amplification products were analyzed by electrophoresis in a 3% agarose gel with 2-log DNA markers (New England Biolabs, Ipswich, MA) as references.

4.2.3 Disruption of *WdRHO1* gene

To disrupt *WdRHO1*, the 1.4-kb *hph* gene cassette was flanked by upstream and downstream *WdRHO1* gene fragments by an overlapping PCR method (*pfx* high fidality PCR kit). A 395-bp upstream fragment of *WdRHO1* was amplified by PCR with the primer PRHO1U (5'-TCCTCCTCGCCCGATTGCA-3') and RHO1PCRUR (5'-AATAGAGTAGGATCCGACCGGGAACCCAGTTAACGTCGACCGTATCGATAAGCTTGATAATGAATTTCGCGACGGATTTCAGCCATG-3', the overlapping sequence with the *hph* gene is framed). The *hph* gene cassette was amplified by PCR with the primer HPH-1(5'-CAAGCTTATCGATACGGTCG-3') and HPH-2 (5'-CCTCGAGGTCGACGTTAA-3'). The 411-bp downstream fragment of *WdRHO1* gene was amplified by PCR with primer PRHO1DF (5'-TGACCTCCACTAGCTCCAGCCAAGCCCAAAAAATGCTCCTTCAATATCAGTTAACGTCGACCTCGAGGGAGCGAGCAATCTCGACATC-3') and PRHO1DR (5'- GCACCCGACGAGGATGAT-3'). The above three PCR products were then used as templates to amplify a 2.2-kb fragment with the primer PRHO1U and PRHO1DR. The 2.2-kb fragment was transformed into competent *W. dermatitidis* haploid or diploid yeast cells by electroporation as described previously (Ye and szaniszlo, 2000). After transformants were selected on YPDA medium containing 50 μg/ml hygromycin B (Invitrogen, Carlsbad, CA), mutants strains were identified by PCR and Southern analysis. The specific primers for the PCR

screening were designed to amplify the *WdRHO1* and *hph* combined hybrid fragment (Fig.3A) and had the following sequences: SRHO1D5R, 5'-TTCCCAATACGAGGTCGCC-3'; SRHO1D3, 5'-AACCAATACGAGGTCGCC-3'. For Southern blotting analysis of the disruption mutant, DNA of wild-type strain Wd8656 and the mutant strain were first digested with *Sal*I, and then after separation by electrophoresis in a 0.8% agarose gel, the resulting fragments were identified with the radiolabled *WdRHO1* probe 1.

4.2.4 Ectopic overexpression of *WdRHO1* in *W. dermatitidis*.

The site-specific, integrative expression vector pYEX303 was used for the expression of *wdrho1* alleles in the nonessential Wd*PKS1* genomic locus of *W. dermatitidis* as described previously (Ye, et al., 1999; Ye and szaniszlo, 2000). The *WdRHO1* wild-type allele *wdrho1*$^{+}$ was amplified by RT-PCR(One-Step RT-PCR kit; QIAGEN) with primers ORHO1F, 5'-GAAGATCTA*ATG*GCTGAAATCCGTCGCA-3', and ORHO1R, 5'-TTTCTAGATTACAAAATCAAGCATTTC-3' (the start and stop codons are indicated by italic letters, and the introduced *Bgl*II and *Xba*I restriction digestion enzyme recognition sites are underlined). To introduce the site specific mutantion, primer ORHO1G14V, 5'-GAAGATCTAATGGCTGAAATCCGTCGCAAGCTTGTCATCGTCGGAGATGTT GCCTGCGGAAAGACTTGTT-3' (the mutant amino acid codon is framed) and primer

ORHO1R are used to amplify the *wdrho1*^{G14V} mutant allele by PCR (high fidelity *pfx* PCR system, Invitrogen). The PCR products were then cloned into pGEM-T vector to generate plasmid pPGRHOA and pPGRHOB. To clone the *WdRHO1* wild-type alleles and constitutively active allele into pYEX303 vector, pPGRHOA and pPGRHOB were digested with *Bgl*II and *Xba*I restriction digestion enzymes, then the release fragments were ligated with the *Bgl*II-and *Xba*I-digested pYEX303 vector to generate pPG1002 and pPG1003 respectively. After being linearized by digestion with *Nar*I, the pPG1002 and pPG1003 plasmids were transformed site-specifically into the nonessential *WdPKS1* locus. After white transformants were obtained for each constructed strain, Southern blotting was applied to confirm the proper ectopic integration of the *WdRHO1* alleles

4.2.5 Northern analysis.

Log-phase, 25°C-cultured *W. dermatitidis* yeast cells were first inoculated into YPDB at 10^6cells/ml and then incubated with shaking in YPDB at 25°C or 37°C. After 24 h, the cells were collected by centrifugation and RNA was isolated with the QIAGEN RNeasy kit. The concentration of RNA was determined using an ND-1000 spectrophotometer (NanoDrop Technologies, Wilmington, DE), and RNA integrity was evaluated by electrophoresis in a 1% agarose gel containing 2 M formaldehyde. Probes were labeled as described above. For the *WdRHO1* probe, the *WdRHO1* fragment from

the pPGRHOA plasmid was used. After Northern hybridization, radioactive signals were detected by exposure to the Kodak film.

4.2.6 Nucleotide sequence accession number

The sequence of *WdRHO1* was submitted to the GenBank database. The accession number is bankit1358378 HM600808.

4.3 RESULTS

4.31 Cloning of the *WdRHO1* gene of *W. dermatitidis.*

A gene (*WdRHO1*) that encodes a putative Rho-like GTPase in *W. dermatitidis* was cloned by gene walking using genomic DNA as a template. The gene walking was initiated at a 379-bp sequence obtained from a PCR product that was amplified with degenerate primers derived from a conserved region of *RHO1* homologs of other fungi. The gene walking extended the 379-bp sequence to 1905-bp, which included the 920-bp *WdRHO1* gene sequence (Fig. 4.3.1). The 579-bp open reading frame encodes a putative polypeptide of 193 amino acids with a predicted molecular

mass of 21.7 kDa and a pI of 5.87. Four introns were found by comparing the cDNA sequence with the genomic *WdRHO1* gene sequence. Comparisons of the derived amino acid sequence of *WdRHO1* in the GenBank databases showed that the deduced WdRho1p protein was highly similar to Ras related Rho-type GTPases, including Cdc42, Rac, and Rho proteins. The most similar homolog of WdRho1p was the Rho1 protein of *A. niger*, which was 92% identical in its derived amino acid sequence. Considerably lower identities were shared with ScRho1p (79%) of *S. cerevisiae* and CaRho1p (82%) of *C. albicans* (Kondoh, et al., 1997). Although the WdRho1p deduced polypeptide was found to have 193 amino acids, 16 fewer than ScRhop and five fewer than CaRho1p, it contained all of the consensus sequences conserved among Rho-type GTPases. Multiple alignments of the amino acids sequences identified several conserved regions among all the Rho1p proteins examined. The consensus sequences, GDGACGKT and DTAGQE (conserved domain III) from the N-terminal are believed to be critical for interaction with the phosphoryl group of GTP (Sanders, 1990). The conserved domain, YVTVFENY (domain II), is an effector domain, which is required for the interaction with GTP-activating protein (GAP) (Sekine, et al., 1989) and the C-terminal CXXL box is highly conserved among the Rho1p homologues (Fig. 4.3.2; X for any amino acid). Note: this geranylgeranylation site has been shown to be essential for C-terminal prenylation and membrane localization (Hancock, et al., 1989; Ziman, et al., 1993). Based on sequence homology, I concluded that *WdRHO1* encodes a structural orthologue of ScRho1p.

Fig.4.3.1 Nucleotide sequence and predicted amino acid sequence of the *Wangiella dermatitidis RHO1* (*WdRHO1*). The start codon is shown in blue and the stop codon is shown in green. The intron sequences are capitalized.

```
CCATCAACAACAACTTGAACCATCTTCACCGTCGACCTGATCCATCACCTTCTAGTCCTATCGTAGTAGAAATAATCT
TACACGGTAGTCTATGACAGTCCAAATCATTCTCGAGCTCTCGTCCTCCTCGCCCGATTGCAGCCATCACTGCACTCA
TTTCCTAGTAGTACTACACAATAGATTTGCGTGTCCTTGTTCTCTCGGGCCCGCCCCGTTGCAGTGCAGTGGCAGTTT
GGTCTTCAAAGCCACATCCACACTGCACTAAACGCTCTAAACCGCCCCCAAAAAGGTGCCTTTTCCTGCCAATCCTCT
CTCAACCTCTTTATACCGTCTCGTCTACTACCAACACTCCTACTCCCTCTCACCTATTCATCATTTCGCGCCCACCAA
CCACTCCATCCTAATCTGACCCAGACCTACAGAAACCACCTCGCAGCCATCACCACTCCTACCGCCCTATCTTTACTT
TCCACCAGACGCCGTCCGCCGCAGCCGCC
    atggctgaaatccgtcgcaagcttgtcatcgtcggagatggtgcc
    M  A  E  I  R  R  K  L  V  I  V  G  D  G  A
    tgcggaaagacttgtttgttgatGTAAGTCTCATATCATCGACCG
    C  G  K  T  C  L  L  I
    TCTCCTACCTACAAAACCTGCAGTGGTTGCTGACATTCTACCCTC
                TGTTGTCCAGtgttttctccaagggcacgttt
                          V  F  S  K  G  T  F
    cctgagGTGCGCAGCTCCCCTTTCATCCCCTTCTCTCAATAAACC
    P  E

    ACTCGAGCGAGCAATCTCGACATCAACCCCCTATCATCGACCGTC
    CAACGCTAGATCCGGTGATCACAACGAGATAAAGTACTAAAATCC
    CACATTTGCAG
         gtctacgtcccaaccgtcttcgagaactacgtcgccgat
         V  Y  V  P  T  V  F  E  N  Y  V  A  D
    gtcgaagtcgatggaaaacacgttgaactcgccctatgggatacg
    V  E  V  D  G  K  H  V  E  L  A  L  W  D  T
    gcaggccaggaagattacgaccgccttcgacctctatcatacccc
    A  G  Q  E  D  Y  D  R  L  R  P  L  S  Y  P
    gactcccacgtcatcttgatttgttttgccatcgattctcccgat
    D  S  H  V  I  L  I  C  F  A  I  D  S  P  D
    tcgctcgataacgtccaggagaagGTATGGGAGCAACTGTTCCAG
    S  L  D  N  V  Q  E  K
    TGTTATGTGACTTGGATCGAGCTGACGCCTTGCATTAG
                          tggatttctgaagtcctgcac
                          W  I  S  E  V  L  H
    ttctgccaaggtctccccatcatcctcgtcgggtgcaaatgcgat
    F  C  Q  G  L  P  I  I  L  V  G  C  K  C  D
    ttgagacacgacccaaagactattgaagagctggcaaagacatct
    L  R  H  D  P  K  T  I  E  E  L  A  K  T  S
    cagaagcccgttacacccgagcagGTTCGTTCGCCCGTGATACCG
    Q  K  P  V  T  P  E  Q
    GTCTATCGATGGCCCCGGGACGCTGACTTTGGATTGTCTAG
                           ggtgaggaagttcgcaagaag
                           G  E  E  V  R  K  K
    atcggtgcctacaagtatctcgagtgctcggccaagaccggccag
    I  G  A  Y  K  Y  L  E  C  S  A  K  T  G  Q
    ggtgttcgcgaagtattcgagaccgctacccgggcggccttgttg
    G  V  R  E  V  F  E  T  A  T  R  A  A  L  L
    acgcgcaagagtggaaagagcaagaaatgcttgattttgtaa
    T  R  K  S  G  K  S  K  K  C  L  I  L  *
ATCAGGCAAACCTCTTTCTCTTGTTGCAGACATGGACCCCCCCCCCCTCGCTTGGCATACTTCTGTGAAGTCCTGCACT
TCTGCCAAGGTCTCCCTATCATCCTCGTCGGGTGCAAATGCGATTTGAGACACGACCCAAAGACCCCCCCCCCTCGCTT
GGCATACTTCTGTGAAATCACTAGTGAATTCGCGGCCGCCTGCAGGTCGACCATATGGGAGAGCTCCCAACGCGTTGG
ATGCATAGCTTGAGTATTCTATAGTGTCACCTAAATAGCTTGGCGTAATCATGGTCATAGCTGTTTCCTGTGTGAAAT
TGTTATCCGCTCACAATTCCACACAACATACGAGCCGGAAGCATAAAGTGTAAAGCCTGGGGTGCCTAATGTGAGCTA
ACTCACATTAATTGCGTTGCGCTCACTGCCCGCTTTCCAGTCGGGAAACCTGTCGTGCCAGCTGCATTAATGAATCGG
CCAACGCGCGGGGAGAGGCGGTTTGCGTATTGGGCGCTCTTCCGCTTCCTCGCTCACTG
```

Fig. 4.3.2 Amino acid sequence alignments of *W. dermatitidis* (WdRho1p), *Penicillium. marneffei* (PmRho1p), *Aspergillus. fumigatus* (AfRho1p), *Paracoccidioides brasiliensis* (PbRhoA), *Neurospora crassa* (NcRho1p), *Cryptococcus neoformans* (CnRho1p), *Schizosaccharomyces pombe* (SpRho1p), *Candida albican* (CaRho1p), and *Xenopus laevis* (XlRhoA). Identical amino acids among the proteins are denoted by asterisks. Boxes indicate the conserved domains among Rho-type GTPases (I, II, III, IV, V). The "G" to "V" mutation site is shown in red and the "D" to "A" mutation site is shown in green.

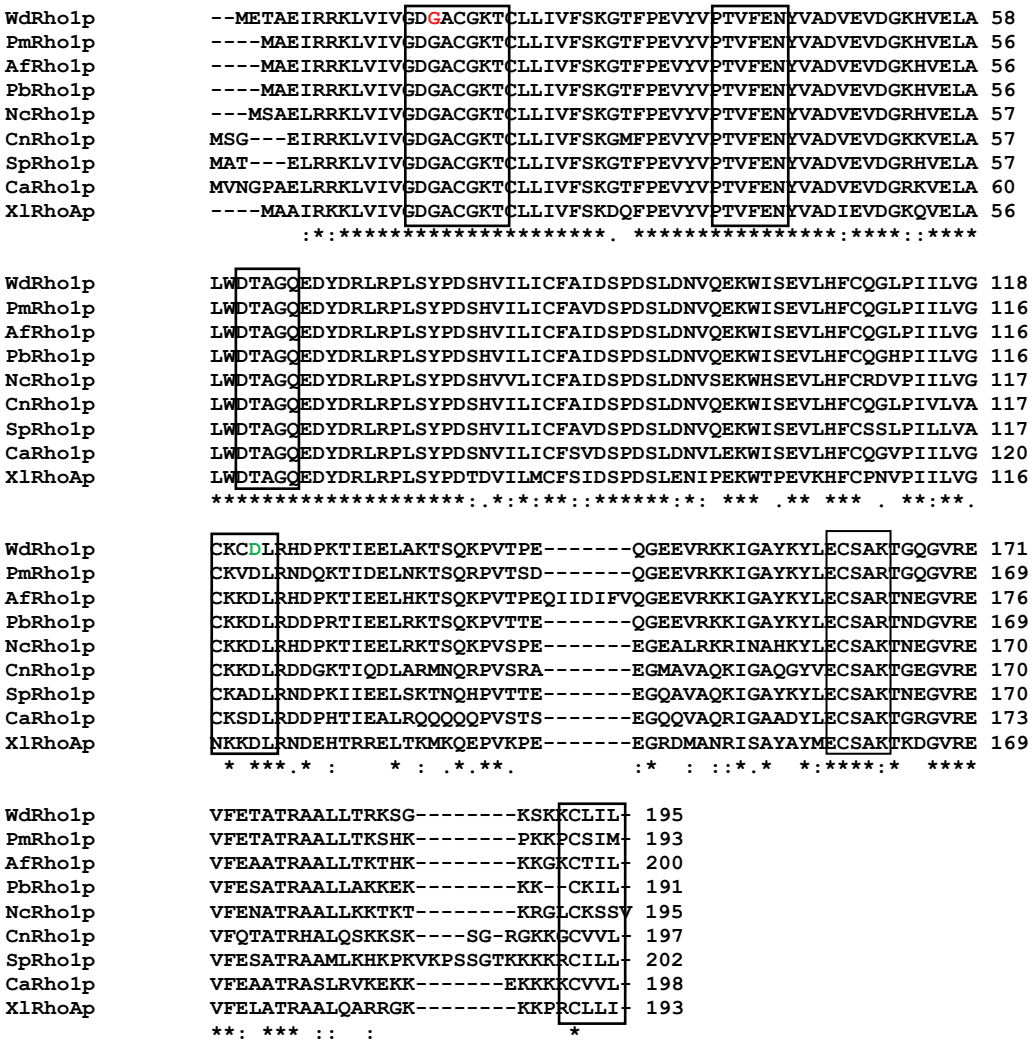

4.32 Loss-of-function studies of the Rho1p allele suggest that *WdRHO1* is an essential gene in *W. dermatitidis.*

To investigate the biological function of WdRho1p in *W. dermatitidis*, I tried to generate the loss-of-function Δ*wdrho1* allele using a targeted gene replacement strategy to delete a 197-bp fragment of the *WdRHO1* gene. The deleted fragment included the start codon and the highly conserved GTP-biding domain within the predicted protein (Fig. 4.3.3A). Considering the possible essentiality of *WdRHO1*, the *WdRHO1* gene loss-of-fuction deletion was carried out in both haploid and synthetic diploid cells of *W. dermatitidis*. Among the 52 hygromycin–resistant haploid transformants analyzed by PCR, none displayed the expected gene replacement, while two transformants from 24 hygromycin–resistant diploid transformants produced a PCR amplification product indicative of gene replacements by homologous recombination. By Southern blot analysis of one of the diploid transformants (*wdrho1*Δ-*d8*), the replacement of a 1-kb *Sal*I fragment, which corresponded to the wild-type *RHO1* allele (rho^{+}), by a 2.4-kb fragment and an additional 1-kb fragment from another wild-type *RHO1* allele was confirmed (Fig. 4.3.3B). Thus, I concluded preliminarily that the *wdrho1*Δ-*d8* strain carried a disrupted copy of the *WdRHO1* gene, as well as one copy of the intact gene. Then to obtain more evidence to support my contention of the essentiality of the *WdRHO1* gene, methylbenzimidazole 2- yl-carbamate (MBC) was used to induce the haploidization (Cooper and Szaniszlo 1993; Ye and Szaniszlo 2000) of diploid

*wdrho1*Δ-*d8*. Since no haploid *wdrho1*Δ strain was produced, I suggest that *WdRHO1* disruption mutants cannot be generated in haploid strains because this gene is essential and no another *RHO1*-like gene in *W.dermatitidis* with partially overlapping function exists.

4.33. Ectopic overexpression of the *wdrho1*$^+$ allele did not affect the growth rate or the cellular morphogenesis of *W. dermatitidis.*

For *W. dermatitidis* there is as yet no tested working regulatory promoter that can be used for down-regulation by an inductor molecule. To circumvent this problem the overexpression promoter *glaA* of the glucoamylase gene from *Aspergillus niger*, which mediates gene expression in the presence of maltose or starch as sole carbon source (Fowler et al., 1990; Ward et al., 1993), was tested previously for reliability in *W. dermatitidis*. This led to the development of a color-selectable and site-specific integrative transformation system for the ectopic overexpression of genes in *W. dermatitidis* (Ye, et al., 1999; Ye, and Szaniszlo, 2000). To study the functional role of WdRho1p, I used this system to ectopically overexpress the wild-type allele *wdrho1*$^+$ under the regulation of the *glaA* promoter by introducing the linearized plasmid pPG1002 into the *W. dermatitidis* genome (Fig. 4.3.4A). The rational for using plasmid pPG1002

Fig.4.3.3. Disruption of *WdRHO1* by replacement with the *hph* selection marker. **(A)** The 1.4-kb *hph* gene cassette was flanked by upstream (395 bp) and downstream (411 bp) *WdRHO1* gene fragments by overlapping PCR. The 2.2-kb fragment was next released from the vector by restriction enzyme digestion and used for the gene knock out. **(B)** Southern blotting analysis of the diploid *WdRHO1* disruption mutant *wdrho1*Δ-*d8* . DNA of wild-type strain Wd8656 and the diploid *RHO1* mutant *wdrho1*Δ-*d8* was digested with *Sal*I. After separation by electrophoresis in a 0.8% agarose gel, the resulting fragments were identified with the radiolabled *WdRHO1* probe.

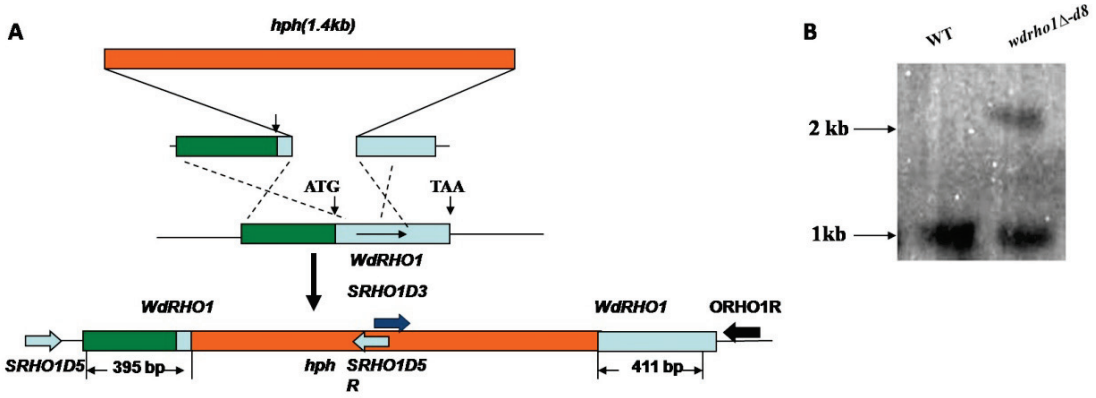

is that it targets and disrupts the *WdPKS1* gene, and thus helps identify suitable transformants not only by their resistance to hygromycin B but also by their albino phenotype (Feng et al., 2001). After a number of hygromycin-resistant albino transformants were selected for the analysis, Southern blotting of one mutant (*wdrho1*^{OE}) revealed a 17-kb *Bam*HI hybridizing fragment, confirming the presence of the newly integrated pPG1002 plasmid containing a functional *wdrho1*$^{+}$ allele in the *WdPKS1* locus (Fig. 4.3.4B). Northern blot analysis confirmed the ectopic overexpression of the *wdrho1*$^{+}$ allele from the plasmid (Fig. 4.3.4C). When I then investigated whether the overexpression of wild-type WdRho1p would affect the growth rate of *W. dermatitidis* at either 25℃ or 37℃ using a serial dilution spot test, I found that the rates were very similar at both temperatures to those of the wild type, as well as the negative control strain *wdpyex303*, which was transformed with plasmid pYEX303 that did not contain the *wdrho1*$^{+}$ allele (Fig. 4.3.5A). Also, no additional phenotype was observed when compared with the negative control strain *wdpyex303* or the wild-type strain. These results indicate that translational or post-translational regulation of WdRho1p affects cell growth more than does transcriptional level regulation of *WdRHO1* gene expression.

4.34 Ectopic overexpression of the constitutively active allele *wdrho1*^{G14V} causes slower growth.

Fig.4.3.4. Ectopic overexpression by transformation of *W. dermatitidis* cells with *WdRHO1* and its mutants alleles. (A) To obtain the *WdRHO1*overexpression plasmid, a 582-bp *WdRHO1* cDNA or the *wdrho1*^{G14V} fragment were cloned into plasmid pYEX303 to generate pPG1002 and pPG1003 respectively. After being linearized by digestion with *Nar*I, the pPG1002 and pPG1003 plasmids were transformed site-specifically into the nonessential *WdPKS1* locus. **(B)** Southern blotting analysis of the *WdRHO1* overexpression mutants *wdrho1*^{OE}. DNA of wild-type strain Wd8656 and *wdrho1*^{OE} were digested with *Bam*HI. After separation by electrophoresis in a 0.8% agarose gel, the resulting fragments were identified with the radiolabled *WdRHO1* probe 1. **(C)** Northern blotting analysis of the radiolabled *WdPKS1* probe 1.

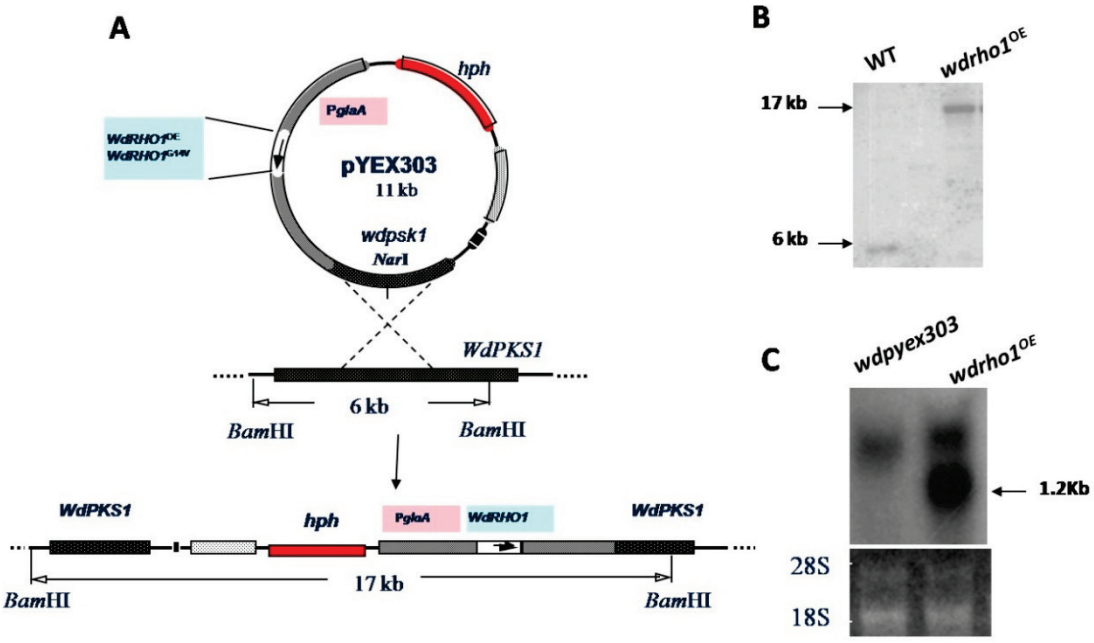

To further investigate the role of WdRho1p in *W. dermatitidis*, I used site-directed mutagenesis to generate a *rho1*^{G14V} gain-of-function allele, in which the conserved number 14 amino acid G residue was changed to V (Fig. 4.3.2, red color font). Then I ectopically overexpressed the *wdrho1*^{G14V} allele without disrupting the wild-type *wdrho1*$^{+}$ allele. This would putatively change the ratio between the active and inactive forms of WdRho1p and allow me to determine whether the phenotype changed because of the overexpression of the constitutively active GTP form of WdRho1p. After the PCR fragment of the *wdrho1*^{G14V} allele was cloned into pYEX303 under the control of the *glaA* promoter to generate the plasmid pPG1003, the ectopic overexpression vector pPG1003 was introduced into wild-type strain to generate hygromycin-resistant albino transformants. From among a total of six albino transformants that grew in the presence of hygromycin B, one was selected for further study and analyzed by Southern blotting with a *WdPKS1*-specific probe. The results revealed a 17-kb *Bam*HI hybridization fragment, confirming the presence of the newly introduced *wdrho1*^{G14V} allele in the *WdPKS1* locus (Fig. 4.3.5B, second band from the left). From this result, I concluded that the overexpression mutant *wdrho1*^{G14V} carries both a *rho1*^{G14V} allele and the wild-type *wdrho1*$^{+}$ allele in its genome, since the pPG1003 construct was confirmed to be specifically integrated only into the *WdPKS1* gene. Phenotypic analysis of *wdrho1*^{G14V} in a dilution assay spot test on YPmaltose agar then revealed it also had a reduced growth rate (Fig. 4.3.5C, second row from right). The retarded growth rate was more severe at 37℃, which may be due the fact that the promoter *glaA* is more active at

37°C than 25°C (Ye et al., 1999). This result indicates that the damaged balance between the active form and inactive form of WdRho1p influences the growth rate of *W. dermatitidis*. In addition, the result suggests that the overexpression of constitutively active WdRho1p has a negative effect on its rate of growth.

4.35 Overexpression of the constitutively active form of WdRho1p in the *wdrho1*^{G14V} mutant promotes pseudohyphal growth.

Because Rho1p in *S. cerevisiae* is involved in multiple signal transduction pathways, characterizations of the cellular and colony morphology of *wdrho1*^{G14V} were carried out. After 48 h incubation at 25°C and 37°C in YPMaltose liquid broth, cells were stained with Calcoflour white and DAPI. Microscopic observations then showed that the *wdrho1*^{G14V} mutant cells produced end-to-end attached budding yeast cells reminiscent of pseudohyphae (Fig. 4.3.6. left panel). Also at 37°C, the mutant cells displayed a higher level of attached cells than those produced at 25°C. in addition, cell separations between mother cells and daughters appeared to be arrested in *W. dermatitidis*, which consequently biased accurate growth assays on plate media. Nonetheless, these results, compared to the unaffected growth rate associated with the overexpression of wild-type WdRho1p, suggest that the active GTP form of WdRho1p is a key element affecting cell separation and growth rates. After four days incubation at 37°C, the colony morphology of mutant *wdrho1*^{G14V} on the YPMaltose agar showed a

Fig.4.3.5. Effects of the overexpression of alleles *wdrho1*^{OE} and *wdrho1*^{G14v} on growth. **(A)** yeast cells of the wild-type 8656, *Wdpyex303*, and *wdrho1*^{OE} strains were spotted with 10^5 ,10^4, 10^3 cells on YPMaltose agar medium, and then incubated at both 25℃ and 37℃ for 48 h. **(B)** Southern blotting analysis of the *wdrho1*^{G14V} mutant allele overexpressed in WT, Hf1^{ts}and Mc3^{ts} strains. DNA of *wdrho1*^{OE} , *wdrho1*^{G14V} , *hf1/rho1*^{G14V} ,and *mc3/rho1*^{G14V} was digested with *Bam*HI. After separation by electrophoresis in a 0.8% agarose gel, the resulting fragments were identified with the radiolabled *WdPKS1* probe 1. **(C)** wild-type 8656, *wdpyex303*, *wdrho1*^{OE}, *wdrho1*^{G14V} , and *wdcdc42*Δ were spotted with 10^4, 10^3, 10^2 cells on YPMaltose agar medium, and then incubated at both 25℃ and 37℃ for 48 h. **(D)** The relative abundance of *WdRHO1* mRNA was analyzed by realtime PCR. Cells of *W. dermatitidis* were incubated in YPD broth at 25°C until log phase. Then ~2x10^{7}cells/ml cells were transferred into pre-warm YPMaltose broth media at 37°C and incubating 2 hours. Each total RNA sample was isolated three times and converted into cDNA. Each cDNA sample was analyzed in three parallel PCR reactions. The average results were used to determine the relative mRNA abundance. The error bars indicate the standard diviations among the percentages.

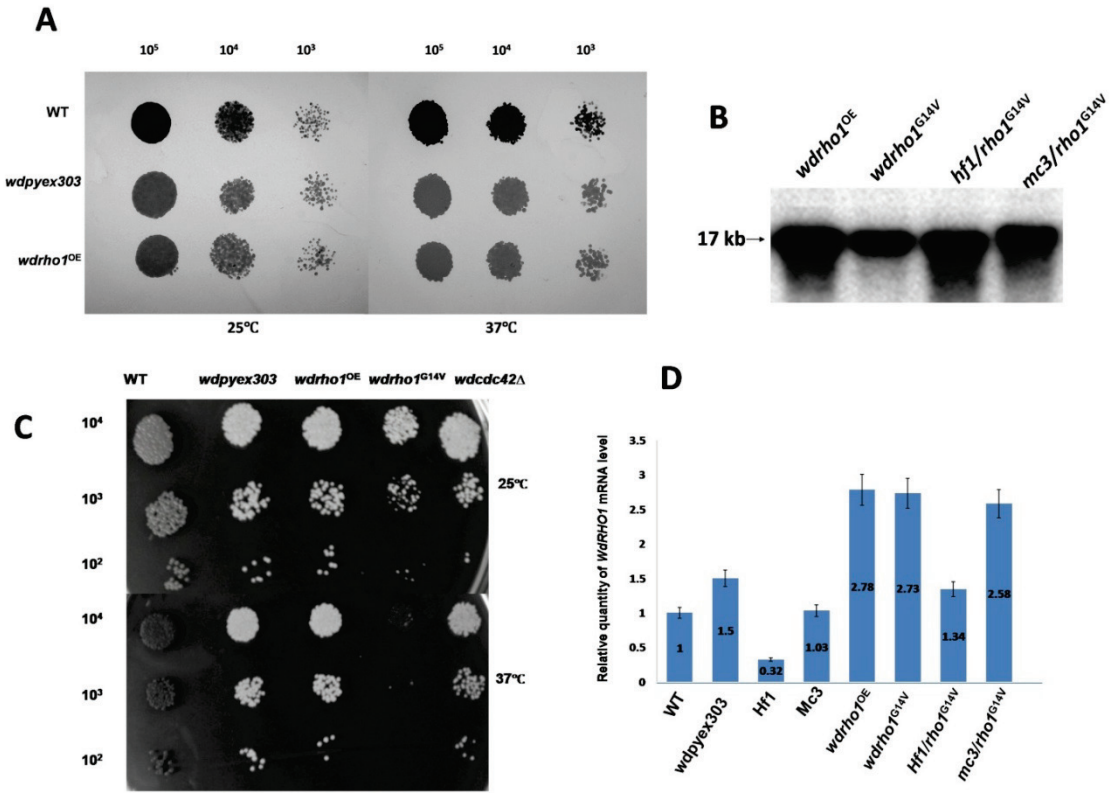

Fig. 4.3.6. Cellular morphology and colony morphology of the overexpression mutant *wdrho1*^{G14V}. Left: Cellular morphology of the control strain *wdpyex303* and the *wdrho1*^{G14V} mutant with the overexpressed constitutively active form of WdRho1p. DIC images (a, c, e and g) of cells of *wdpyex303* (a, b, e, and f) and *wdrho1*^{G14V} (c, d, g and h) stained with Calcoflour white and DAPI (b, d, f, h). In each case, cells ($1x10^7$ cells/ml) grown at 25℃ were transferred to fresh 25℃ (upper panel) or pre-warmed 37℃ (lower panel) YPMaltose broth and then sampled and observed microscopically in a time-course manner. The cells shown were sampled after culture for 48 h and photographed at the same magnification with visible or fluorescent light using a 40 x objective lens. The bars in each image represent 10 µm. **Right:** Comparison of colony morphology of control strain *wdpyex303* and constitutively active WdRho1p overexpression mutant strain *wdrho1*^{G14V} on YPMaltose agar medium after incubation at 37℃ for 4 days.

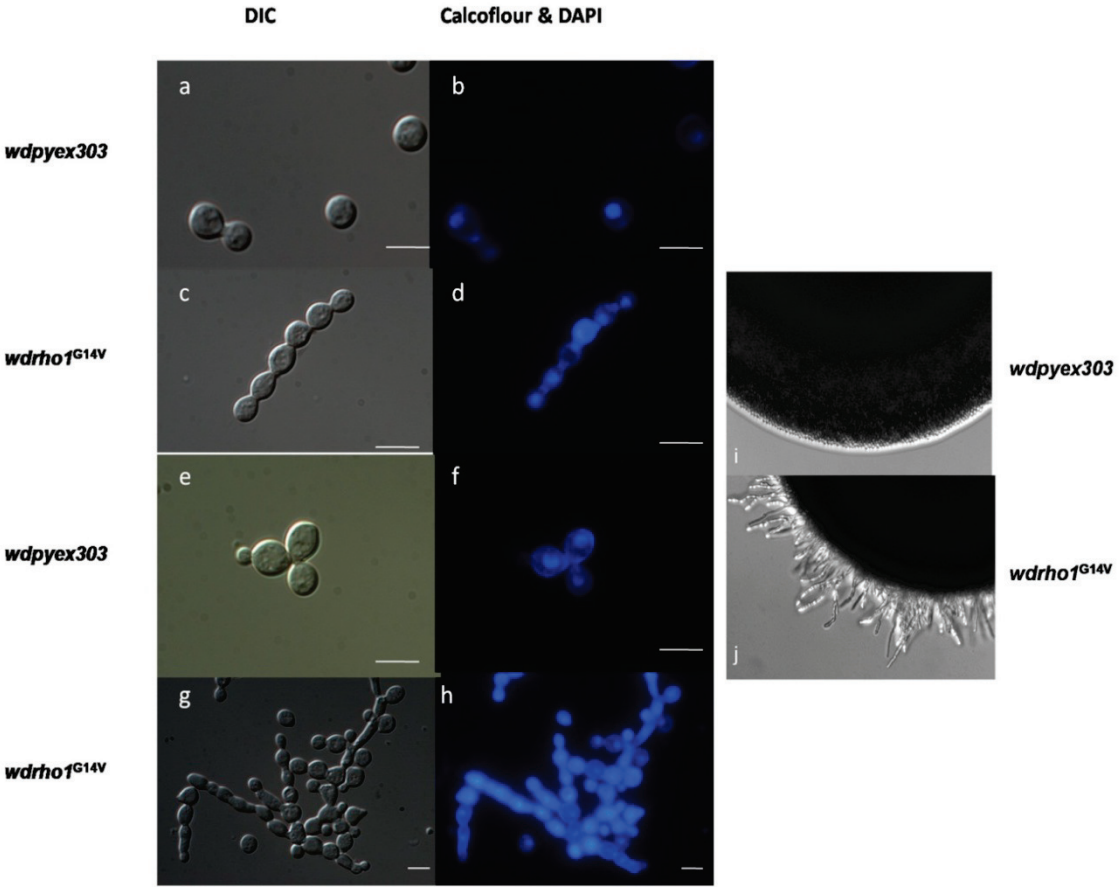

fuzzy edge whereas the negative control mutant *wdpyex303* showed a smooth colony edge. Furthermore, when the fuzzy edge of a *wdrho1*^{G14V} colony was picked and examined microscopically, it contained cells of the pseudohyphal type and not of the true hyphal type (Fig. 4.3.6. right panel).

4.36 Overexpression of the constitutively active form of Rho1p in the *wdrho1*^{G14V} mutant inhibits the true hyphal growth.

In *C.albican*, the switch between pseudohyphae and true hyphae can be regulated under the expression level of transcription factor gene *UME6* (Carlisle, et al., 2008). To investigate if the pseudohyphal growth caused by *wdrho1*G14V allele is associated with reduced true hyphae formation, I evaluated the effects of overexpression of the constitutively active WdRho1p on hyphal growth in *W. dermatitidis*. On starch agar medium, a widely-used glucose limitation and hyphae-inducing medium, the *wdrho1*^{G14V} mutant was observed to have dramatically reduced hyphal growth at both 25°C and 37°C compared to the *wdpyex303* negative control strain (Fig. 4.3.7). On PDA, a well known nitrogen-poor, hyphae-inducing and conidia-inducing medium, a similar reduction in true hyphae formation was observed (data not shown). These results suggest that the constitutively active WdRho1p negatively regulated the production of polarized true hyphal growth and may genetically interact with Ume6p.

Fig. 4.3.7. Effect of overexpression of the constitutively active form of WdRho1p on hyphal growth in the wild-type strain. The control strain *wdpyex303* and constitutively active WdRho1p overexpression mutant strain *wdrho1*^{G14V} were grown on a starch agar medium (induces hyphal growth in the wild-type strain) at 25℃ or at 37℃. Samples were observed microscopically in a time-course manner. All cells are shown at the same magnification with visible light using a 10x objective lens.

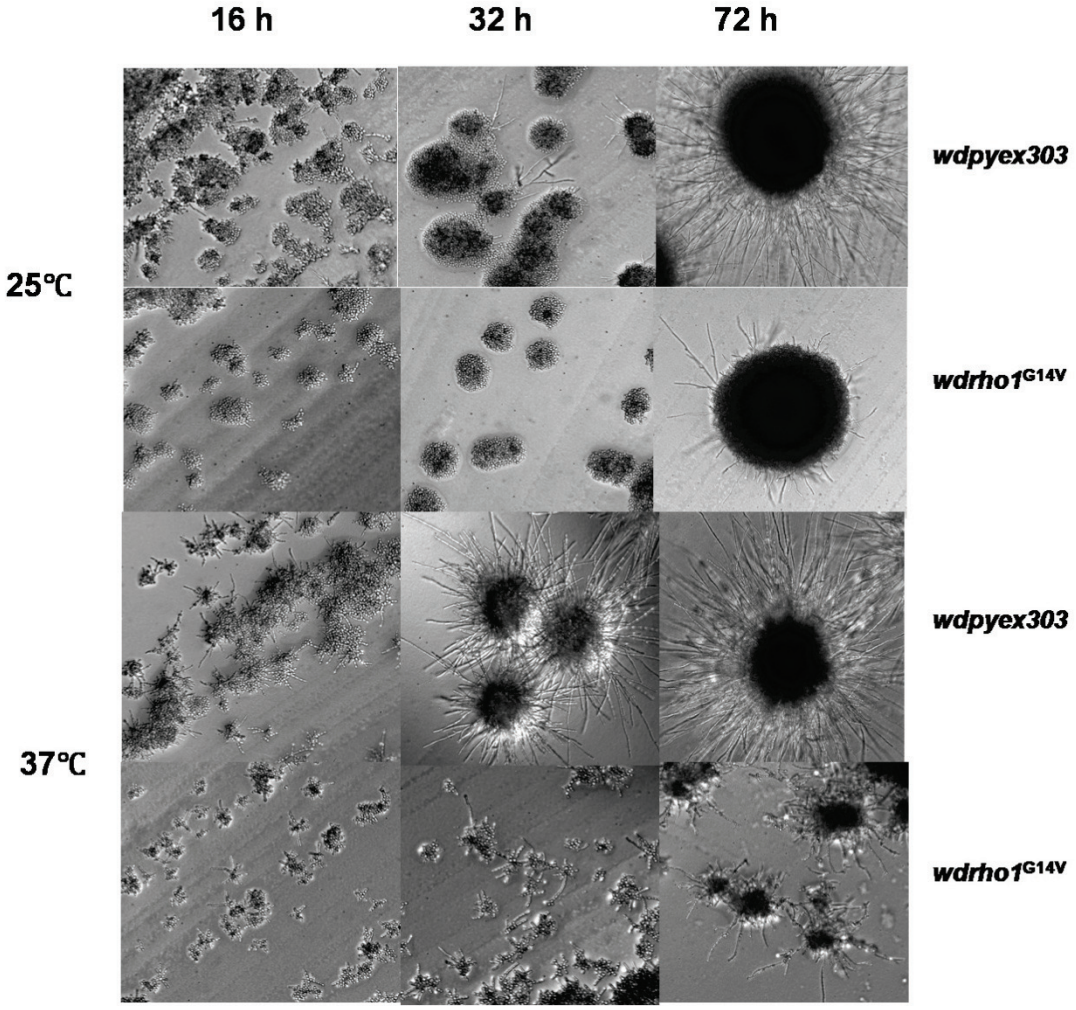

4.37 Ectopic overexpression of mutant allele *wdrho1*^{G14V} in the *W. dermatitidis* ts mutants Hf1 and Mc3 (*wdcdc2*) has different effects.

The two existing temperature-sensitive morphological mutants Hf1 and Mc3 (Abramczyk, et al., 2009) were chosen to generate double mutants that would overexpress the constitutively active form of WdRho1p. The Hf1 ts mutant behaves like wild-type at 25°C, but displays increased filamentous true hyphal growth when incubated in YPDB at 37°C (Fig. 4.3.8A). In contrast, the Mc3 ts mutant can be induced to form isotropically enlarged, so called sclerotic cells, planate cells and sclerotic bodies, depending upon whether they have no internal septa, one internal septum or multiple internal septa respectively, when incubated at 37°C in YPDB (Fig. 4.3.8A). The ectopic overexpression vector pPG1003 was introduced into the Hf1 and Mc3 to generate strains *hf1/wdrho1*^{G14V} and *mc3/wdrho1*^{G14V} respectively. After Southern blotting analysis confirmed the ectopic integration of pPG1003 into *WdPKS1* (Fig. 4.3.5B, lane 3 and 4 from left), I characterized the growth pattern of the double mutant *hf1/wdrho1*^{G14V}. To my surprise, the growth rate did not show the expected variation when compared to the Hf1 ts mutant at either 25°C or 37°C (Fig. 4.3.8B). This result indicates that the mutation in the Hf1 ts mutant may block the signal transduction by the active GTP form of WdRho1p of downstream effectors. To further investigate if the induced hyphal growth at 37°C in Hf1 can be inhibited by the overexpression of

constitutively active WdRho1p, I inoculated the Hf1 and *hf1/wdrho1*^{G14V} onto the surface of YPMaltose agar plate medium and incubated both at 37°C for seven days. The colony morphology showed retarded hyphal growth in the *hf1/wdrho1*^{G14V} mutant (Fig. 4.3.8C). The cellular morphology of the *hf1/wdrho1*^{G14V} mutant in YPMaltose broth medium also displayed pseudohyphal growth both at 25°C and 37°C (Fig. 4.3.8D). This was especially apparent at 37°C, when Hf1 displayed its characteristic temperature-induced filamentous true hyphal growth, whereas the *hf1/wdrho1*^{G14V} mutant produced the pseudohyphal form. These results reflect the fact that the temperature-induced hyphal growth in the Hf1 ts mutant can be inhibited by the overexpression of the *wdrho1*^{G14V} allele. Furthermore, the above observations provide additional evidence to support the idea that the active GTP form of WdRho1p negatively regulates polarized true hyphal growth. More interestingly, the hyphal growth induced on the starch medium was not inhibited by overexpression of *wdrho1*^{G14V} allele in the *hf1/wdrho1*^{G14V} mutant (Fig. 4.3.9). One possible explanation for this is that with the Hf1 mutant, the starch-induced hyphal growth results from a different mechanism than that producing the temperature-induced hyphal growth. In addition, I postulate that the signaling pathway controlling growth rates shares a common intermediate signaling molecule, which is mutated in Hf1 ts mutant, with the carbon-poor-induced hyphal growth signaling pathway and that this signaling molecule brings about its effect downstream of WdRho1p in the signaling pathway.

Fig. 4.3.8. Effect of overexpression of the constitutively active form of WdRho1p on cell growth and morphological development in strain Hf1. **(A)** Diagrams of development of ts mutants Hf1 and Mc3 after shift from 25ºC to 37ºC: note the WT strain remains yeast-like at 37ºC. **(B)** Hf1 and hf1/*wdrho1*^{G14V} were spotted with 10^4, 10^3, 10^2 cells on YPMaltose agar medium, and then incubated at both 25ºC and 37ºC for 48 h. **(C)** Comparison of colony morphology of control strain Hf1 and the constitutively active WdRho1p overexpression mutant strain *hf1/wdrho1*^{G14V} on YPMaltose agar medium after incubation at 37ºC for 7 days. **(D)** Cellular morphology of Hf1 and the constitutively active WdRho1p overexpression mutant strain *hf1/wdrho1*^{G14V}. DIC images (a, c, e and g) of cells of Hf1 (a, b, e, and f) and *hf1wd/rho1*^{G14V} (c, d, g and f) stained with Calcoflour white and DAPI (b, d, f, h). In each case, cells ($1x10^7$ cells/ml) grown at 25ºC were transferred to fresh 25ºC (upper four panels) or pre-warmed 37ºC (lower four panels) YPMaltose broth and then sampled and observed microscopically in a time-course manner. The cells shown here were sampled after culture for 48 h and photographed at the same magnification with visible light or fluorescent light and a 40x objective lens. The bars in each image represent 10 μm.

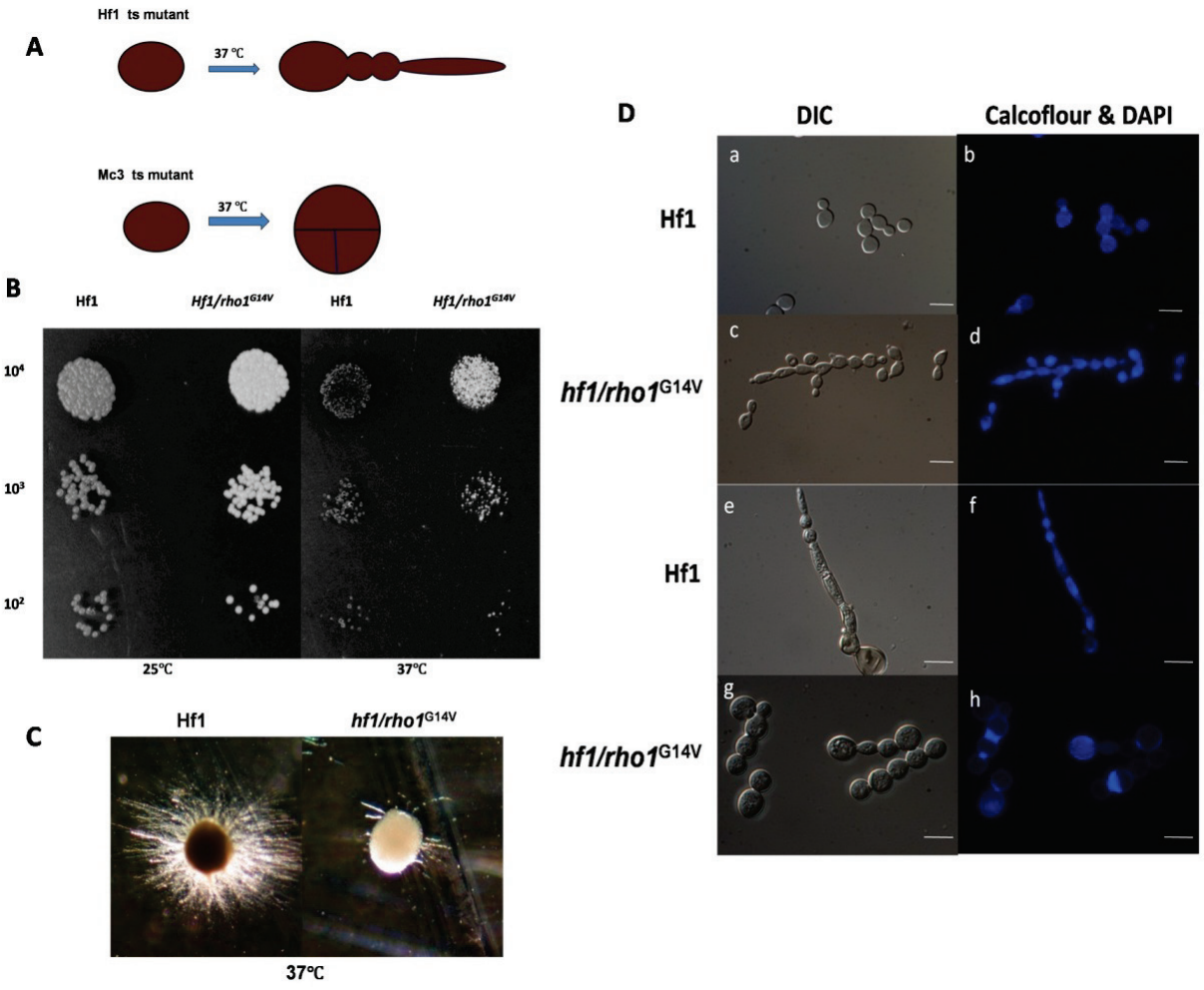
A
Hf1 ts mutant
37 ℃
Mc3 ts mutant
37 ℃
B
Hf1
Hf1/rho1G14V
Hf1
Hf1/rho1G14V
10⁴
10³
10²
25℃
37℃
C
Hf1
hf1/rho1G14V
37℃
D
DIC
Calcoflour & DAPI
Hf1
hf1/rho1G14V
Hf1
hf1/rho1G14V
a
b
c
d
e
f
g
h

Fig. 4.3.9. Effect of the overexpression of the constitutively active form of WdRho1p on hyphal growth in the ts Hf1 strain. The control strain Hf1 and constitutively active WdRho1p overexpression mutant strain *hf1/rho1*^{G14V} were grown on a starch agar medium at 25℃ or at 37℃. Samples were observed microscopically in a time-course manner. All cells are shown at the same magnification with visible light using a 10x objective lens.

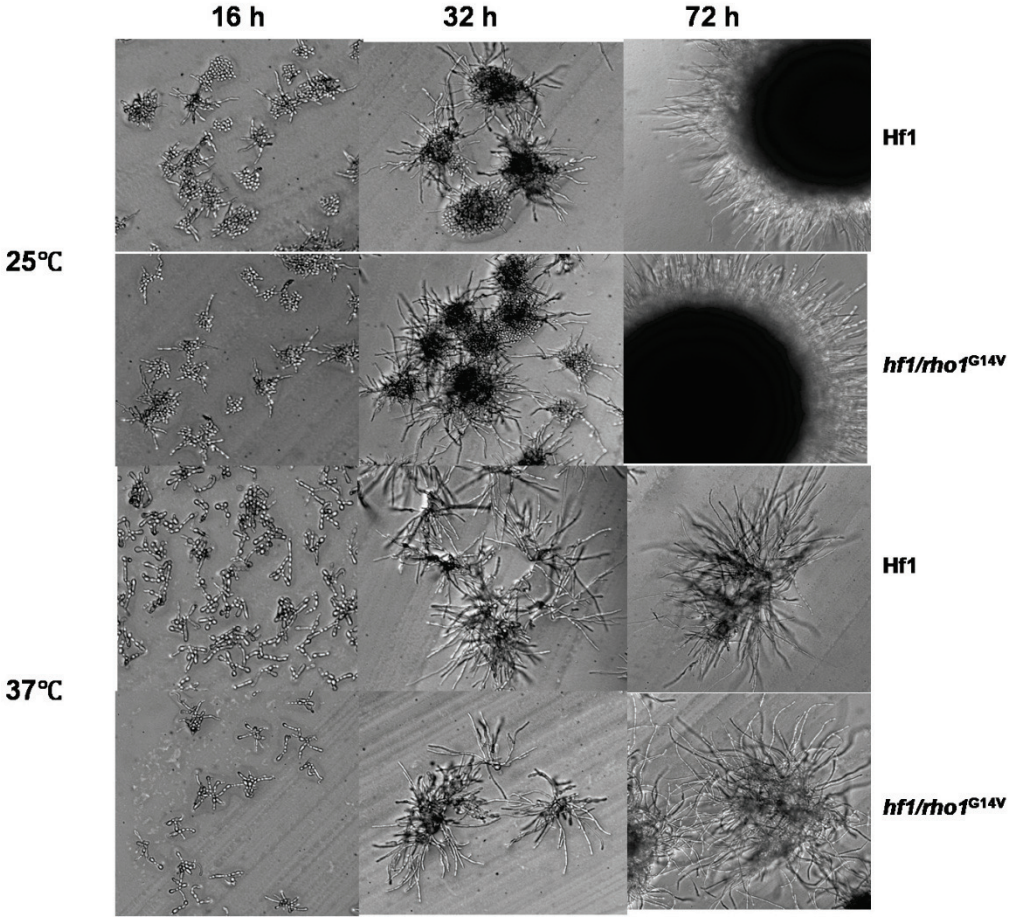

However, when I overexpressed the constitutively active form of WdRho1p in the Mc3 ts mutant, the growth pattern of the *mc3/wdrho1*^{G14V} mutant was different than that of the *hf1wd/rho1*^{G14V} mutant. Although there was no obvious change in the growth rate at 25°C, the dilution spot growth assay results showed that the growth rate of the *mc3/wdrho1*^{G14V} mutant at 37°C decreased (Fig. 4.3.10, left). When I investigated the cellular morphologies of the cells that developed at 37°C, the planate cells of the *mc3wd/rho1*^{G14V} mutant showed a larger size and a shape that was less spherical than that of the typical sclerotic forms produced by the Mc3 ts mutant at 37°C (Fig. 4.3.10, right), suggesting that overexpression of the constitutively active WdRho1p may promote cell expansion by speeding up cell wall synthesis. On hypha-inducing starch medium, the Mc3 ts mutant showed true hyphal growth at 25°C, but inhibited hyphal growth at 37°C, whereas the *mc3/wdrho1*^{G14V} mutant displayed reduced hyphal growth at 25°C and pseudohyphal growth at 37°C (Fig. 4.3.11). Finally when I examined the fuzzy edge of the *mc3wd/rho1*^{G14V} mutant colonies at 37°C on starch media, only pseudohyphae and neither moniliform nor true hyphae were observed (data not shown).

4.38 Overexpression of the constitutively active form of WdRho1p in the *WdCDC42* knock-out strain significantly reduced growth.

The GTPases Cdc42p and Rho1p both belong to the Rho GTPase protein family. In *S. cerevisiae*, knock outs of *CDC42* or *RHO1* are lethal. In *W. dermatitidis,*

Fig. 4.3.10. Effect of overexpression of constitutively active form of WdRho1p on cell growth and morphological development in the ts strain Mc3. Left. Mc3 and *mc3/rho1*^{G14V} were spotted with 10^4, 10^3, 10^2 cells on YPMaltose agar medium, and then incubated at both 25℃ and 37 ℃ for 48 h. **Right.** Cellular morphology of Mc3 and constitutively active WdRho1p overexpressed in mutant strain *mc3/rho1*^{G14V}. DIC images (a, c, e and g) of cells of Mc3 (a, b, e, and f) and *mc3/rho1*^{G14V} (c, d, g and f) stained with Calcoflour white and DAPI (b, d, f, h). In each case, cells ($1x10^7$ cells/ml) grown at 25℃ were transferred to fresh 25℃ (top four panels) or pre-warmed 37℃ (lower four panels) YPMaltose broth and then sampled and observed microscopically in a time-course manner. The cells shown here were sampled after culture for 48 h and photographed at the same magnification with visible light or fluorescent light using a 40x objective lens. The bars in each image represent 10 µm.

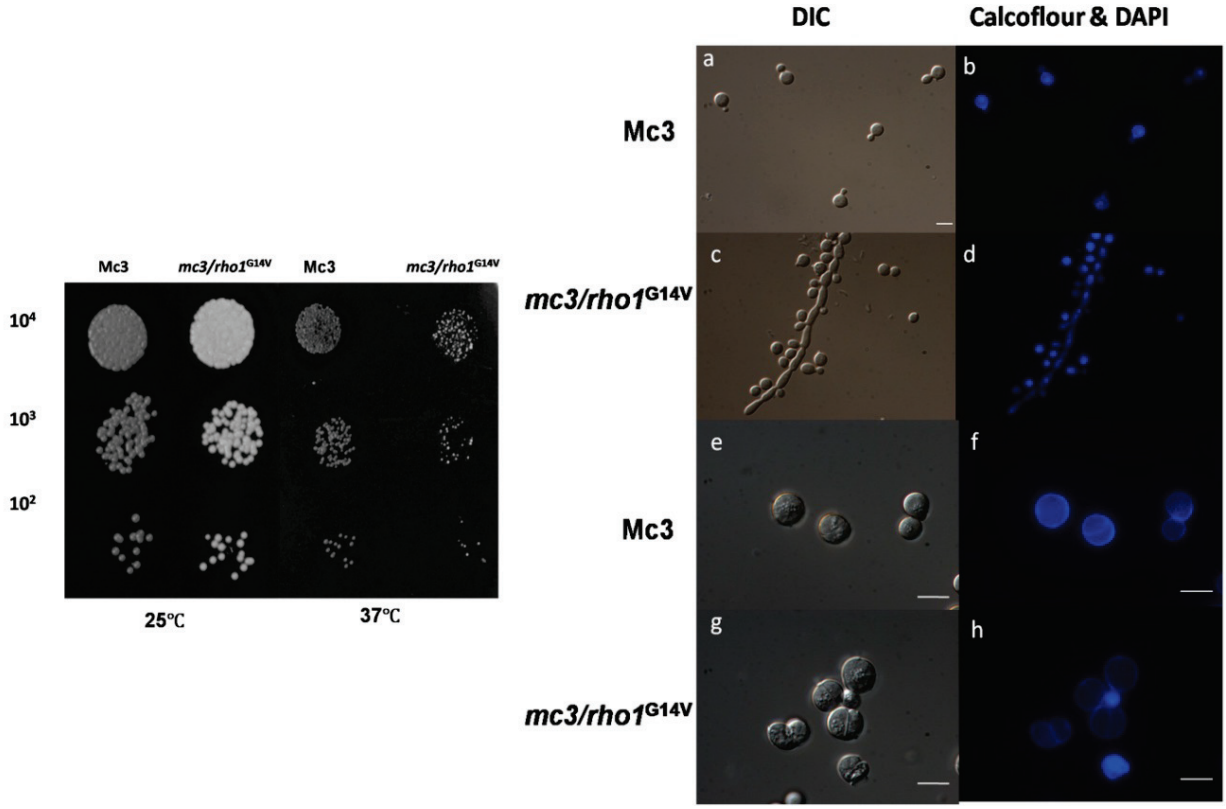

Fig.4.3.11. Effect of overexpression of the constitutively active form of WdRho1p on the hyphal growth in the ts Mc3 strain. The control strain Mc3 and the constitutively active WdRho1p overexpression strain *mc3/wdrho1*^{G14V} were grown on a starch agar medium at 25℃ or at 37℃. Samples were observed microscopically with visible light using a 10x objective lens in a time-course manner. All cells are shown at the same magnification.

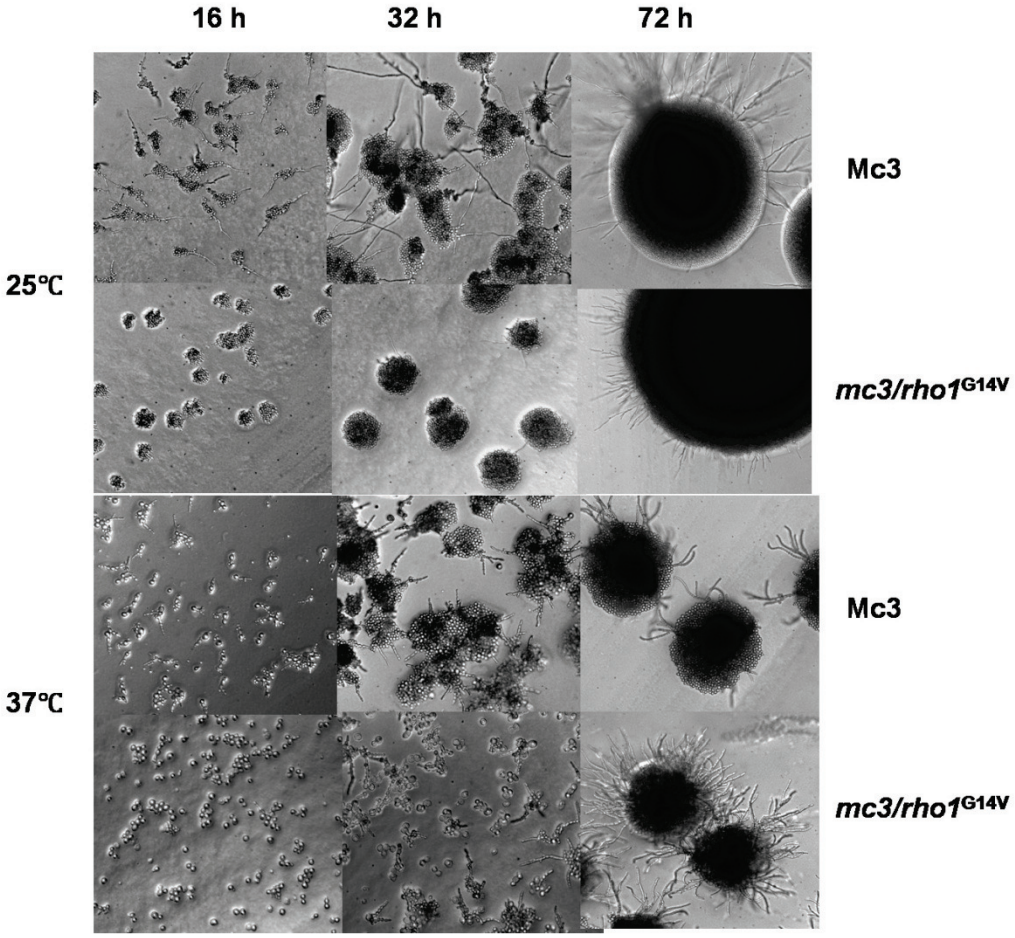

WdCDC42 knock out mutant is not only viable, but also displays a phenotype mostly identical to the wild-type, albeit with infrequent and slender planate cells (Ye, and P. J. Szaniszlo, 2000). The deduced amino acid sequences of the WdCdc42p and WdRho1p ORFs are both 193 amino acids and they also share several conserved domains. To investigate the genetic interaction between *WdCDC42* and *WdRHO1*, the *wdrho1*^{G14V} allele was overexpressed in the *WdCDC42* knock-out strain, after Southern blotting analysis confirmed the target-specific integration (Fig. 4.3.12A). Realtime RT-PCR analysis confirmed that *WdRHO1* mRNA was overexpressed ectopically from the integrated pPG1003 construct and that the mRNA level of the glucan synthase gene *WdFKS1* remained constant (Fig. 4.3.12B). Dilution spot growth assay results revealed extremely slow growth patterns for the double mutant at both 25°C and 37°C (Fig. 4.3.12.C). When I screened the transformants nine days after the linearized pPG1003 plasmid was introduced into the *wdcdc42*Δ mutant, no albino colonies of even the smallest size were observed, whereas colonies of the wild type were normally visible after two to three days (data not shown). The cellular morphology of the *wdcdc42*Δ/*wdrho1*^{G14V} double mutant revealed an elongated cell shape with small bud tips (Fig. 4.3.12D): the cells seem to have difficulty in enlarging the bud, a situation similar to that seen when yeast cells are inhibited in growth by severe Ca^{2+} limitation (Szaniszlo et al., 1993; Karrupayal and Szaniszlo, 1997). Moreover, the filamentous

Fig. 4.3.12. Effect of overexpression of the constitutively active form of WdRho1p on cell growth and morphological development in the *WdCDC42* knock out strain. **(A)** Southern blotting analysis of the *wdrho1*^{G14V} mutant allele over-expressed in the *WdCDC42* knock-out strain. After the DNA of *wdcdc42*Δ/*wdrho1*^{G14V} double mutant was digested with *Bam*HI and separated by electrophoresis in a 0.8% agarose gel, the resulting fragments were identified with the radiolabled the *WdPKS1* probe 1. **(B)** The relative abundance of *WdRHO1* mRNA was analyzed by realtime PCR. Cells of *wdcdc42*Δ and *wdcdc42*Δ/*wdrho1*^{G14V} were incubated in YPD broth at 37°C until log phase. Total RNA (2 μg) was reverse transcribed into cDNA. Primers used in the real-time RT-PCR were specific for *WdFKS1* and *WdRHO1*. The *wdcdc42*Δ/*wdrho1*^{G14V} double mutant showed higher levels of *WdRHO1* mRNA expression at 37°C. The error bars indicate the standard diviations among the percentages **(C)** Mutants *wdcdc42*Δ, *wdrho1*^{G14V} and *wdcdc42*Δ/*wdrho1*^{G14V} were spotted with 10^4, 10^3, 10^2 cells on YPMaltose agar medium, and then incubated at both 25℃ and 37℃ for 48 h. **(D)** Cellular morphology of the double mutant *wdcdc42*Δ/*wdrho1*^{G14V} . DIC images of cells of *wdpyex303* (a), *wdrho1*^{G14V} (b), *wdcdc42*Δ (c) and *wdcdc42*Δ/*wdrho1*^{G14V} (d). In each case, cells ($1x10^7$ cells/ml) grown at 25℃ were transferred to fresh 25℃ YPMaltose broth and then sampled and observed microscopically in a time-course manner. The cells shown were sampled after culture for 72 h and photographed at the same magnification with visible light or fluorescent light using a 40x objective lens. The bars in each image represent 5 μm. **(E)** Effect of overexpression of constitutively active WdRho1p on hyphal growth in the *WdCDC42* knock out strain. Cells of *wdpyex303* (e), *wdrho1*^{G14V} (f), *wdcdc42*Δ (g) and *wdcdc42*Δ/*wdrho1*^{G14V} (h) were grown on a starch agar medium at 25℃ for 72 h. Samples were observed microscopically. All cells are shown at the same magnification with visible light using a 10x objective lens

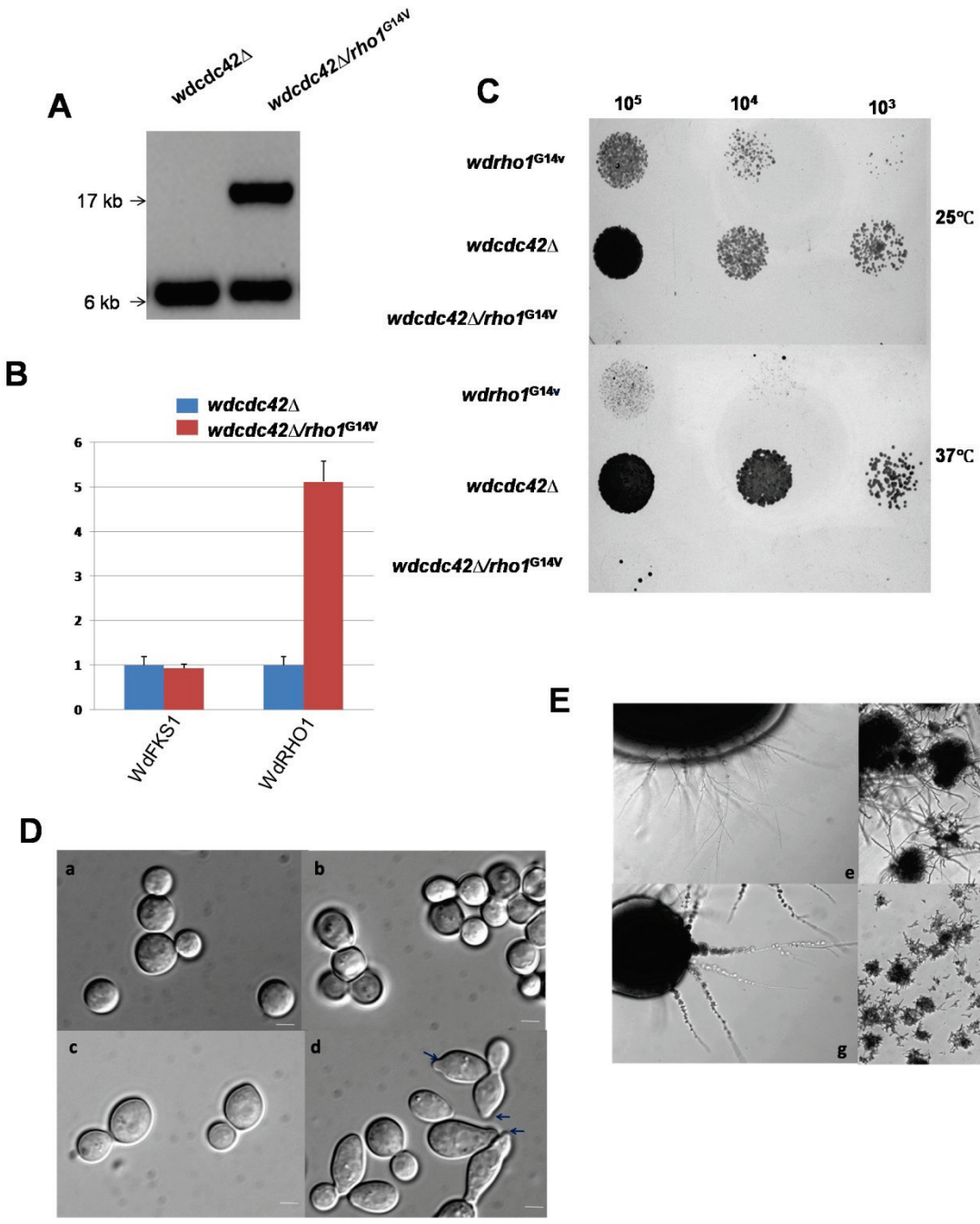
A
wdcdc42Δ
wdcdc42Δ/rho1G14V
17 kb
6 kb
B
wdcdc42Δ
wdcdc42Δ/rho1G14V
6
5
4
3
2
1
0
WdFKS1
WdRHO1
C
10^5
10^4
10^3
wdrho1G14v
wdcdc42Δ
wdcdc42Δ/rho1G14V
25℃
wdrho1G14v
wdcdc42Δ
wdcdc42Δ/rho1G14V
37℃
D
a
b
c
d
E
e
f
g
h

growth of the *wdcdc42*Δ/*wdrho1*^{G14V} mutant was very poor, which may due to the dramatically retarded growth rate (Fig. 4.3.12Eh). Considering the unaffected growth rate of the *wdcdc42*Δ knock out mutant (Ye, and Szaniszlo, 2000) and the slow growth of the *wdrho1*^{G14V} mutant, the amplified effect of overexpression of the constitutively active WdRho1p on the growth rate of the *wdcdc42*Δ mutant may indicate that the GDP form WdRho1p or it downstream effectors substitute for Cdc42p during the budding process and that a partial functional overlap exists between WdRho1p and WdCdc42p functions.

4.4 DISCUSSION

The discovery that GTP can activate β-(1,3)-glucan synthase activity was first documented in *S. cerevisiae* and shortly thereafter in *W. dermatitidis* and a number of other fungi (Shematek, et al., 1980; Szaniszlo, et al., 1985; Kang, et al., 1986). These findings were then followed by the discovery that the Rho1p GTPase of *S. cerevisiae* is able to regulate glucan synthase activity through exchange of GTP and GDP (Drgonova et al., 1996; Qadota et al., 1996). However, other than the investigations of the role of Rho1p in the cell wall *β*-1,3-glucan synthesis, Rho1p has been studied mainly with an intense and extensive focus on the responses of Rho1p to stimuli, its regulation of cytoskeletal rearrangements, and its importance to morphogenesis, motility, and cytokinesis. In *S. cerevisiae* and *S. pombe* (Arellano, et al., 1997; Levin, 2005), the

RHO1 knockout and the constitutively active form of Rho1p overexpression are lethal, whereas in *Yarrowia lipolytica* and *Fusarium oxysporum,* the *RHO1* disruption strains are viable (Nonaka, et al., 1995; Leon, et al., 2003; Martinez-Rocha, et al. 2008). In this study, I explored the role of the small GTPase WdRho1p in the cellular development and polymorphic transitions of the black filamentous and condidiogenous fungal pathogen of humans *W. dermatitidis*.

The *WdRHO1* fragment was amplified by degenerate PCR, which generated three different size products. After TA cloning into the pGEMT vector, all three PCR products were sequenced and blasted in the GenBank database. One of the fragments was a homolog of *RHO1* and the other two fragments showed homology to *RHO2* and *RHO4* (data not shown). A subsequent gene knock out experiment led me to conclude the essentiality of *WdRHO1*. Several lines of evidence support this conclusion. First was my inability to isolate a single strain with *WdRHO1* disrupted, even after numerous attempted gene knock out transformations. Second was my success with relative ease in knocking out *WdRHO1* in a synthetic diploid strain. Further evidence came from the fact that the MBC-induced haplodization never produced a haploid strain in which the *WdRHO1* gene was replaced by homologous recombination. All these results lead me to suggest that *WdRHO1* is a single copy essential gene in *W. dermatitidis*.

Overexpression of the *rho1*$^{+}$ allele in *S. pombe* causes the production of larger cells, with aberrant cell separation and septum abnormality (Arellano, et al., 1996). Although the overexpression of the *wdrho1*$^{+}$ allele in *W. dermatitidis* did not produce a phenotype similar to the one reported for *S. pombe*, the *wdrho1*^{OE} mutant showed a growth pattern similar to that of the control strain *wdpyex303*, as well as to that of the wild-type strain. When I characterized the cellular morphology of the *wdrho1*^{OE} mutant, no multiple septa or loss of polarity were observed, again in the manner of *wdpyex303* and the wild-type strain. In *S. pombe*, overexpression of thr *rho1*$^{+}$ allele also causes the formation of thicker cell walls than those observed in the wild type (Arellano, et al., 1996). However, with *W. dermatitidis* I found it difficult to chraracterize the change on the cell wall caused by overexpression of the *wdrho1*$^{+}$ allele. This was because the overexpression strategy in *S. pombe* did not involve an additional gene disruption: the ectopic overexpression strategy in *W. dermatitidis* involved the disruption of the *WdPKS1* gene, which generates an albino mutant and thus may have additionally affected its cell wall composition, structure and integraty. In addition, while my realtime RT-PCR data showed that the disruption of the *WdPKS1* gene with the pYEX303 vector did not affect the mRNA expression level of *WdFKS1* gene, which encodes the catalytic subunit of glucan synthase, it did increased the mRNA level of *WdRHO1* (Fig. 4.3.5D). Thus with the *wdpyex303* and *wdrho1*^{OE} strains, although both had increased mRNA levels of *WdRHO1*, their growth rates did not change. Taken

together, I believe these results indicate that the WdRho1p needs to be activated to affect the growth rate of *W. dermatitidis*.

The *rho1*^{G14V} allele, which encodes a mutated protein that prevents the dissociation of GTP and arrests Rho1p in a constitutively active form, was determined to affect polarized growth and cell wall integrity in the ascomycetous yeasts *S. cerevisiae*, *S. pombe*, and the basidiomycetous yeast *C. neoformans* (Saka *et al*., 2001; Arellano, et al., 1996; Chang and Penoyer, 2000; Kohno, et al., 1996). Similarly in *W. dermatitidis*, my results suggest that the *wdrho1*^{G14V} allele, unlike the *wdrho1*$^{+}$ allele, plays a significant role in cellular development and polarity determination. Also, the overexpression of the constitutively active form of WdRho1p slows down its rate of growth, even though the GTP form of Rho1p activates glucan synthase and promotes cell wall synthesis. As reported for *S. pombe*, the expression of the constitutively active *rho1*^{G15V} causes cell lethality (Arellano, et al., 1996). The reason why it is not lethal in *W. dermatitidis*, when the *wdrho1*^{G14V} allele is overexpressed, may be due to the fact that the *glaA* promoter is not a highly inducible promoter in this particular fungus. Furthermore, I can't exclude the possibility that other Rho-type GTPases are probably activated by the active WdRho1p to maintain viability. From my Realtime RT-PCR data, expression levels of WdRho1p increased only about three fold compared with that of wild-type (Fig. 4.3.5D). Nonetheless, the changed ratio between the GDT and the GTP form of WdRho1p produced several obviously different phenotypes, which

allowed me to study the functional role of WdRho1p in *W. dermatitidis*. Since the *W. dermatitidis* wild-type cells grow slightly faster at 37°C than 25°C (see for example Roberts and Szaniszlo, 1978) and the active GTP form of Rho1p retards its rate of growth, I assume that in wild-type cells less of the GTP form of Rho1p is present at 37°C than is present at 25°C. The production of yeast cell clusters by the *wdrho1*^{G14V}, mutant, which I assumed to be pseudohyphae because they appear to be in reality simply to be end-to-end attached, but polarized, individual yeast cells, indicates an abnormal and impaired cell separation function.

In filamentous fungi, the mechanism of switching between pseudohyphae and true hyphae is under intense investigation (Wang and Szaniszlo, 2007; Liu, et al., 2008). The production of pseudohyphal growth indicates the maintenance of polarity and the retardation of true hyphal growth. As expected, the overexpression of the *wdrho1*^{G14V} allele in *W. dermatitidis* retarded true hyphal growth when incubated on hyphal-inducing starch medium. A similar trend was documented in *A. nidulans*, in which the overexpression of constitutively active Rho1p causes reduced germ tube formation (Guest, et al., 2004). Nonetheless, the overexpression of dominant negative allele *wdrho1*^{D122A} in *W. dermatitidis* did not result in an aberrant phenotype (data not shown). Additional characterizations are needed to investigate this particular functional role of WdRho1p.

The initial observation of the similar growth rate of the *hf1/wdrho1*^{G14V} double mutant and Hf1 (Fig. 4.3.8B), suggests that the Hf1 ts mutant possesses a mutated gene product, which may stop another signal from activating WdRho1p. The unchanged trend of hyphal growth in the *hf1/wdrho1*^{G14V} mutant (Fig. 4.3.9) provides additional evidence for this hypothesis. However, the *hf1/wdrho1*^{G14V} mutant produces true hyphae or moniliform hyphal morphotype swithching to the pseudohyphal morphotype switch at 37°C on YPMaltose broth (Fig. 4.3.8D). It is also inhibited in true hyphal growth at 37°C on YPMaltose agar (Fig. 4.3.8C). Therefore, to more precisely characterize the role of the *wdrho1*^{G14V} allele, the overexpression of *wdrho1*$^{+}$ allele in Hf1 was investigated as the control. The double mutant *hf1/wdrho1*^{OE} did not display the switch of true hyphae to pseudohyphae with elevated temperature in the YPMaltose medium (data not shown). Although a *mc3/wdrho1*^{OE} control mutant may have brought more detailed insights of genetic interaction between Mc3 ts mutation and *WdRHO1,* I failed to obtain that double mutant, probably because the transformation efficiency with Mc3 mutant is extremely low (P.J. Szaniszlo, personal communication). Nonetheless, and based on the above observation, I suggest that the carbon source limitation-induced true hyphal growth pathway has a different, or partially different, signal transduction pathway than that of the temperature stress-induced hyphal growth pathway that is altered in the Hf1 ts mutant. I further suggest that the mutated gene product in Hf1 may be involved both in a signaling pathway regulating growth rates and a carbon source poor, inducing-hyphal growth pathway. However the related observations were very

different in the Mc3 mutant background. While the ts mutated gene product in Mc3 only blocks the signal from active WdRho1p in growth rate regulation at 25°C, the suppression effect of active WdRho1p was observed in *mc3/wdrho1*^{G14V} both at 37°C and in the carbon-poor-inducing starch medium (Fig. 4.3.10 and 4.3.11).

The level of expression of the filament-specific transcription factor UME6 in *C. albican* was recently reported to determine the production of either pseudohyphal growth or true hyphae growth (Carlisle, et al., 2009). The dominant pseudohyphal growth associated with overexpression of the *wdrho1*^{G14V} allele may indicate there is a regulatory connection between WdRho1p and UME6p in *W. dermatitidis*. Moreover, it is interesting to note that although I observed a reduced mRNA level of *WdRHO1*in the Hf1 mutant and an increased mRNA level of *WdRHO1* in the *hf1rho1*^{G14V} mutant using realtime RT-PCR, the growth patterns of the Hf1 and *hf1rho1*^{G14V} mutant were similar. One possible explanation for this is that a blocking of the signal transduction from an active WdRho1p results in the down regulation of *WdRHO1* gene expression, which in turn may indicate that *WdRHO1* expression is regulated by a feedback loop. Other possibilities no doubt exist and more experiments are needed to clarify the mechanism.

Although the *wdcdc42*Δ/*wdrho*^{G14V} double mutant derived in this study exhibits a supressed budding process and a greatly retarded growth rate, the recently obtained *wdcdc42*Δ/*wdrho*$^{+}$ control mutant displayed a growth rate similar to that of the

*wdcdc42*Δ mutant. However, the *wdcdc42*Δ/*wdrho*$^{+}$ mutant still showed the clustered cell pattern, which is similar to that of the *wdrho*^{G14V} mutant, but not like that of the *wdcdc42*Δ mutant (data not shown). Considering that the *wdrho*$^{+}$ mutant did not display the clustered pseudohyphal morphology, the loss of WdCdc42p may have caused a changed balance between the speed of yeast cell budding and yeast cell separation. In addition, recent investigations of Pxl1p suggest that Cdc42p and Rho1p *S. cerevisiae* possibly compete with each other during budding (Gao, et al., 2004). This is in agreement with my previous assumption that the WdRho1p has a partial functional overlap with WdCdc42p during budding. Nonetheless, the mechanism governing the precise coordination of Cdc42p and WdRho1p during polarized budding growth is still blurred, even though these two Rho family GTPases are involved in related events.

4.5 SUMMARY

My studies of the WdRho1p GTPase of *W. dermatitidis* demonstrated its importance in regulating the growth rate and the yeast-to-true hyphal and yeast-to-pseudohyphal transitions in *W. dermatitidis*. Although possibly more than one Rho1p homolog exist in *Fusarium oxysporum* (Martinez-Rocha, et al., 2008), several lines of evidence support the essentiality of the *WdRHO1* homolog in *W. dermatitidis*. With the help of a site-specific mutagenesis and ectopic overexpression system, I was able to characterize the

functional role of WdRho1p, in spite of the fact that a gene replacement study was not applicable. In the end, this study resulted in a focus more on the mechanisms of polarized hyphal growth, which is a key element in fungal pathogenicity (Madhani and Fink, 1998), than on the role of WdRho1 in cell wall synthesis as the regulatory component of glucan synthase. My results documented for the first time that the ectopic overexpression of the *wdrho1*$^{+}$ allele does not affect the growth rate of *W. dermatitidis*, whereas the constitutively active *wdrho1*^{G14V} allele slows growth and represses true filamentous hyphal growth by promoting pseudohyphal growth in this filamentous, but polymorphic, conidiogenous fungus. Also my results indicated that the overexpression of constitutively active WdRho1p is sufficient to control polarized hyphal biogenesis by promoting pseudophal growth. Other interesting results were observed with the Hf1 and Mc3 ts mutants, which suggested that the identification of the mutations responsible for the Hf1 and Mc3 phenotypes will extend our knowledge about fungal stress response signal transduction pathways in this pathogen. In addition, future investigations of the regulatory relationships among Ume6p, WdRho1p and the GEF proteins may reveal other subtle mechanisms for the regulation of morphological switching and its contribution to the pathogenicity of *W. dermatitidis* and other filamentous fungi.

Chapter 5: WdRac1p is the key protein regulating polarized hyphal growth and shares partial overlapping function with WdCdc42p in *Wangiella dermatitidis.*

5.1 INTRODUCTION

5.1.1 The function of the Rho-type GTPases.

Rho-type GTPase family members, including Cdc42, Rac, and Rho proteins, are signaling molecules. Like other Ras proteins, they act as molecular switches by transducing signals in the GTP-bound form, but not in the inactive GDP-bound form (Boguski and McCormick, 1993; Bourne, et al., 1991). Originally, the Rho-type family GTPases were thought only to play a role in the actin cytoskeleton organization (Hall, 1998; Hancock, et al., 1989; Ridley, 1994; Ridley, 1995; Symons, 1995; Tapon and Hall, 1997; Van Aelst and D'Souza-Schorey, 1997). However, recently evidence has emerged that indicates it has multiple roles in various vital cellular activities. These cellular processes include regulation of gene expression, activiation of kinase cascades, cell cycle controls, membrane trafficking, and induction of apotosis (Bazenet, et al., 1998; Block, et al., 1995; Chuang, et al., 1997; D'Souza-Schorey, 1997; Khosravi-Far,

et al., 1994; Minden, et al., 1995; Qiu, et al., 1995; Ridley, et al., 1995; Ridley, et al., 1992; Zohn, et al., 1998).

5.1.2 Cdc42p is essential for the polarized growth in fungi.

5.1.2.1 Cdc42p regulates polarisome assembly and actin organization.

In *S. cerevisiae*, Cdc42p plays crucial roles in the regulation of cell polarity by mediating the transfer of positional information to the morphogenetic machinery via the actin cytoskeleton and signal transduction (reviewed in Johnson, 1999). In *S. cerevisiae* and *S. pombe*, the *CDC42* gene is essential for cell viability (Johnson and Pringle, 1990; Miller and Johnson, 1994) The specific roles and the mechanism of Cdc42p action in the generation of hyphal polarity are poorly defined, although many Cdc42p target proteins have been identified. Localized and triggered activation of Cdc42p is required and crucial for polarized morphogenesis (Fig. 5.1.1B). In general, the GTP-bound and the GDP-bound forms of Cdc42p function differently and use different effectors to recruit components of the morphogenetic machinery. Specifically the GDP-bound form, but not the GTP-bound form of Cdc42p recruits effectors to form the polarisome in an expanding yeast cell bud (Fig. 5.1.1B), and possibly also in an elongating hyphal tip. Also, the GTP-bound form of Cdc42p triggers actin filament assembly and localization

Fig.5.1.1 Role of Cdc42p in the polarized growth. A. Cdc42p localizes to the bud tip and recruits effectors to promote apical growth. **B**. GDP form of Cdc42p recruits Msb3p/Msb4p, as well as Spa2p and Bni1p, to establish the polarisome, whereas the GTP-bound form of Cdc42p targets Gic1p/Gic2p to organize the actin cytoskeleton. (Modified from Mahlert, et al., 2006).

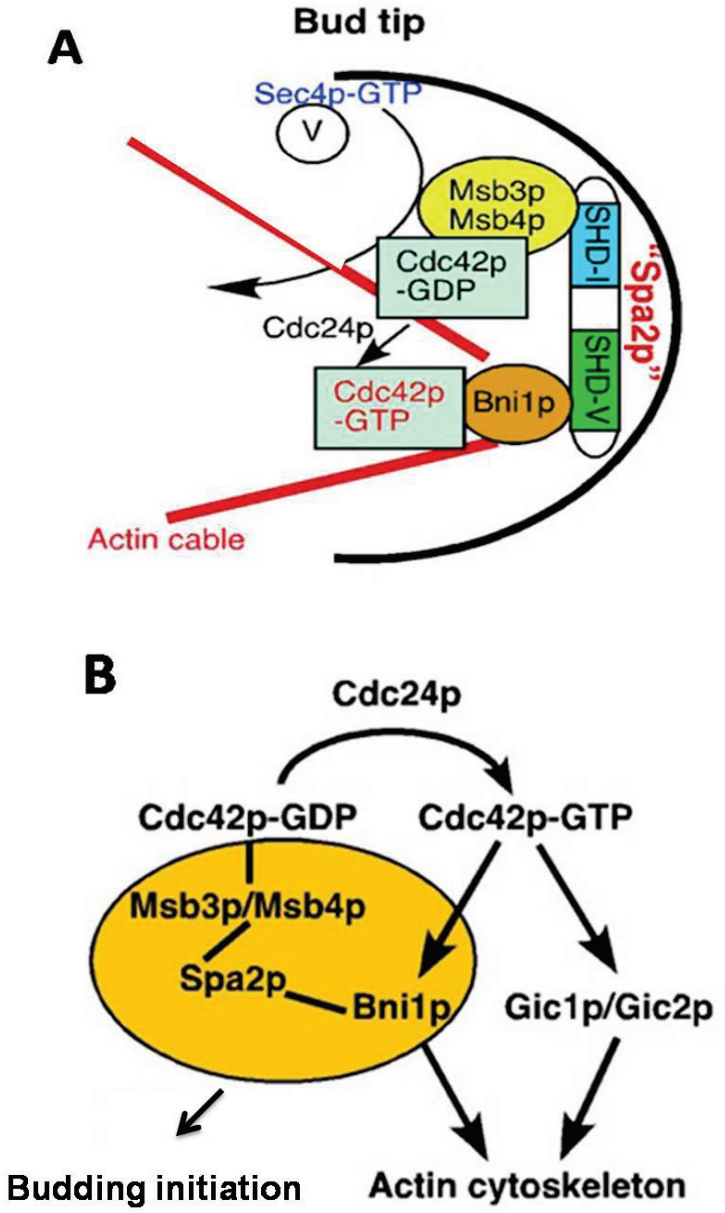

by affecting the conformation of the scaffold proteins WASP and formin (Rohatgi, et al., 2000; Alberts, 2001).

5.1.2.2 Cdc42p is involved in septin ring assembly.

Septins are GTP-binding proteins that possess a characteristic primary structure. Typical septins have a variable N-terminal region, a conserved core that includes the element of a GTP-binding site, and a variable C-terminal region. Septin monomers assemble into hetero-oligomeric (multi-septin) complexes (Fig. 5.1.2). In *S. cerevisiae* septins are assembled into a ring in a yeast mother cell before bud formation and remain there as a collar subjacent to the plasma membrane at the yeast mother-bud neck after a new bud emerges and grows during most of the yeast budding growth cycle. Although significant effort has been dedicated to deciphering the Cdc42p effector pathways important for actin polarization, little is known about how Cdc42p mediates septin ring assembly (Fig. 5.1.2). Several effectors of Cdc42p have been identified, including the p21-activated kinase (PAK)-like kinases Ste20p, Cla4p, and Skm1p, a formin family protein Bni1p, and Gic1p and Gic2p (Pruyne and Bretscher, 2000). Newer evidence shows that Cdc42p is required for the loading the septins to the septin ring complex (Gladfelter, et al., 2002; see Fig. 4.1.3).

5.1.3 Functional roles of Cdc42p in animal cell.

Fig.5.1.2. Model of the polymerization of septin complexes into paired, linear filaments in *S. cerevisiae*. End-to-end association of Cdc3 in one Cdc3–Cdc12–Cdc11 complex with Cdc11 in another complex yields filaments with a defined polarity; Cdc10 serves as a bridge to stabilize and pair the strands. (Modified from Versele and Thorner, 2005).

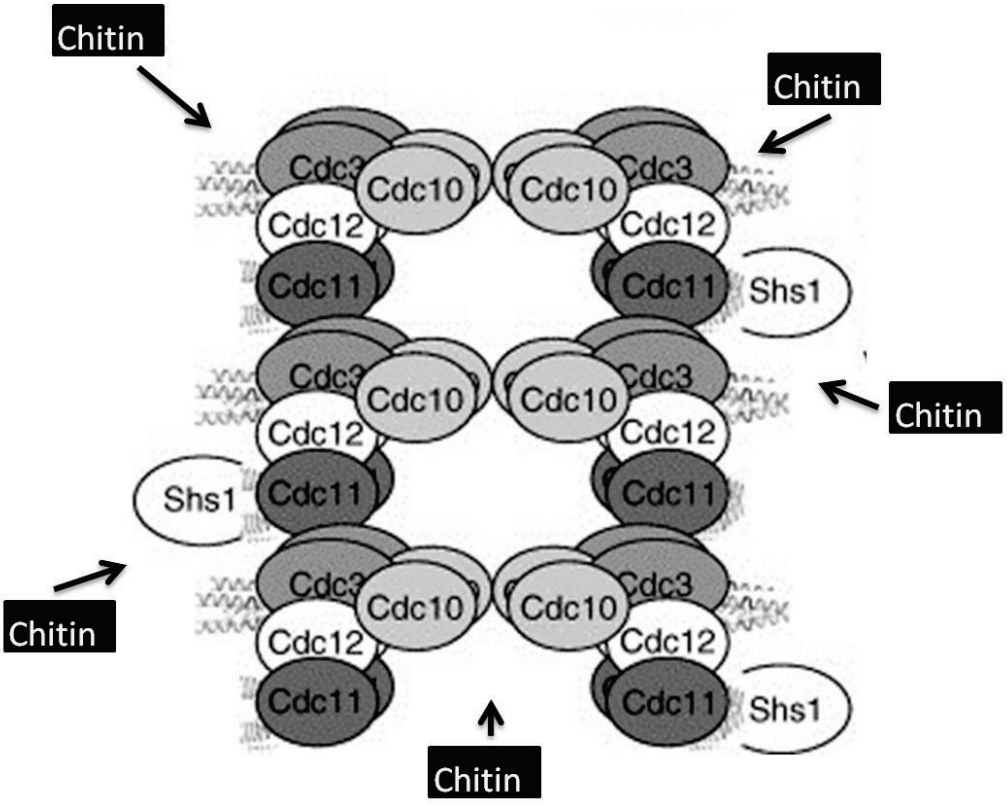

Fig.5.1.3. Model for the role of Cdc42p GTP hydrolysis in septin ring assembly in *S. cerevisiae*. GTP-bound Cdc42p (red) is proposed to bind to septin filaments (green) in a complex together with other assembly factors (blue). Interaction of the assembly complex with the ring is reversible. This model shows the importance of Cdc42p GTP hydrolysis in septin ring assembly. (Modified from Gladfelter, et al., 2002).

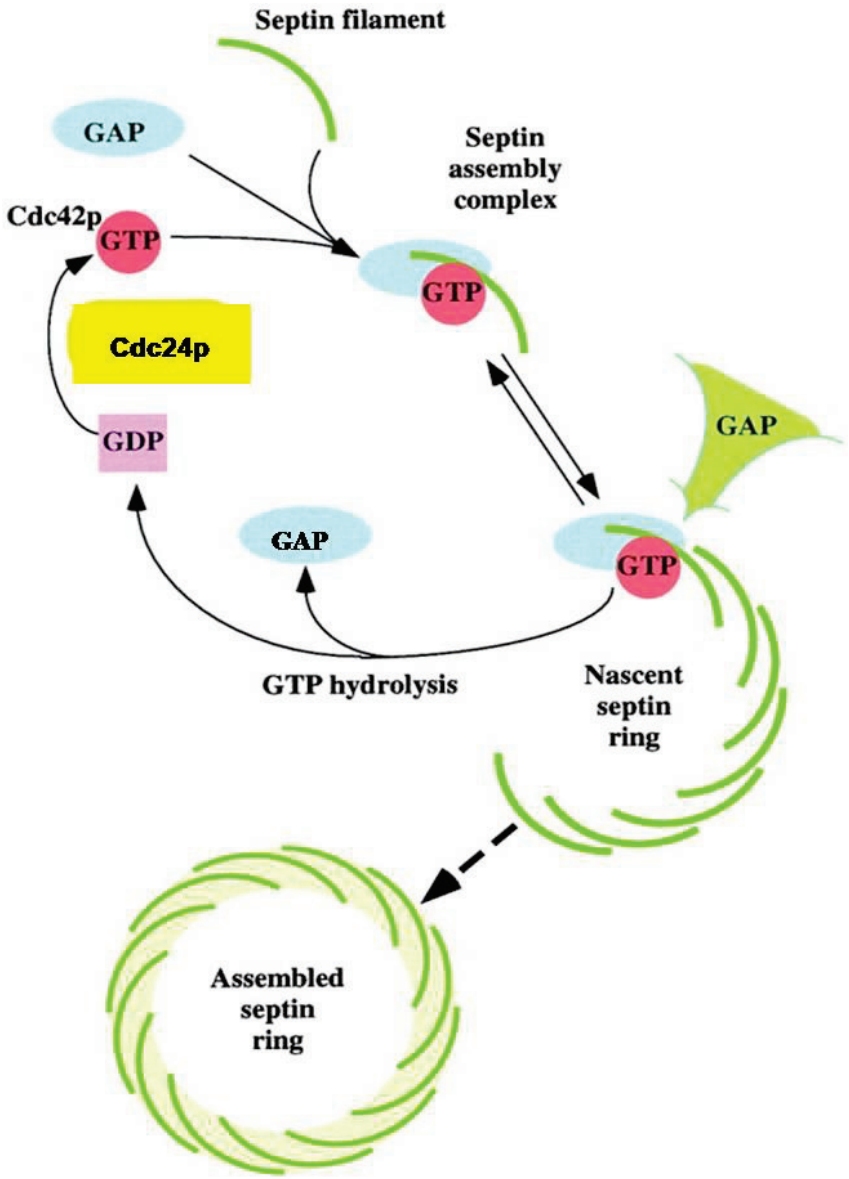

Cdc42p homologues and regulators have been studied in several other organisms, including humans. The biological functions for human Cdc42p are similar to those in *S. cerevisiae* and involve actin cytoskeleton reorganization (Nobes and Hall, 1995), and transcriptional activation through the JNK/SAPK signaling pathway (Minden, et al., 1995, Coso, et al., 1995). In addition, Cdc42p also modulates localized vesicle trafficking via the multiprotein exocyst (Zhang, et al., 2001).

5.1.4 Functional roles of Cdc42p in filamentous fungi.

Although filamentous fungi possess highly conserved homologues of Cdc42p, their specific role in the generation of hyphal polarity is poorly defined. The biological functions mediated by Cdc42p GTPase have attracted broad interest, although its mechanism of regulating cellular morphogenesis is still largely obscured. In *W. dermatitidis*, the finding that the deletion of a *CDC42* gene does not result in lethality in all organisms was first reported by Ye and Szaniszlo (2000). Subsequently other results have shown that the *CDC42* homolog is not essential in a number of other filamentous, conidiogenous fungi. Othe results with *W. dermatitidis* have shown that WdCdc42p is also not required for polarized hyphal growth and that the constitutively active form of WdCdc42p negatively regulates polarized true hyphal extensition (Ye and Szaniszlo, 2000). However, Cdc42p is required for the establishment of hyphal polarity in *Ashbya gossypii* and *C. albicans* (Wendland and Philippsen, 2001; Ushinsky, et al., 2002), both

of which are closely related to *S. cerevisiae*. Moreover, recent observations suggest that Cdc42p is only required for the maintenance of hyphal polarity in *Penicillium marneffei*, *Claviceps purpurea*, and *Colletotrichum trifolii* (Boyce, et al., 2001; Scheffer, et al., 2005; Chen, et al., 2006). Thus it remains possible that filamentous fungi may utilize Cdc42p-independent mechanisms to establish axes of cell polarity.

5.1.5 Functional roles of Rac1p and the relationship with Cdc42p.

Unlike the yeast species *S. cerevisiae* and *S. pombe*, in which Rac1p is missing, conidiogenous filamentous fungi possess both Rac1p and Cdc42p homologues. In *P. marneffei* and *Colletotrichum trifolii*, dominant mutations that lock Rac1p in a GTP- or GDP-bound state affect hyphal morphogenesis, suggesting a possible role in hyphal polarity maintenance (Chen and Dickman, 2004; Boyce, et al., 2003). Similarly in *Yarrowia lipolytica*, Rac1p is not essential for cell viability or actin organization but is required for hyphal growth (Hurtado, et al., 2000), whereas in *Cryptococcus neoformans* while Rac1p is not required for actin cytoskeleton organization, it is required for haploid filamentation and mating (Vallim, et al., 2005). In *C. albicans*, in contrast, a divergent Rac1p homolog is reported to be required for polarity establishment only under certain conditions, but it does not appear to share any detectable functional overlap with Cdc42p (Bassilana and Arkowitz, 2006). Interestingly in the basidiomycete *Ustilago maydis* Rac1p appears more important than

Cdc42p for the establishment of hyphal polarity, although analyses of double mutants imply that they share at least one function (Mahlert, et al., 2006). Thus in fungi, the functions of Cdc42p and Rac1p seem to vary considerably.

In addition to Cdc42p, animal cells use the related GTPase Rac1p to generate cell polarity. In general, Rac1p and Cdc42p appear to act in a sequential manner to direct the formation of cellular projections in migratory cells and neurons (Arimura and Kaibuchi, 2005). Both GTPases function within an interconnected web of signaling pathways (Wiggin, et al., 2005).

In *W. dermatitidis*, cells without WdCdc42p are viable and polarized hyphal growth is not inhibited. Since Rac1p does not exist in *S. cerevisiae* and recent evidence indicates it has a role in the polarized hyphal growth in filamentous fungi, I hypothesized that WdRac1p may share overlapping function with WdCdc42p and can complement the loss of function of WdCdc42p. Should this be true, then my research in this area was expected to increase our understanding of the subtle interaction between Rho-type GTPases by investigating the functional roles of WdRac1p and WdCdc42p and their interaction during fungal cellular development and differentiation.

5.2 MATERIALS AND METHODS

5.2.1 Strains, culture conditions.

The *W. dermatitidis* strains used in this research are listed in Table 4.1. Routine culture of *W. dermatitidis* was on YPD agar (YPDA) and in YPD broth (YPDB), as described previously (Liu et al., 2004). For the detection of the filamentous growth, *W. dermatitidis* was grown on SD minimal medium. The composition of SD broth was prepared as follow: 1% dextrose (or maltose), 0.17% Difco^{TM} yeast nitrogen base without amino acids and ammonium sulfate (Difco Scientific, Detriot, Mich.), 0.2% ammonium nitrate, and 0.1% asparagine (Sigma, USA). The pH was adjusted to 6.5.

5.2.2 Gene walking and cloning.

Gene walking from a 486-bp *WdRAC1* gene fragment (amplified previously by Xiangcang Ye, unpublished data) was carried out in two directions by using the DNA walking Speedup^{TM} premix kit (Seegene, Korea) with two sets of primers: 5' upstream walking primers; 5TSP1, 5'-TCATGGTGGATGGGAAACC-3', 5TSP2, 5'-ACGGGATTGACGAGCTGACA-3',5TSP3,5'-AGCGTGTTTGACGAGGCG-3'; 3' downstream walking primers: 3TSP1, 5'-CCTCGTCAAACACGCTTT-3', 3TSP2, 5'-TGTCAGCTCGTCAATCCCGT-3', 3TSp3, 5'- GGTTTCCCATCCACCATGAC-3'.

Table 5.1. Strains used in this research.

Strain	Genotype	Reference(s) or source
3u2m-428	*Mcm2/cdc1 mcm3/cdc2 met ura mel3 mel4*	Cooper and Szaniszlo, 1993
W. dermatitidis 8656	Wild type	ATCC 34100
*wdrac1*Δ*-d8*	*wdrac1*::*hph*	This study
wdpyex303	*wdpks1*::pYEX303-*hph*	This study
*wdcdc42*Δ	*wdcdc42*Δ::*sur++*	Ye and Szaniszlo, 2000
wdrac1^{OE}	*wdrac1 wdpks1*::pYEX303-*hph- wdrac1*$^{+}$	This study
wdrac1^{G16V}	*wdrac1 wdpks1*::pYEX303-*hph- wdrac1*^{G16V}	This study
*wdcdc42*Δ/ *wdrac1*^{G16V}	*wdcdc42*Δ::*sur++ wdrac1 wdpks1*::pYEX303-*hph- wdrac1*^{G16V}	This study
*wdcdc42*Δ/ *wdrac1*^{OE}	*wdcdc42*Δ::*sur++ wdrac1 wdpks1*::pYEX303-*hph- wdrac1*$^{+}$	This study
*wdcdc42*Δ/ *wdcdc42*^{G14V}	*wdcdc42*Δ::*sur++ wdpks1*::pYEX303-*hph-wdcdc42*^{G14V}	Ye and Szaniszlo, 2000
*wdcdc42*Δ/ *wdcdc42*^{OE}	*wdcdc42*Δ::*sur++ wdpks1*::pYEX303-*hph-wdcdc42*$^{+}$	Ye and Szaniszlo, 2000

*hph**: hygromycin resistance gene. *sur*++: sulfonylurea resistance gene.

^{OE} : Overexpression of wild-type allele

The PCR products generated by the gene walking were cloned in pGEM-T vector and sequenced by the Core Facility of Institute of Cellular and Molecular Biology, The University of Texas at Austin, using BigDye technology (Applied Biosystems, Foster City, CA). The locations of introns, first predicted in silico by alignments and by consensus splice sequences, were then confirmed by the comparison of the cDNA sequence produced by reverse transcription-PCR (RT-PCR) using the One-Step RT-PCR kit (QIAGEN, Valencia, CA) with the genomic DNA sequence. For the RT-PCR, RNA was extracted with hot acidic phenol from cells grown in YPDB for 24 h at 37°C and treated with RQ1 RNase-free DNase (Promega). After the RT-PCR was carried out, the amplification products were analyzed after electrophoresis in a 3% agarose gel together with 2-log DNA markers (New England Biolabs, Ipswich, MA) as references.

5.2.3 Disruption of *WdRAC1* gene.

To disrupt the *WdRAC1* gene, the 1.4-kb *hph* gene cassette was flanked by upstream and downstream with *WdRAC1* gene fragments using an overlapping PCR method (*pfx* high fidality PCR kit). The 495-bp upstream fragment of *WdRAC1* was amplified by PCR with the primers PRAC1U (5'-GCGCGGTGGTCTTTGCTC-3') and RAC1PCRUR (5'- AATAGAGTAGGATCCGACCGGGAACCCAGTTAACG TCGACCGTATCGATAAGCTTGATAATGAATTTCTCCCCCGTCACCACACAT-3'; the overlapping sequence with the *hph* gene is framed). The *hph* gene cassette was

amplified by PCR with the primer HPH-1(5'-CAAGCTTATCGATACGGTCG-3') and HPH-2 (5'- CCTCGAGGTCGACGTTAA-3'). The 426-bp downstream fragment of *WdRAC1* was amplified by PCR with primers PRAC1DF (5'-TGACCTCCACTAGCTCCAGCCAAGCCCAA AAAATGCTCCTTCAATATCAGTTAACGTCGACCTCGAGG ATAAAGCCACGGCCGATAG-3') and PRAC1DR (5'-TCGGGGAACACGTTGAAGA-3'). The resulting three PCR products were used as template to amplify a 2.3-kb fragment with the primers PRAC1U and PRAC1DR. The 2.3-kb fragment was then used to transform competent *W. dermatitidis* haploid and diploid yeast cells by electroporation as described previously (Ye and Szaniszlo, 2000). After transformants were selected on YPDA medium containing 50 μg/ml hygromycin B (Invitrogen, Carlsbad, CA), *wdrac1* mutants strains were identified by PCR and Southern analysis. The specific primers for the PCR screening were designed to amplify the *WdRAC1* and *hph* combined hybrid fragment (Fig. 5.3.3A) and had the following sequences: SRAC1D5R, 5'-TCCCAATACGAGGTCGCC-3'; SRHO1D3, 5'-AACCAATACGAGGTCGCC-3'. For Southern blotting analysis of the disruption mutant, DNA of wild-type strain Wd8656 and the mutant strain were digested with *Sal*I. After separation by electrophoresis in a 0.8% agarose gel, the resulting fragments were identified with the radiolabled *WdRAC1* probe 1.

5.2.4. Ectopic overexpression of *WdRAC1* in *W. dermatitidis*.

The site-specific, integrative expression vector pYEX303 was used for the overexpression of *wdrac1* alleles in the nonessential *WdPKS1* genomic locus of *W. dermatitidis*, as described previously (Ye, et al., 1999; Ye and Szaniszlo, 2000). The *WdRAC1* wild-type allele *wdrac1*$^{+}$ was amplified by RT-PCR (One-Step RT-PCR Kit; QIAGEN) with primers ORAC1F, 5'-GAAGATCTA*ATG*GCGCAAGCGACGCAG-3', and ORAC1R, 5'-TTTCTAGACCTAAAGAATGCTGCACCTCG-3' (the start and stop codons are indicated by italic letters, and the introduced *Bgl*II and *Xba*I restriction digestion enzyme recognition sites are underlined). To introduce the site-specific mutations, primer ORAC1G16V, 5'-GAAGATCTAATGGCGCAAGCGACGCAGTCAATAAAATGTGTGGTGACGGGG GATGGTGCTGTGGGAAAGACTTGT-3' (the mutant amino acid codon is framed) and primer ORAC1R were used to amplify the *wdrac1*^{G16V} mutant allele by PCR using the high fidelity *pfx* PCR system (Invitrogen). The PCR products were then cloned into pGEM-T vector to generate plasmids pPGRACA and pPGRACB. To clone the *WdRAC1* wild-type allele and constitutively active allele into the pYEX303 vector, pPGRACA and pPGRACB were digested with *Bgl*II and *Xba*I restriction digestion enzymes, after which the released fragments were ligated with the *Bgl*II- and *Xba*I-digested pYEX303 vector to generate pPG2001 and pPG2002 respectively. After being linearized by digestion with *Nar*I, the pPG2001 and pPG2002 plasmids were transformed site-specifically into the nonessential *WdPKS1* locus. After hygromycin

B resistant, white transformants of each type were isolated, Southern blotting was used to confirm the site-specific ectopic integration of each *WdRAC1* allele.

5.2.5 Nucleotide sequence accession number.

The sequence of *WdRAC1* was submitted to the GenBank database. The accession number is bankit 1358378 HM600809.

5.3 RESULTS

5.31 Cloning and chacterization of the *WdRAC1* gene of *W. dermatitidis.*

The *WdRAC1* gene encoding a putative Rho-like GTPase of *W. dermatitidis* was cloned by gene walking from a 486-bp PCR product, which was amplified from *W. dermatitidis* 8656 genomic DNA with degenerate primers derived from a conserved region of *RAC1* homologs of diverse fungi (Xiangcang ye, unpublished data). The gene walking extended the 486-bp sequence to 1652-bp, which included a 711-bp *WdRAC1* gene sequence (Fig. 5.3.1). The 594-bp open reading frame encoded a putative polypeptide of 197 amino acids with a predicted molecular mass of 21.7 kDa and a pI of 8.21. One 63-bp and one 54-bp intron was found by comparing the cDNA sequence

with the genomic *WdRAC1* gene sequence. When compared with the derived amino acid sequences of other *RAC1* genes in the GenBank databases, the deduced WdRac1p protein was found to be highly similar to most other Rho-type GTPases. The most similar homolog of WdRac1p was the Rac1 protein of the *Paracoccidioides. brasiliensis*, which was 96% identical in its derived amino acid sequence. Lower identities were shared with CnRho1p (79%) of the *C. neoformans*. Although the deduced polypeptide was found to have 197 amino acids, four amino acids more than WdRho1p and WdCdc42p, it did contain all of the consensus sequences that are conserved among the Rho-type GTPases. Multiple alignment of these Rac1p amino acids sequences displayed several conserved regions among all the Rac1p proteins (Fig. 5.3.2). The consensus elements GXXXXGK (GDGAVGK, residues 14 to 20, X for any amino acid) and DXXG (DTAG, residues 62 to 65) are present and are believed critical for interactions with the phosphate portion of GTP (Sanders, 1990). Conserved motifs are also present at regions implicated in interaction with the GTPase-activating protein (YIPTVFDNY, residues 35 to 43) (Sekine, et al., 1989) The CXXL (CSIL, residues 193 to 197) geranylgeranylation site is reported to be essential for the C-terminal prenylation and for membrane localization prior to biological activity (Hancock, et al., 1989; Ziman, et al., 1993). Also the conserved motif TKXD (TKLD, residues 119 to 123) is said to be responsible for nucleotide specificity in Rac1 (Delmer, et al., 1995).

5.32 *WdRAC1* is not an essential gene and does not play important roles in the growth patterns of *W. dermatitidis.*

To investigate the biological function of WdRAc1p in *W. dermatitidis*, I generated the loss-of-function *wdrac1*Δ allele in the haploid wild-type strain using a targeted gene replacement that deleted a 572-bp fragment inside the *WdRAC1* gene (Fig. 5.3.3A). Southern blot analysis of one of the transformants, *wdrac1*Δ-*5*, confirmed the replacement of a 1.2-kb *Bgl*I fragment, corresponding to the wild-type *RAC1* allele with a 2-kb fragment (Fig. 5.3.3B). The *WdRAC1* deletion mutant *wdrac1*Δ-5 was viable and showed a very similar phenotype to the wild-type strain when incubated in rich YPD medium (Fig. 5.3.5A). To investigate further the role of WdRac1p in true hyphal growth in *W. dermatitidis*, I used site-directed mutagenesis to generate a *wdrac1*^{G16V} gain-of-function allele, in which the conserved #16 amino acid G residue was changed to V, which prevents the hydrolysis of GTP to GDP and keeps the WdRac1p in the constitutively active form. For the ectopic overexpression study of WdRac1p, the color-selectable and site-specific integrative transformation system was again applied as previously described (Ye, et al., 1999; Ye and Szaniszlo, 2000). The wild-type allele *wdrac1*$^{+}$ and the constitutively active allele *wdrac1*^{G16V} were cloned under the regulation of promoter *glaA* (Fig. 5.3.3C). By introducing the linearized plasmid pPG2001and pPG2002 into the *W. dermatitidis* wild-type strain or the *WdCDC42* knock out strain, the plasmids targeted and disrupted the *WdPKS1* gene,

Fig. 5.3.1. Open reading frame (ORF) and predicted amino acid sequence of *Wangiella dermatitidis RAC1*. Two intron sequences are shown in the red. The start codon is shown in blue and the stop codon is also shown in red.

```
ACCGCTTCATTGACTGGGCACCCGCTCTGGGCGCCGTCAGCGGTGCACCAT  -510
CCCCAACTTTCAGCCTAGGCCTCCCTACGGACACTCCCGCCGGGCAGGCTG  -459
CGCGGTGGTCTTTGCTCCTCTTGCCGCCCCGGACCCTGAACCCTCTAGCCA  -408
ACTTGCCTCCTTGCCCCGATACAACCACTGGCACCGTGACCTGCTACCTGG  -357
TACCACTCACACTGCAGTAGCGTACGCCCCTTCTCACCTGCGCATGCTTTG  -306
TACAGCTCTGCGACTGCCCTGCTCCATACACCTGTCATTCCACTTGTGCCT  -255
ACTCCTATCGCCCTGCTTGATCCTCTCCCAGACTGCAGGCCTGCCTACCTC  -204
TGTCGTGCAACCATCGGGCCCTGTGGGCTTGTTGACTTTTACAGAGACGCG  -153
CCCAGTTGCTGGACACGGTTCGCGTCAACAGATCAACGCCTTGGCCAGCTT  -102
GACGCTGAGACGACAAAATCATCGCTCGGGAATTCTTGACGACAGAAGACT  -51
CGCCCCCGAGAAAGAGCAGCCTGCGTTTGCCCCAGATCCATCCTCACAGAC  0
      atggcgcaagcgacgcagtcaataaaatgtgtggtgacgggggat
      M  A  Q  A  T  Q  S  I  K  C  V  V  T  G  D
      ggtgctgtgggaaagacttgtttgctcatatcctataccacgaat
      G  A  V  G  K  T  C  L  L  I  S  Y  T  T  N
      gccttcccgggcgaatatatccctactgtctttgacaactactca
      A  F  P  G  E  Y  I  P  T  V  F  D  N  Y  S
      gctagtgtcatggtggatgggaaacccgtctctctgggattgtgg
      A  S  V  M  V  D  G  K  P  V  S  L  G  L  W
      gatactgctggtcaggaagactacgatagattgcggccctttca
      D  T  A  G  Q  E  D  Y  D  R  L  R  P  L  S
      tacccgcagacggacgtctttttgatatgcttttccattgtatct
      Y  P  Q  T  D  V  F  L  I  C  F  S  I  V  S
     cctcccagtttcgacaatgtcaaggcgaaaGTGAGCACCACTACC
     P  P  S  F  D  N  V  K  A  K
     CTATCTGCCTTGTTTACGGGATTGACGAGCTGACAGCCTGGCATT

     TAGtggtaccctgaaatc---------------------------
        W  Y  P  E  I
      gagcatcacgcccccggtgtgcccatcatcctcgtcggaaccaaa
      E  H  H  A  P  G  V  P  I  I  L  V  G  T  K
      ctggatttgagggacgataaagccacggccgatagtctgagggcg
      L  D  L  R  D  D  K  A  T  A  D  S  L  R  A
      aaaaaaatggaacctgtatcatacgagcaggcacttgctgtggcc
      K  K  M  E  P  V  S  Y  E  Q  A  L  A  V  A
      aaagaaattaaagcggtcaaatatctggagtgctccgcattgaca
      K  E  I  K  A  V  K  Y  L  E  C  S  A  L  T
      CaacgaaatctcaaaagcgtgtttgacgaagcgatcagGTAATAA
      Q  R  N  L  K  S  V  F  D  E  A  I  R
      ACCAACATTTATAGCAAATTTCACCACGGTGCTGACCTGCATTCT

      ---------------------------------- AGagccgta
                                            A  V
      cttaaccctcgaccaaccactacgaagaagaaatcgaggtgcagc
      L  N  P  R  P  T  T  T  K  K  K  S  R  C  S
      attcttag
      I  L  *
CAGTGTTTTTTGGGAGGCGACATTTTGGGTGTTCTTTTGGGATGGCAAGGG  762
GTTTCAGGGACGCATTGCAAAAAGGTGGACATAGACACTTTCACAGCTTCG  813
CTGCTTCGTCCTCCATCGTTCGCTCAACTTCAACTCCGACATAGGTGTGGT  864
TGAGATTGTAGAAGAGAATCTCTCCATCATACGAATAATAAATGAGCAATC  915
TAATTGGAAGAACGCACATTGACCGGAGGCGTTGAATCTTCAACGTGTTCC  966
CCGA                                                  1017
```

Fig. 5.3.2. Sequence alignment. **A.** Amino acid sequence alignment of Rac1p of *Wangiella dermatitidis* (WdRac1p) and the Rac proteins from *Paracoccidioides brasiliensis* (PbRac1p), *Aspergillus nidulans* (AnRac1p), *Neurospora crassa* (NcRho1p), *Drosophila melanogaster* (DmRac1), *Cryptococcus neoformans* (CnRho1p). **B.** Cladogram of the the Rac1p of fungi species

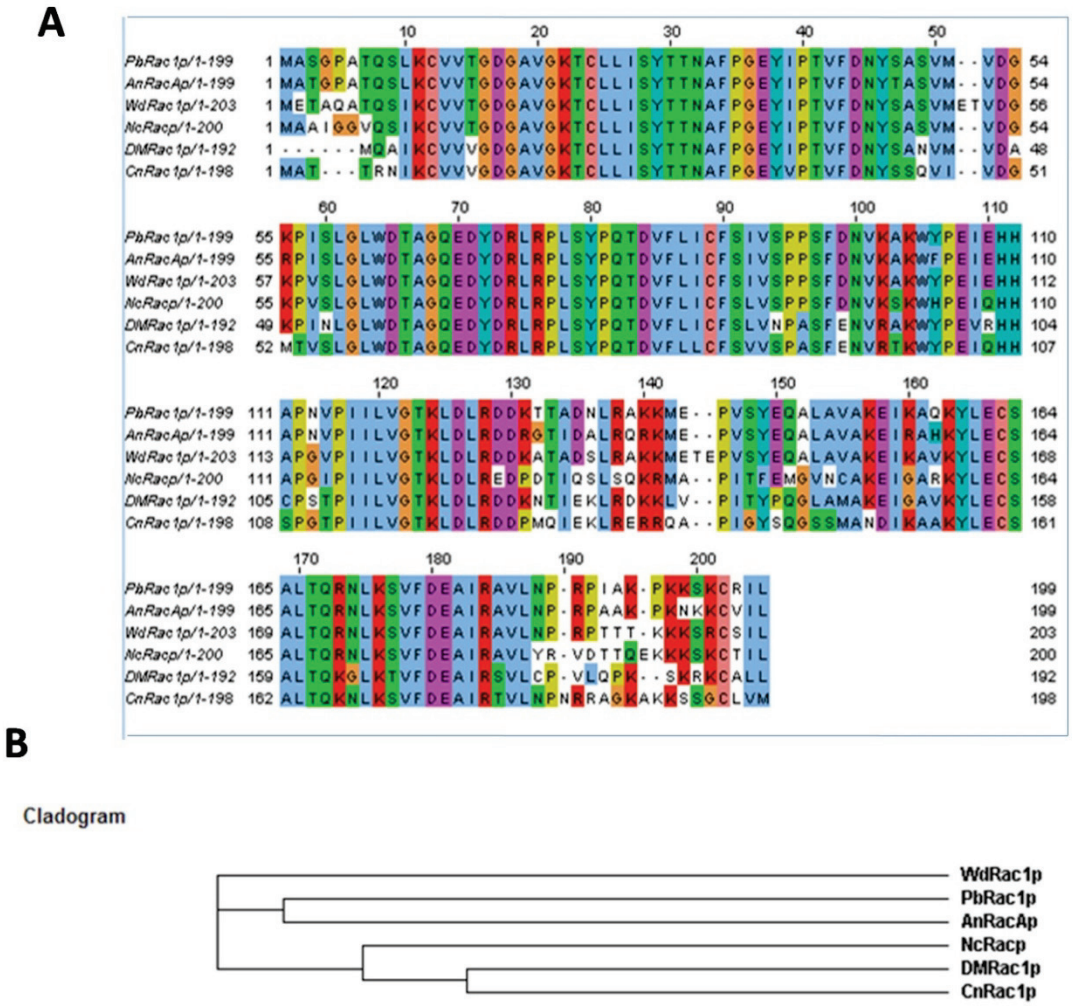

which to my knowledge only generates an albino cellular phenotype (Feng, et al., 2001). Hygromycin-resistant albino transformants were selected for the analysis. Southern blotting analysis of all of the resulting albino transformants revealed a 17-kb *Bam*HI-hybridizing fragment, confirming the presence in the *W. dermatitidis* genome of the newly integrated pPG2001 or pPG2002 plasmids that contained the functional *wdrac1*$^{+}$ or *wdrac1*^{G16V} alleles respectively (Fig. 5.3.3D). Realtime RT-PCR results then provided evidence for the overexpression of these *wdrac1* wild-type and mutant alleles (Fig. 5.3.4B). Results from a dilution spot growth analysis then showed that the growth rate of the *wdrac1*Δ-5 mutant was very similar to that of the wild type strain, as well as that of the overexpression mutant *wdrac1*^{OE} or the overexpression mutant *wdrac1*^{G14V}. Nonetheless, the *wdrac1*^{OE} and the *wdrac1*^{G14V} mutants showed slightly accelerated growth rates when incubated at 37℃ on YPMaltose agar plate medium (Fig. 5.3.4A). When I studied the cellular morphology of the *WdRAC1* mutants in YPMaltose broth medium at 37℃, the wild type, and the *wdrac1*Δ-5, *wdrac1*^{OE}, and *wdrac1*^{G16V} mutants all displayed similar cellular morphology, although *wdrac1*^{G16V} showed an elongated cell shape, whereas the *wdrac1*Δ-5 mutant was more sperical (Fig. 5.3.5A). The elongated cell shape of *wdrac1*^{G14V}, compared to *wdrac1*Δ-5 and *wdrac1*^{OE}, indicates that the active form of the Rac1 GTPase might be more polarized during yeast growth.

Fig. 5.3.3. Genetic manipulations of the *WdRAC1* gene. **(A)** Disruption of *WdRAC1* by replacement with a *hph* selection marker. The 1.4-kb *hph* gene cassette was flanked with upstream and downstream *WdRAC1* gene fragments by overlapping PCR. This fragment was cloned into pGEM-T easy vector and confirmed by sequencing to be properly oriented. The 2.3-kb fragment was released from the vector by restriction enzyme digestion and used for the gene knock out. **(B)** Southern blotting analysis of the *WdRAC1* disruption mutant *wdrac1*Δ-5 . DNA of wild-type strain Wd8656 and the *wdrac1*Δ-*5* were digested with *Bgl*I. After separation by electrophoresis in a 0.8% agarose gel, the resulting fragments were identified with a radiolabled *WdRAC1* probe. **(C)** Ectopic overexpression strategy after transformation of *W. dermatitidis* yeast cells with *WdRAC1* and its mutant alleles under the regulation of the *glaA* promoter. To obtain the *WdRAC1*over-expression plasmid, a 594-bp *WdRAC1* cDNA or the *wdrac1*^{G16V} fragment were cloned into plasmid pYEX303. After being linearized by digestion with *Nar*I, the plasmid was transformed site-specifically into the nonessential *WdPKS1* locus. **(D)** Southern blotting analysis of the *WdRAC1* overexpression mutant alleles:*wdrac1*^{OE} and *wdrac1*^{G16V}. DNA of the wild-type strain Wd8656, *wdrac1*Δ-*5*, *wdcdc42*Δ-*11*, *wdrho1*^{OE}, *wdrac1*^{G18V} and *wdcdc42*Δ/*wdrac1*^{G16V} were digested with *Bam*HI. After separation by electrophoresis in a 0.8% agarose gel, the resulting fragments were identified with the radiolabled *WdPKS1* probe 1.

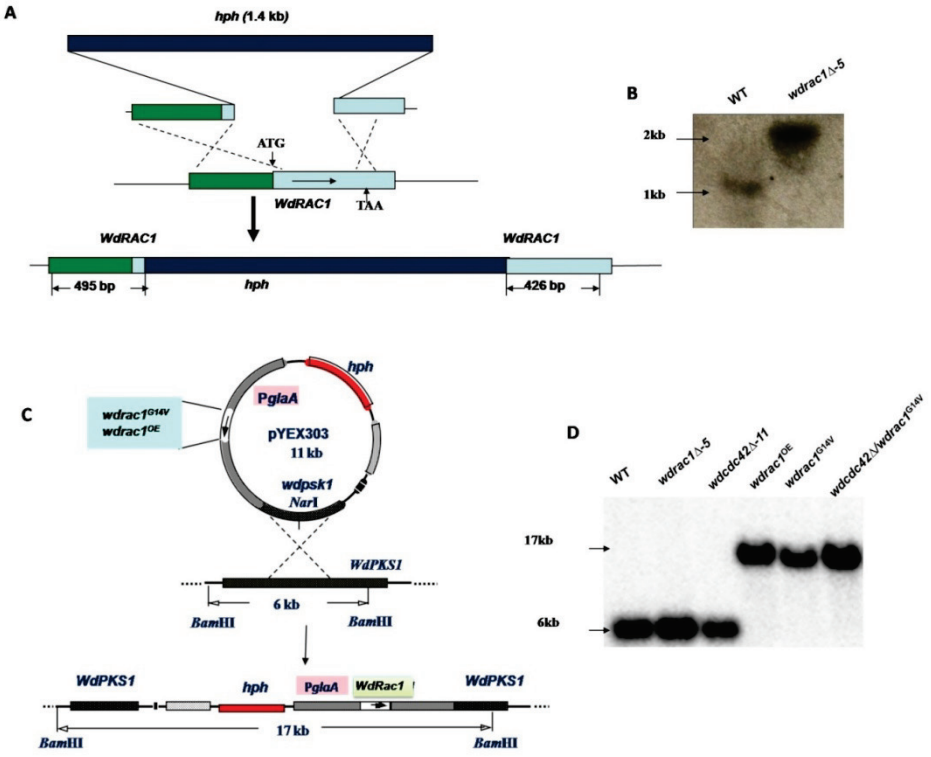

Fig. 5.3.4. Growth rates and expression analysis of the *WdRAC1* mutants. (A) The wild-type strain Wd8656, *wdrac1*Δ*-5*, *wdrac1*^{OE}, *wdrac1*^{G16V} and *wdcdc42*Δ/*wdrac1*^{G16V} were spotted with 10^5,10^4,10^3,10^2 cells on YPMaltose agar medium, and then incubated at both 25℃ and 37 ℃ for 48 h. (B) The abundance of *WdRAC1* mRNA in the *WdRAC1* mutants relative to that of the housekeeping gene *WdACT1* was calculated after real time PCR and is shown in the form of bars. The error bar in each bar indicates one standard deviation.

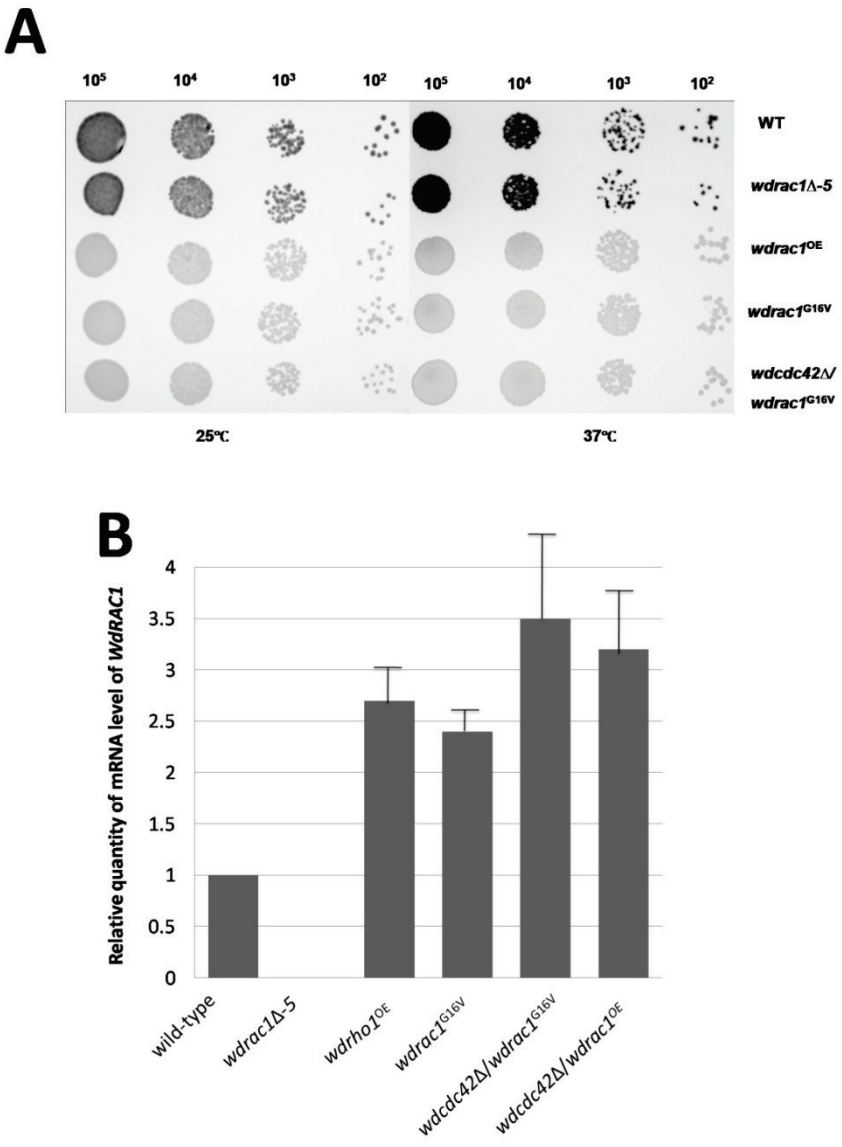

Fig. 5.3.5. Cellular morphology comparisions of the wild-type strain and the *WdRAC1* mutants *wdrac1*Δ-5, *wdrho1*^{OE}, and *wdrac1*^{G16V} grown in carbon-rich complete and minimal media. (A) Cells ($1x10^7$ cells/ml) grown at 25℃ were transferred to pre-warmed 37℃ YPMaltose broth and then sampled and observed microscopically in a time-course manner. The cells shown here were sampled after culture for 48 h and photographed at the same magnification with visible light or fluorescent light using a 40x objective lens. Calcoflour white staining was applied to all the samples. The bars in each image represent 10 μm. (B) Cells ($1x10^7$ cells/ml) grown at 25℃ were transferred to pre-warmed 37℃ broth minimal medium with maltose and then sampled and observed microscopically in a time-course manner. The cells shown here were sampled after culture for 72 h and photographed at the same magnification with visible light using a 40x objective lens. The bars in each image represent 10 μm.

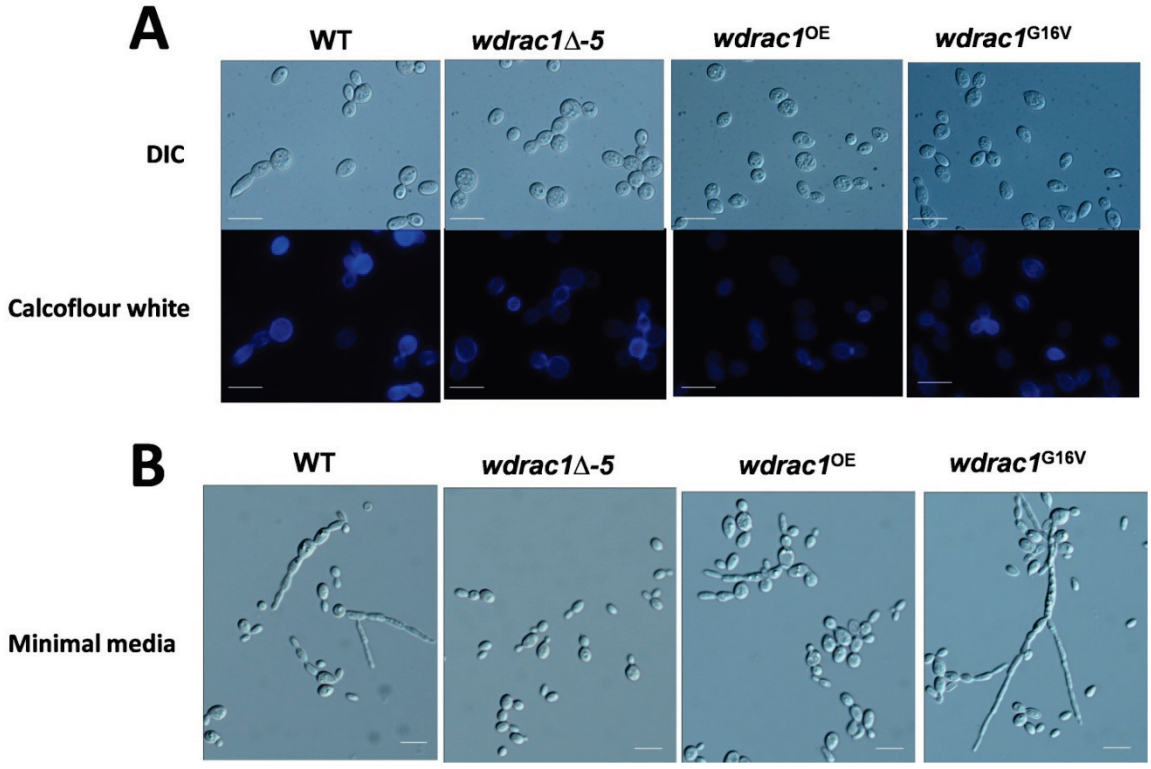

5.33 The *wdrac1* allele is required for the establishment of polarized true hyphal growth, but only in a nitrogen-poor minimal medium.

The more enlongated cellular morphology of *wdrac1*^{G16V} yeast cells in carbon rich YPMaltose media indicates that there was a role for the *wdrac1* alleles in true hyphal growth (hyphae with parallel side walls in optical section; Fig. 5.3.5A). In contrast, when the *WdRAC1* mutants were incubated in a carbon-rich minimal medium at 37℃ for 72 h and checked for true hyphal growth none was observed in *wdrac1*Δ-*5* and *wdrac1*^{OE}, whereas the *wdrac1*^{G16V} and wild-type strain both showed considerable true hyphal growth and the length of the true hyphae in *wdrac1*^{G16V} was much longer than that of the wild-type strain cultured identically. To understand if the retarded hyphal growth of the *wdrac1*Δ-*5* and *wdrac1*^{OE} mutants was due to the same mechanism, I increased the incubation time for these two mutants to seven days. Although a small number of true hyphae were still observed with *wdrac1*^{OE}, the *wdrac1*Δ-*5* still showed the yeast form (data not shown). These observations suggested the following: 1) WdRac1p is required for polarized true hyphal growth; 2) overexpression of the constitutively active allele *wdrac1*^{G16V} promotes the polarized hyphal growth, whereas overexpression of *wdrac1*$^{+}$ allele delays the production of true hyphae in carbon-rich minimal media.

5.34 The *wdcdc42* allele plays important roles in maintaining cell wall integrity, septin ring establishment and hyphal branching.

It was previously documented that although the *wdcdc42*Δ mutant displays a similar phenotype as the wild-type strain when incubated in YPD or minimal medium at both 25℃ and 37℃, the constitutively active form of WdCdc42p plays a negative role in hyphal growth (Ye and Szaniszlo, 2000). However, when I incubated the *wdcdc42*Δ mutant in YPMaltose broth medium at 37℃ for two days, a large number of cells showed lysis (Fig. 5.3.6C), while no such lysed cells were observed at 25°C, which means that WdCdc42p may play a role in maintaining cell wall integrity during temperature stress. More interestingly, the loss of cell wall integrity was observed only when the carbon source was maltose instead of glucose, which was provided in the YPD and minimal media but not in the YPMaltose medium. Furthermore the loss of cell wall integrity in the *wdcdc42*Δ mutant was also observed in a medium with xylose as the sole carbon source (data not shown). To my knowledge there is no similar report with *W. dermatitidis* and any other fungi. Additionally, I observed darker bud necks in yeast of the *wdcdc42*Δ mutant after 48 h when cells were incubated at 37℃ in YPD and stained with Calcoflour (Fig. 5.3.6A). Similar results were found in YPMaltose and minimal medium (data not shown). However at 25℃, after 48 h incubation in all of these same three media, a large amount bright fluorescence was present in the bud necks after staining.

Fig. 5.3.6. Cellular morphologies of the *wdcdc42*Δ mutant in three media. (A) *wdcdc42*Δ mutant cells ($1x10^7$ cells/ml) grown at 25℃ were transferred to pre-warmed 37℃ YPMaltose broth. After 48 h, cells were stained with Calcoflour white and photographed at the same magnification with visible light or fluorescent light using a 40x objective lens. (B) *wdcdc42*Δ mutant cells ($1x10^7$ cells/ml) grown at 25℃ were transferred to pre-warmed 37℃ minimal medium for 72 h and photographed with visible light using a 40x objective lens. (C) *wdcdc42*Δ mutant cells ($1x10^7$ cells/ml) grown at 25℃ were transferred to pre-warmed 37℃ YPMaltose or YPD broth. After 48 h, cells were photographed with visible light using a 40x objective lens. The bars in each image represent 10 μm.

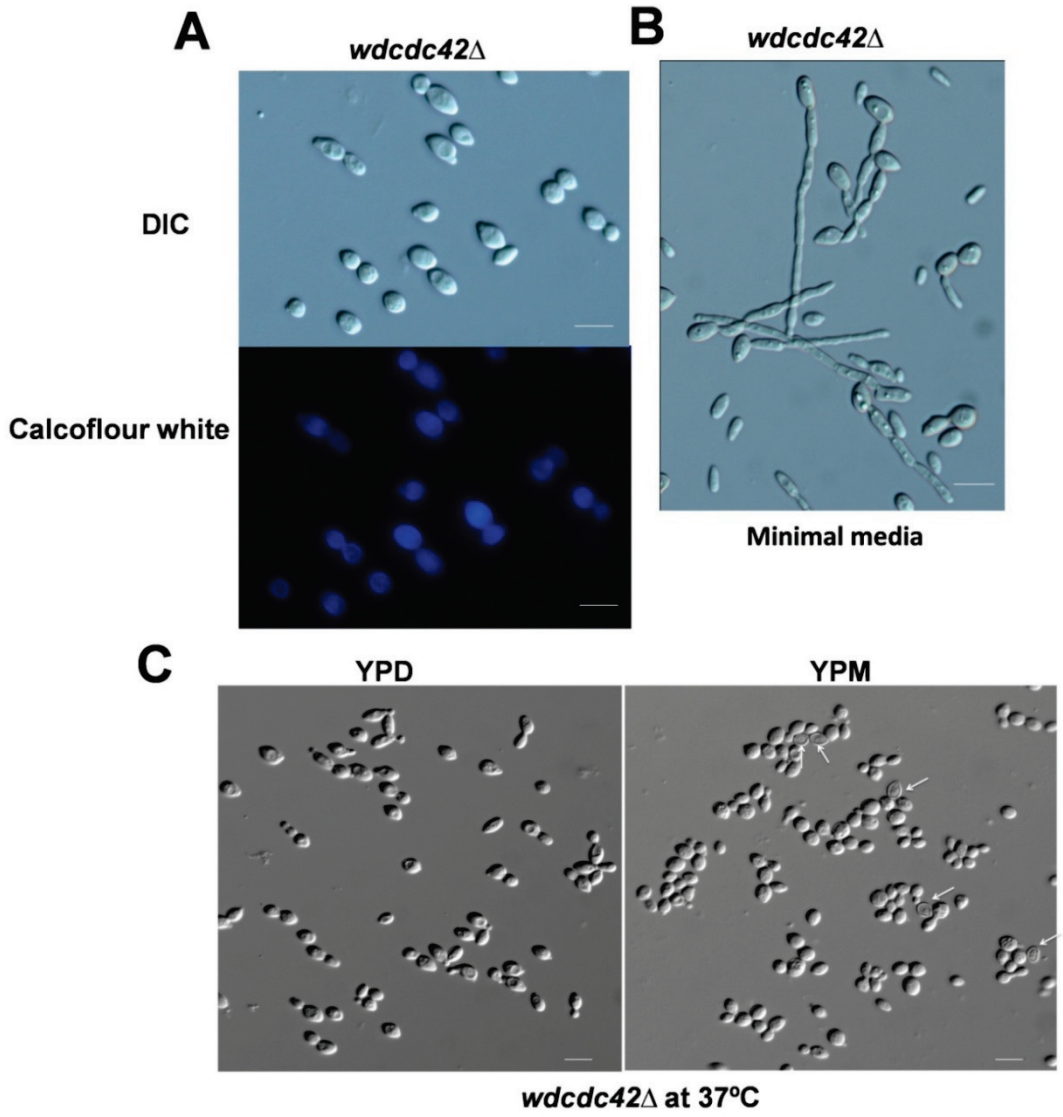

In *S. cerevisiae,* Cdc42p is required to interact with septin filaments to form a "septin assembly complex," which allows docking of the complex to the assembling septin ring (Gladfelter, et al., 2002). My results suggest that a similar biological process may happened in *W. dermatitidis*, because the dark neck may be caused by a damaged septin ring assembly, which affects chitin deposition into the budding neck. In addition, I noticed that the hyphal growth of the *wdcdc42*Δ mutant in the hyphae-inducing minimal medium lost its branching pattern, whereas in the wild-type strain and in the *wdrac1*^{G16V} mutant, the normal branch pattern was maintained (Fig. 5.3.5B and 5.3.6B). A similar result has been documented in the fungal plant pathogen *Colletotrichum trifolii*, in which overexpression of dominant negative Cdc42p causes virtually no hyphal branching (Chen, et al., 2006).

5.35 The double mutant *wdcdc42*Δ/*wdrac1*^{G16V} shows induced germ tube formation in YPMaltose medium and shows enhanced true hyphal growth in minimal medium.

In *W. dermatitidis*, Ye and Szaniszlo (2000) first reported that not only is *WdCDC42* not an essential gene, but also that the *wdcdc42*Δ deletion mutant is phenotypically very similar to wild-type. Because of those observations, current opinion holds that a homolog of Rac1p might be able to replace the lost function of WdCdc42p. In *Ustilago maydis*, there is at least one important functional overlap between its Rac1

and Cdc42, since the depletion of both Rac1p and Cdc42p is lethal. (Mahlert, et al., 2006). Nonetheless, in *C. albicans,* not only do its Rac1p and Cdc42p show different dynamics at the membrane level, but also they have different roles in cell development (Bassilana and Arkowitz, 2006). Furthermore, the teo proteins complement each other, even though they are highly similar to one another. My inability to obtain the double deletion of both *WdCDC42* and *WdRAC1* suggests that the same important functional overlap exists between them in *W. dermatitidis*. Thus, to investigate the genetic interactions, if any, between *WdCDC42* and *WdRAC1*, I overexpressed the constitutively active allele *wdrac1*^{G16V}, as well as the wild-type *rac1*$^{+}$ allele as the control, in the *WdCDC42* knock out mutant *wdcdc42*Δ in order to generate the two double mutants *wdcdc42*Δ*/wdrac1*^{G16V} and *wdcdc42*Δ*/wdrac1*^{OE}. Observations of the double mutant, *wdcdc42*Δ*/wdrac1*^{G16V} showed it had a slightly accelerated rate of growth when incubated at 37℃ on YPMaltose agar plate medium when using a dilution spot growrh assay (Fig. 5.3.4A). Since WdCdc42p plays a negative role in true hyphal growth and the *wdrac1*^{G16V} mutant displays an elongated cell shape, indicating it has a positive role in polarized growth, I postulated the the double mutant *wdcdc42*Δ*/wdrac1*^{G16V} would show polarized growth. As expected, I found that the *wdcdc42*Δ*/wdrac1*^{G16V} double mutant indeed produced many more germ tubes instead of yeast with buds among a population of cells (Fig. 5.3.7A), whereas the *wdcdc42*Δ mutant, the *wdrac1*^{G16V} mutant and the *wdcdc42*Δ*/wdrac1*^{OE} double mutant did not display the germ tube morphology. To further investigate germ-tube formation in the

*wdcdc42*Δ*/wdrac1*^{G16V} double mutant, I incubated this mutant in YPMaltose broth media at both 25℃ and 37℃ and took samples in the time-course manner to determine germ tube and bud percentages. At both at 25℃ and 37℃, germ-tube formation by the *wdcdc42*Δ*/wdrac1*^{G16V} mutant increased and reached a very high percentage by 24 h (Fig. 5.3.7B). However after 48 h, the germ tube formation at 37℃ started to fall, whereas the germ-tube formation at 25℃ continued to increase. This may be due to the fact that the higher growth rate at 37℃ leads to cell entering stationary phase earlier than that of 25℃ and to the fact that the cells with germ tubes don't increase in number whereas those with buds do.. The induced germ-tube growth of the *wdcdc42*Δ*/wdrac1*^{G16V} mutant, but not the *wdcdc42*Δ, *wdrac1*^{G16V} or *wdcdc42*Δ*/wdrac1*^{OE} mutants supports a negative effect concept for WdCdc42p and a positive effect concept for a constitutively active form of WdRac1p in polarized hyphal growth.

Since the *wdcdc42*Δ*/wdrac1*^{G16V} mutant displayed induced germ-tube formation in YPMaltose broth and agar media, I wondered if it would display enhanced polarized true hyphal formation in the hyphae-inducing minimal medium. As expected, the *wdcdc42*Δ*/wdrac1*^{G16V} mutant showed more hyphal filament extensions than did the wild-type strain and the *wdcdc42*Δ and *wdrac1*^{G16V} mutants. However, the *wdcdc42*Δ*/wdrac1*^{OE} and *wdcdc42*Δ/*wdcdc42*^{G14V} mutants showed repressed true hyphal growth in the minimal medium. The repression effect of the constitutively active

wdcdc42^{G14V} allele on true hyphal growth was reported previously (Ye and Szaniszlo, 2000). In addition, the retarded hyphal growth of *wdcdc42*Δ*/wdrac1*^{OE}, compared with the enhanced hyphal growth of *wdcdc42*Δ*/wdrac1*^{G16V}, suggests that WdRac1p is the key protein deciding the morphological switch and the activation of WdRac1p is required for the process. The retarded hyphal growth caused by WdRac1p overexpression may be due to recruiting competition between the GTP form and the GDP form of WdRac1p, and this competition may decide whether there will be a morphological switch in *W. dermatitidis*. Interestingly, in *C. albican*, the *RAC1* deletion mutant shows no hyphal growth in embedded media (Mahlert, et al., 2006). However, no report about the role of constitutively active Rac1p in *C. albican* addresses this point.

5.36 WdCdc42p and WdRac1p share partial overlapping functions.

As described previously, WdCdc42p plays a negative role in hyphal growth while WdRac1p plays a positive role. However, it seems that WdRac1p is not a substitute protein for WdCdc42p since they play different roles in the hyphal growth. However, I could not exclude the possibility of overlapping function between them. To discover if the overexpression of *rac1* alleles in the *wdcdc42*Δ mutant can complement the function of WdCdc42p, I compared the phenotypes that the *wdcdc42*Δ mutant displays with those of *wdcdc42*Δ*/wdcdc42*^{G14V} *wdcdc42*Δ*/wdrac1*^{OE} and *wdcdc42*Δ*/wdrac1*^{G16V}. To my surprise, the *wdcdc42*Δ*/wdrac1*^{G16V} mutant can

Fig.5.3.7. Cellular morphology of the *wdcdc42*Δ/*wdrac1*^{G16V} double mutants. (A) Cells (1x10^7 cells/ml) grown at 25℃ were transferred to pre-warmed 37℃ YPMaltose broth. After 48 h, cells were stained with Calcoflour white and photographed at the same magnification with visible light or fluorescent light using a 40x objective lens. **(B)** Germ-tube formation patterns at 48 h. Cells (1x10^7 cells/ml) of *wdcdc42*Δ/*wdrac1*^{G16V} grown at 25℃ were transferred to a fresh 25℃ YPMaltose broth or pre-warmed 37℃ maltose-containing YP broth. The cells with germ tubes were counted among every 1000 budded cells in the time-course manner. The error bars indicate one standard deviation. **(C)** Mutants cells (1x10^7 cells/ml) grown at 25℃ were transferred to pre-warmed 37℃ minimal midum for 72 h and photographed with visible light using a 40x objective lens. The bars in each image represent 10 μm.

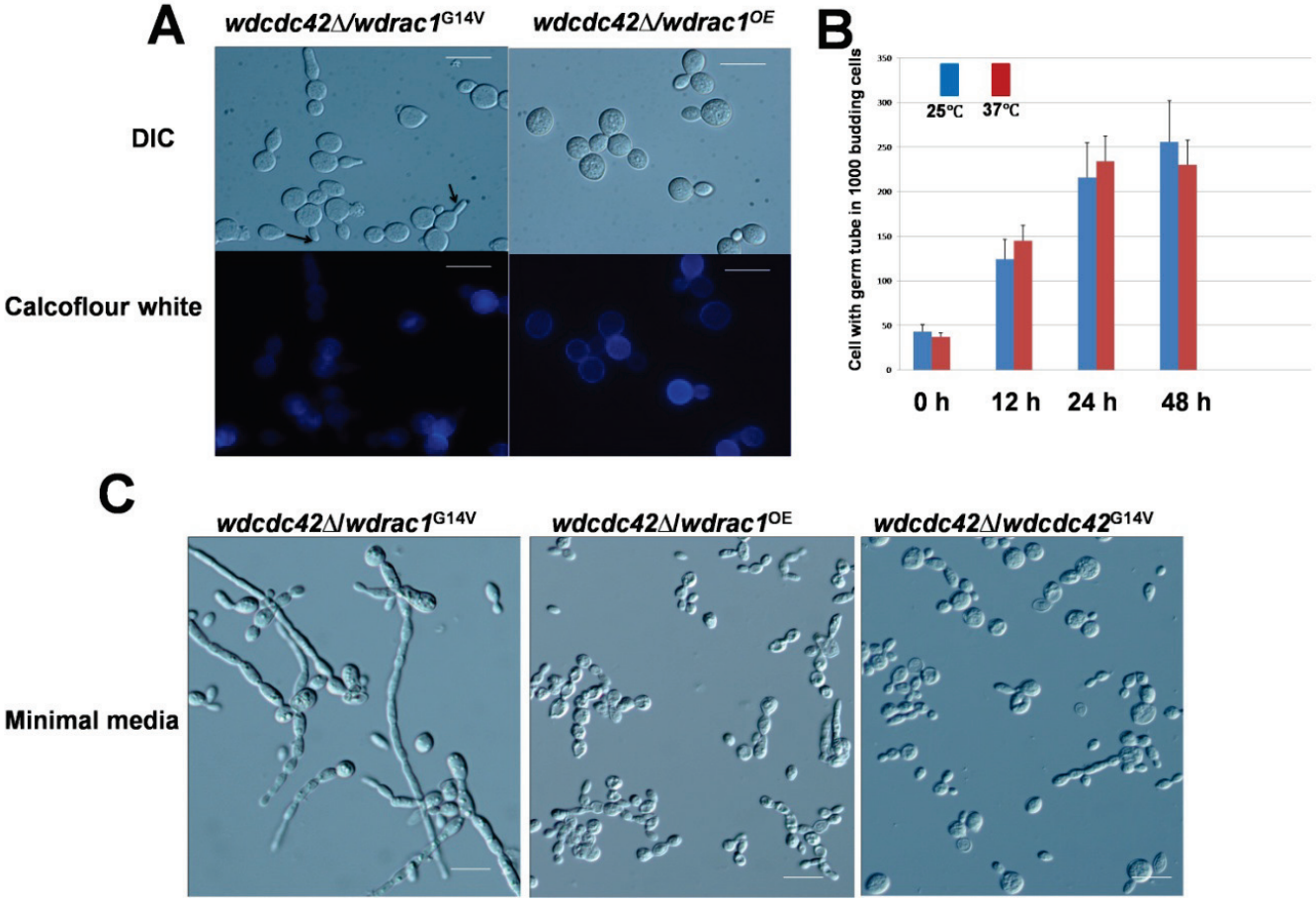

Fig.5.3.8. Constitutively active WdRac1p complements the function of WdCdc42p in septin ring formation. **(A)** Cells ($1x10^7$ cells/ml) grown at 25℃ were transferred to pre-warmed 37℃ YPMaltose broth. After 48 h, cells were stained with Calcoflour white and photographed at the same magnification with visible light or fluorescent light using a 40x objective lens. **(B)** Percentages of cells among the strains having reduced fluorescence in their bud necks. Cells ($1x10^7$ cells/ml) grown at 25℃ were transferred to 25℃ or pre-warmed 37℃ YPD broth. After culturing for 48 h, the numbers of cells with bright budding necks were counted among every 1000 budding cells, which only had one bud. The error bars indicate one standard diviation among the percentages. **(C)** Percentages of cells among the strains exhibiting a loss of cell wall integrity among mutants. Cells ($1x10^7$ cells/ml) grown at 25℃ were transferred to 25℃ or pre-warmed 37℃ YPMaltose broth. The tendency to lyse were quantified under microscope after culturing for 48 h

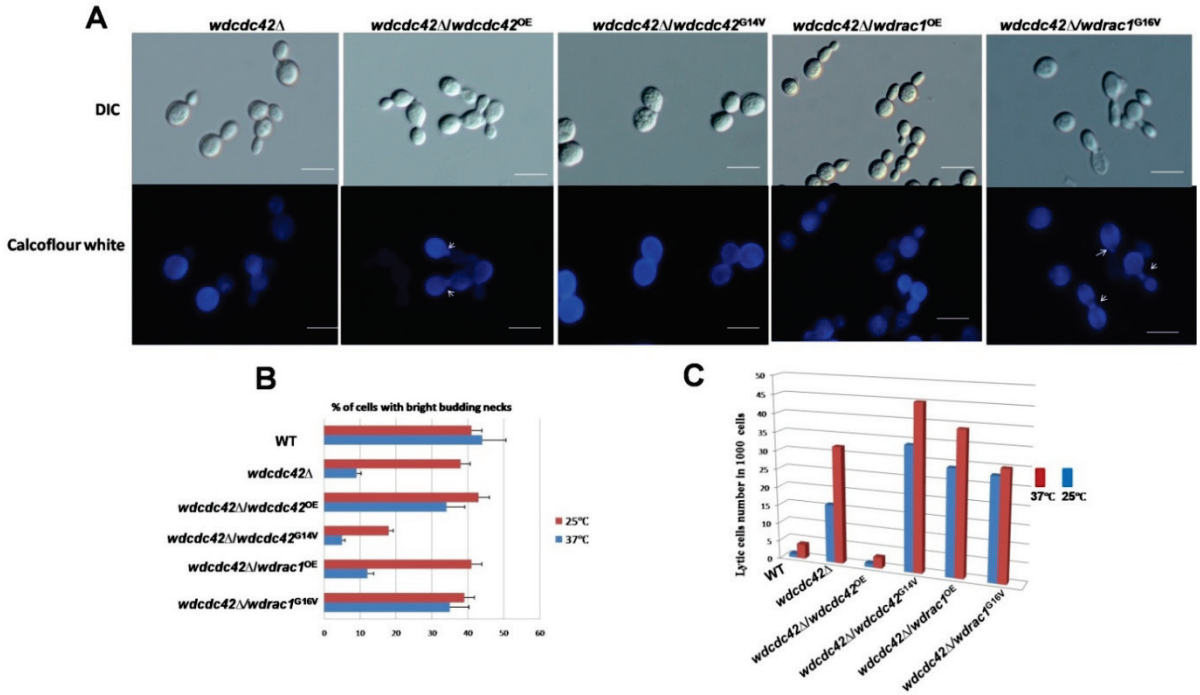

complement the loss of branching in the *wdcdc42*Δ mutant. In Fig. 5.3.6B, it can be seen that the *wdcdc42*Δ mutant displayed a type of true hyphal growth that is devoid of branches, whereas the more typical branching hyphal growth is exhibited by the *wdcdc42*Δ*/wdrac1*^{G16V}mutant (Fig. 5.3.7C). This observation suggests that an overlapping function in branch formation during hyphal growth exists between WdCdc42p and WdRac1p. More surprisingly, the *wdcdc42*Δ*/wdrac1*^{G16V} mutant displayed the bright budding neck when incubated in YPD broth at 37°C (Fig. 5.3.8A), as well as did the complemented *wdcdc42*Δ*/wdcdc42*^{OE} strain. However, the *wdcdc42*Δ*/wdrac1*^{OE} and *wdcdc42*Δ*/wdcdc42*^{G16V} mutants still displayed the dark budding necks in the manner of the *wdcdc42* mutant (Fig. 5.3.8A). My quantitative study of the various phenotypes provides additional support for my above results (Fig. 5.3.8B). To investigate if the overexpression of WdRac1p can rescue the lysis phenotype cause by the functional loss of WdCdc42p, the *wdcdc42*$^{+}$, *wdcdc42*^{G14V}, *wdrac1*$^{+}$ or *wdrac1*^{G16V} alleles in the *wdcdc42*Δ mutant were overexpressed and characterized in YPMaltose broth at 37°C for 48 h. The number of lysed cells was counted among every 1000 cells. Whereas the overexpression of the *wdcdc42*$^{+}$allele significantly reduced the lysed cell number, the overexpression of all the other alleles did not effectively reduce that number (Fig. 5.3.8C). This result indicates that in the same manner as the active form of WdCdc42p, both the inactive and the active forms of WdRac1p could not complement the role of WdCdc42p in the temperature stress response.

Fig.5.3.9. The *wdcdc42*Δ/*wdrac1*^{G16V} mutant displays an interrupted carotenogenesis pathway. The albino strains *pyex303* , *wdrac1*^{OE}, *wdrac1*^{G16V} *wdcdc42*Δ/*wdcdc42*^{G14V}, *wdcdc42*Δ/*wdrac1*^{OE} and *wdcdc42*Δ/*wdrac1*^{G16V} were streaked on the minimal medium with maltose or YPM and incubated in the presence or absence of light at 25℃ for 5 days: the plates incubated in the dark were wrapped with tin foil, whereas the plates incubated in the light were exposed directly visible room light. The resulting growth was photographed with digital camera. Note the loss of pink color in the *wdcdc42*Δ/*wdcdc42*^{G14V} mutant.

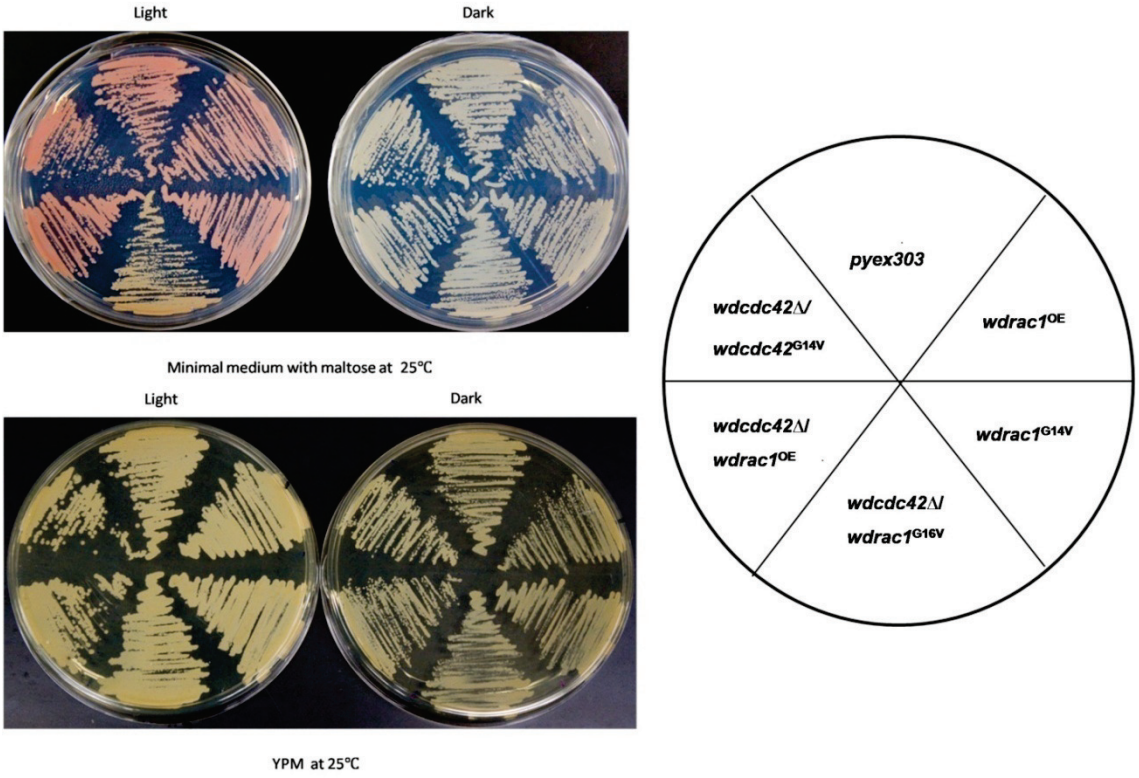

5.37 The *wdcdc42*Δ/*wdrac1*^{G16V}mutant has an interrupted carotenogenesis pathway.

An unexpected discovery about the *wdcdc42*Δ/*wdrac1*^{G16V}mutant was obtained coincidently when I incubated the *wdcdc42*Δ/*wdrac1*^{G16V}mutant on SD minimal medium under standard room light. In *W. dermatitidis*, carotenogenesis can be induced under visible light, which gives albino cells a pink color on SD minimal medium not the rich YPD medium (Geis and Szaniszlo, 1984). Although the pink color caused by carotenogenesis can not be observed with the wild-type strain, because it is absent or is masked by the black melanin in the cell wall, albino mutants often display the pink color when carotenogenesis is activated by light. However, the *wdcdc42*Δ/*wdrac1*^{G16V}mutant showed little or no pink color after incubation on the minimal medium under the visible light. When I compared this *wdcdc42*Δ/*wdrac1*^{G16V}mutant with the other albino mutants, I found that *wdcdc42*Δ/*wdrac1*^{G16V} was the only mutant that did not produce the pink color (Fig. 5.3.9.). Since both the *wdrac1*^{G16V} and *wdcdc42*Δ/*wdrac1*^{OE} mutants displayed the pink color, I concluded that the deletion of *WdCDC42* allele, as well as the activation of WdRac1p, is required for the disruption of carotenogenesis.

5.4 DISCUSSION

In this study, I identified and characterized the *RAC1* homolog of *W. dermatitidis*. This GTPase is highly similar to Rac1 proteins found in other organisms and to WdCdc42p and WdRho1p (Fig. 5.4.1). Because the consensus element, the GDGAVGK domain, was found in all of these three GTPase, I was able to generate the constitutively-active, gain-of-function alleles *wdrac1*^{G16V} and *wdrho1*^{G14V} to compare them with the previously derived *wdcdc42*^{G14V} mutant (Ye and Szaniszlo, 2000). This CXXL (CSIL, residues 193 to 197 in WdRac1p) geranylgeranylation site indicates that WdRac1p is also a signal molecule that is involved in a signal transduction pathway.

Neither *WdCDC42* nor *WdRAC1* are essential for viability in *W. dermatitidis.*

Until the *CDC42* deletion mutants in the human pathogenic fungus *Wangiella dermatitidis* and the plant pathogenic fungus *Claviceps purpurea* were reported to be viable (Scheffer *et al*., 2005; Ye and Szaniszlo, 2000), the *CDC42* gene was long considered to be an essential gene in all eukaryotes (Johnson, 1999). Similar to the findings with *WdCDC42*, the *WdRAC1* gene is also not an essential gene in *W. dermatitidis*, since I was able to derive the *WdRAC1* deletion mutant. Not only are the mutants with deletions of *WdCDC42* and *WdRAC1* viable, but they have also have

Fig.5.4.1 Amino acid sequence alignments of WdRho1p, WdCdc42p and WdRac1p of *Wangiella. dermatitidis.* The red frame shows the aminio acid "G" to "V" switch sites and the black frame shows the CXXL conserved geranylgeranylation site domain.

growth patterns that are similar to that of the wild-type strain. Furthermore, neither the *WdCDC42* deletion mutant nor the *WdRAC1* deletion mutant displayed an abnormal budding ability or aberrant buds at 25°C, except for the *wdcdc42*Δ mutant, which displayed a lack of fluorescence in the bud neck at 37°C after staining with Calcoflour white. In addition, the overexpression of the *wdrac1*^{G16V} allele did not lead to the lethal phenotype and a similar observation was previously reported for the overexpression of the *wdcdc42*^{G14V} allele (Ye and Szaniszlo, 2000). However, it has been documented that the overexpression of constitutive active Rac1p under control of the inducible P*crg* promoter is lethal in the dimorphic fungus *Ustilago maydis* (Mahlert, et al., 2006). The reason why it is not lethal in *W. dermatitidis* when the constitutively active *wdrac1*^{G16V} allele is overexpressed may due to the following possibilities: First, the *glaA* promoter is not a very highly inducible promoter and thus a lethal event caused by the overexpression of the *wdrac1*^{G16V} allele, if possible, is dosage sensitive. Second, the *wdrac1*^{G16V} mutant still expresses the wild-type WdRac1 protein, which may have adversely diluted the effect of overexpression of the constitutively active WdRac1p.

WdCDC42 plays an important role in polarized growth and genetically interacts with WdRAC1

The overexpression of Cdc42p in *S. cerevisiae* perturbs the pattern of bud site selection (Johnson and Pringle, 1990). Other evidence support the role of Cdc42p in

the establishment of polarized growth, including it importance in the initiation of the polarisome and the regulation of the localization (Evangelista, et al., 1997; Dong, et al., 2003; Rida and Surana, 2005), which indicates a role for Cdc42p in branch initiation during hyphal growth. In *Colletotrichum trifolii*, overexpression of dominant negative Cdc42p causes virtually no hyphal branching (Chen, et al., 2006). Similarly, there were no branching-hyphae observed in the *WdCDC42* deletion mutant strain, which provided additional support on the role of WdCdc42p in branch formation. Even though WdCdc42p and WdRac1p displayed opposite roles in the regulation of true hyphal growth, they still may be involved in the same biological process because the active form of WdRac1p not only was able to restore the branches, which could not be observed in the *WdCDC42* deletion mutant during true hyphal growth, but also can apparently increase the bright Calcofluor staining of the bud neck of yeast cells..

The *WdCDC42* complementation strain *wdcdc42*Δ*/wdcdc42*^{OE} showed the bright budding neck, which provides addition evidence to support that the WdCdc42p is required for the septin ring assembly at the yeast bud neck. Meanwhile, when compared with *wdcdc42*Δ*/wdcdc42*^{G14V} and *wdcdc42*Δ*/wdcdc42*^{OE}, very rare bright bud necks were observed in the *wdcdc42*Δ*/wdcdc42*^{G14V} mutant (Fig. 5.3.8A). From the quantitative data (Fig. 5.3.8B), I notice that the *wdcdc42*Δ*/wdcdc42*^{G14V} mutant showed significantly less bright bud necks even at 25°C, which may due to a negative effect on cell polarity establishment by the active form of WdCdc42p (Ye and Szaniszlo, 2000).

This result indicates that similar to the role of Cdc42p in *S. cerevisiae*, in *W. dermatitidis* the GDT form of WdCdc42p is also essential for reloading the septin fiber and that the constitutively active GTP form of WdCdc42p prevents this process, thus leading to the septin assembly failure. Interestingly, the overexpression of GTP form of WdRac1p can complement the lost function of WdCdc42p in the septin ring assembly. In *S. cerevisiae,* the hydrolysis of GTP by Cdc42p is necessary to release the septin fiber to the septin ring complex. The mechanism by which the active form of WdRac1p can complement the dark budding neck phenotype caused by the loss of WdCdc42p, may explain why the active form of WdRac1p can recover the ability of branch formation during hyphal growth. In this case the active form WdRac1p may be able to substitute for WdCdc42 and thus interact with the polarisome component to initiate the polarized growth, which caused the recovery of septin ring formation and branch initiation. It is also possible that the constitutively active WdRac1p may use a different mechanism to assemble the septin ring or the active WdRac1p may activate other protein to take part in the assembly.

Although the *wdcdc42*Δ mutant displayed the dark budding neck, when I incubated the *wdcdc42*Δ mutant in the hyphae-inducing minimal medium, bright stained septa were observed in hyphae (Fig. 5.4.2A). Similarly, the hyphae of the *wdcdc42*Δ/*wdrac1*^{G16V} double mutant were divided into multiple compartments by the bright septa. This observation indicates that during polarized hyphal growth, the loss

of the functional WdCdc42p can be compensated for by another protein, possibly WdRac1p, when the cell is developing septa in hyphae, because the active WdRac1p can restore septin ring formation in the *WdCDC42* deletion background when incubated in the rich media. Additional evidence from my realtime RT-PCR results showed that both *WdCDC42* and *WdRAC1* mRNA expression levels increased when cells were transferred from the rich YPMaltose medium to hyphae-inducing minimal medium (Fig. 5.4.2B). This means that the expression of *WdRAC1* is reacting to the hyphae-inducing environment. After comparing septum formation of the *wdcdc42*Δ mutant in rich medium with that of in the hyphae-inducing minimal medium, I suggest that WdRac1p is inactive mostly in rich media, and that the WdRac1p is activated when incubated in the hyphae-inducing minimal media.

Does a *WdCDC42* paralog exist?

The realtime RT-PCR detected a high level of signal when I ran realtime RT-PCR with the *WdCDC42* primers and probe to amplify the cDNA sample from the *wdcdc42*Δ mutant, which was incubated at 25°C. So it is possible a *WdCDC42* paralog may exist. The *wdcdc42*Δ mutant was confirmed to be a deletion of *WdCDC42* gene by Southern blotting (Ye and Szaniszlo 2000). However, the northern blotting results showed two hybridization bands: one is 1.8 kb major band, another was a 1.5-kb unidentified band. Thus it is very possible that this second band is the paralog not

Fig. 5.4.2 Septum formation comparison between *wdcdc42*Δ and *wdcdc42*Δ/*wdrac1*^{G16V} in maltose-containing minimal medium. **(A)** Cells ($1x10^7$cells/ml) of *wdcdc42*Δ and *wdcdc42*Δ/*wdrac1*^{G16V} grown at 25℃ were transferred to pre-warmed 37℃ maltose-containing minimal media and then sampled and observed microscopically at 72 h and photographed at the same magnification with visible light or fluorescent light using a 100x objective lens. Calcoflour white staining was applied to all the samples. White arrows indicate the bright septa. The bars in each image represent 5 µm. **(B)** The relative abundance of *WdCDC42* and *WdRAC1* mRNA was analyzed by realtime PCR. Wild-type cells were incubated in YPD broth at 37°C until log phase and then the cells were collected by centrifugation, transferred into 37°C pre-warm minimal medium and incubated for 2 h. In each case 2 µg total RNA was reverse transcribed into cDNA. Primers used for the real-time RT-PCR were specific for *WdACT1*, *WdCDC42 and WdRAC1*. The relative mRNA abundance of housekeeping *WdACT1* mRNA to those of *WdCDC42* and *WdRAC1* was calculated and are shown as bars. The error bars in each bar indicate one standard deviation.

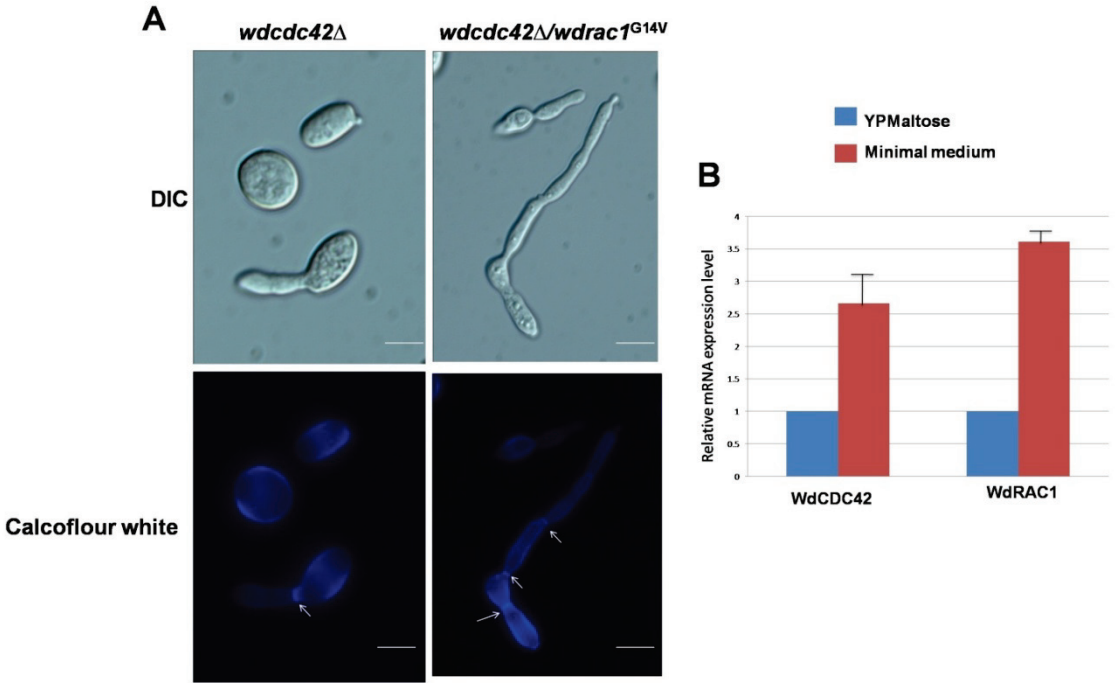

WdRac1p that keeps the *WdCDC42* knock-out strain viable. That said, I still could not exclude the possibility that another GTPase or protein, which is very similar to WdCdc42p, can back up the function of WdCdc42p. It is interesting that when the *wdcdc42*Δ mutant was incubated at 37°C, the mRNA expression level detected with the *WdCDC42* primers and probe dropped dramatically (Fig. 5.4.3A). This result may explain why the *wdcdc42*Δ mutant exhibited the lysis phenotype when incubated in YPMaltose at 37°C. Because at the higher temperature, the putative *WdCDC42* paralog expression drops and thus could not complement for the loss of function of WdCdc42p, the cells could not maintain viability since in many fungi, *CDC42* homologs are essential genes (Johnson and Pringle, 1990; Miller and Johnson, 1994).

WdCdc42p and WdRac1p play different roles during the induction of true hyphal growth.

Although the amino acids sequence alignment showed similar conserved domains in WdCdc42p and WdRac1p, the actual functions of these two GTPase during morphological switching (vegetative dimorphism and polymorphism) varied. First, both the *wdcdc42*Δ mutant and the *wdrac1*^{G16V} mutant displayed similar induced true hyphal growth forms. Second, previous studies of WdCdc42p in *W. dermatitidis*

Fig.5.4.3. **Expression analysis of *WdCDC42* and *WdRAC1.* (A)** Expression of a putative *WdCDC42* paralog. Cells ($1x10^7$ cells/ml) grown at 25℃ were transferred to 25℃ or pre-warmed 37℃ YPD broth for 2 h. The relative abundance of the mRNA of *WdCDC42* expressed by the *wdcdc42*Δ mutant was analyzed by realtime PCR. The relative mRNA abundance in relation to the housekeeping gene *WdACT1* mRNA was calculated and is shown in the form of the bars. The error bars in each bar indicate one standard deviation. **(B)** Deletion of *WdCDC42* increases the *WdRAC1* mRNA expression level. Cells ($1x10^7$ cells/ml) grown at 25℃ were transferred to 25℃ or pre-warmed 37℃ YPD broth for 2 h. The relative abundance of mRNA of *WdRAC1* from WT strain and *wdcdc42*Δ mutants were analyzed by realtime PCR. The relative mRNA abundance compared to that of housekeep *WdACT1* mRNA was calculated and shown in the form of bar. The error bars in each bar indicate one standard deviation.

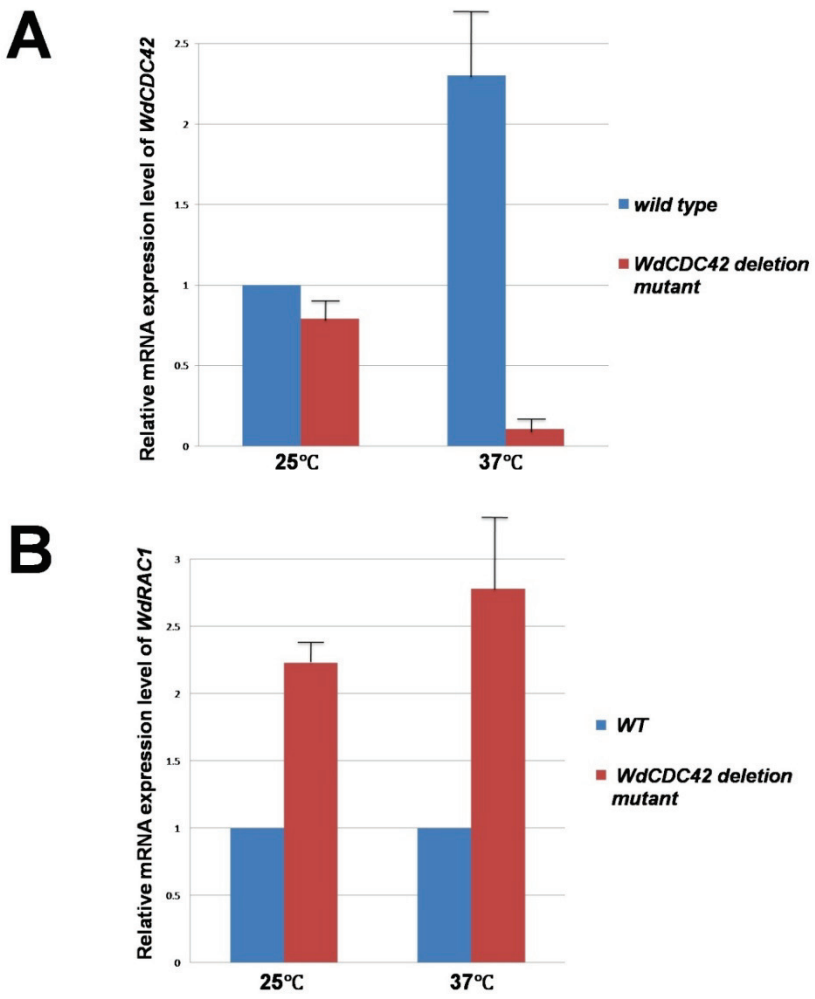

documented its negative role on polarized true hyphal growth (Ye and Szaniszlo, 2000): the overexpression of the constitutively active WdCdc42p represses true hyphal growth on the hyphae-inducing starch agar medium. Third, in this study, the *wdcdc42*Δ mutant showed induced hyphae whereas the *wdrac1*Δ*-5* mutant showed no true hyphal growth. Futhermore, the overexpression of the constitutively active WdRac1p enhanced the true hyphal growth. Especially with the *wdrac1*^{G16V} mutant, the length of its hyphae was obviously longer than that of the wild-type strain after incubation for the same time. Fourth, the *wdrac1*Δ*-5*, *wdrac1*^{OE}, *wdcdc42*Δ/*wdcdc42*^{G14V}, *wdcdc42*Δ/*wdcdc42*^{OE} mutants displayed retarded polarized true hyphal growth. When I incubated all of these mutants longer than seven days however, *wdrac1*^{OE} and *wdcdc42*Δ/*wdcdc42*^{OE} displayed the polarized true hyphal growth typical of the wild type, whereas still no hyphae were observed to be produced by the *wdrac1*Δ*-5* and *wdcdc42*Δ/*wdcdc42*^{G14V} mutants. It seems that the hyphal formation was retarded in *wdrac1*^{OE} and *wdcdc42*Δ/*wdcdc42*^{OE} and was repressed in *wdrac1*Δ*-5* and *wdcdc42*Δ/*wdcdc42*^{G14V}. The retarded hyphal growth in *wdrac1*^{OE} indicates that WdRac1p needs to be activated to promote the formation of true hyphae. In general, the data suggest that the GTP form of WdRac1p has a significant positive effect on the promoting hyphal growth, while the GTP form of WdCdc42p negatively regulates the hyphal growth.

In addition, my observations indicate that the guanine nucleotide exchange factor (GEF) for WdRac1p needs to be activated during true hyphal growth. It seems that the

Fig.5.4.4 Model for the role of WdCdc42p and WdRac1p during yeast budding and the even more polarized hyphal growth of *W. dermatitidis*. The orange dots represent WdCdc42p and the green dots represent WdRac1p. The WdCdc42p GDP form is required for septin to assemble and septum formation to occur in the bud neck of a yeast cell at 37℃. Overexpression of the WdRac1p GTP form not only can complement the functional loss of *WdCDC42*Δ during septin assembly but also can positively promote hyphal growth and allow septa to form in the hyphae. Overexpression of the WdRac1p GTP form can recover the hyphal branching property, which is lost in the *wdcdc42*Δ mutant. WdCdc42p and WdRac1p may compete in a dosage-sensitive manner and this competition then may decide the nature of the resulting vegetative cell growth in a way that leads to yeast budding or to a more polarized true hyphal form of growth.

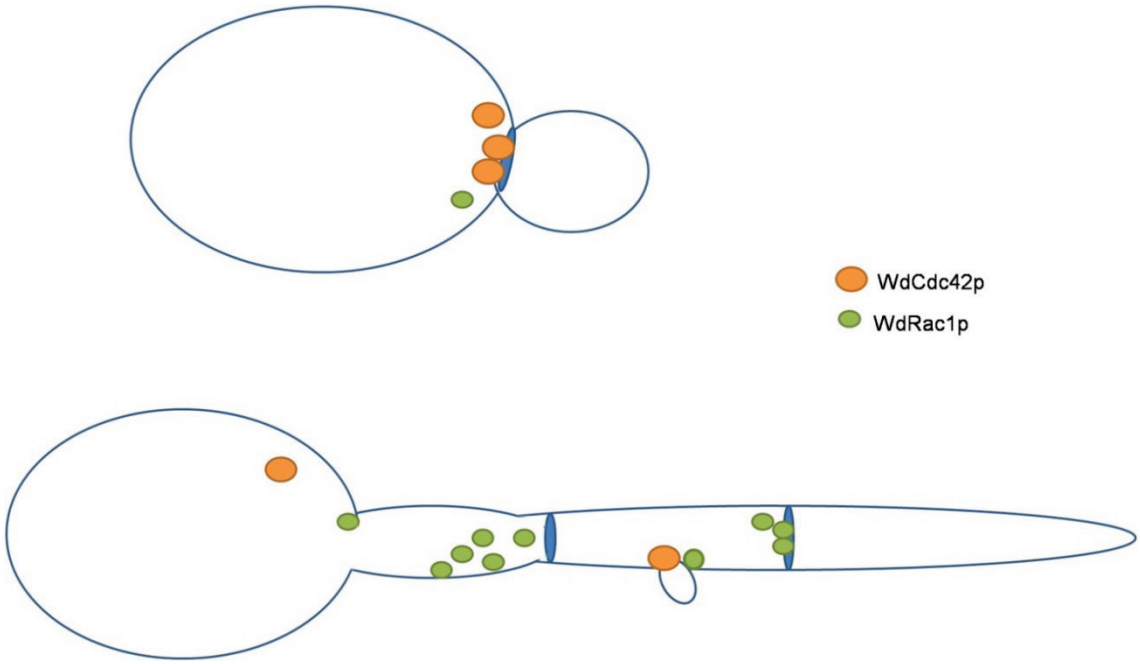

overexpression of the *wdrac1*$^{+}$ allele in *W. dermatitidis* does not have an effect on the activation the GEF, which controls the activity of WdRac1p. Also the GDP form of WdRac1p may compete with the GTP form of WdRac1p for recruiting the same downstream protein. My Realtime RT-PCR results showed that the *WdRAC1* mRNA expression level increases in the *wdcdc42*Δ mutants (Fig. 5.4.3B), which revealed that the over abundance of WdCdc42p may inhibit the mRNA expression of *WdRAC1*. This in turn may indicate that a competitive mechanism exists in the genetic interaction between *WdCDC42* and *WdRAC1* in *W. dermatitidis*. Although it was reported that Cdc42p and Rac1p share an overlapping function in polarity establishment in *A. nidulans* (Virag, et al., 2007), I conclude that in *W. dermatitidis*, WdRac1p plays a pivot role in the polarized true hyphal growth and WdCdc42p and WdRac1p play different roles during the induction of true hyphae (Fig. 5.4.4).

5.5 SUMMARY

In this study, I first cloned and characterized the *WdRAC1* gene from *W. dermatitidis* and demonstrated that WdRac1p activity can affect polarized true hyphal growth although the the various *WdRAC1* mutants I derived have little effect on the budding pattern of a yeast cell. In addition, I discovered three new phenotypes associated with the *WdCDC42* deletion mutant: first, the *wdcdc42*Δ mutants displayed cell lysis when incubated in YPMaltose at 37ºC; second, the dark bud neck in yeast cells after

Calcoflour staining; third, the *wdcdc42*Δ mutants displayed no branching during true hyphal growth. Interestingly, the overexpression of *wdrac1*^{G16V} can complement two of the three phenotypes cause by the *WdCDC42* deletion. Moreover, I proposed different roles for WdCdc42p and WdRac1p and that there is a competition mechanism between them. This study revealed the subtle relationship between Rho GTPases and provided more clues about the regulation of morphological vegetative switching in dimorphic and polymorphic filamentous fungi.

REFERENCES

Abramczyk, D., C. Park, and P. J. Szaniszlo. Cytolocalization of the class V chitin synthase in the yeast, hyphal and sclerotic morphotypes of *Wangiella* (*Exophiala*) *dermatitidis*. Fungal Gen. Biol. 46 (2009) 28-41

Arellano, M., A. Duran and P. Perez. 1996. Rhol GTPase activates the (1-3)-*β*-D-glucan synthase and is involved in *Schizosaccharomyces pombe* morphogenesis The EMBO Journal **15:**4584-4591

Arellano, M., A. Duran, and P. Perez. 1997. Localisation of the *Schizosaccharomyces pombe* Rho1p GTPase and its involvement in the organisation of the actin cytoskeleton. J. Cell Sci. **110:** 2547–2555

Arimura, N., and K. **Kaibuchi.** 2005 Key regulators in neuronal polarity. Neuron **48:** 881–884.

Bazenet, C. E., M. A. Mota, and L. L. Rubin. 1998. The small GTP-binding protein Cdc42 is required for nerve growth factor withdrawal-induced neuronal death. Proc. Natl. Acad. Sci. USA **95:**3984–3989

Bassilana, M and B. A. Arkowitz. 2006. Rac1 and Cdc42 Have Different Roles in *Candida albicans* Development. Eukaryot. Cell **5:** 321–329

Beauvais, A., J. M. Bruneau, P. C. Mol, M. J. Buitrago, R. Legrand and J. P. Latge. 2001. Glucan synthase complex of *Aspergillus fumigatus*. J. Bacteriol. **183:** pp. 2273–2279

Bickle, M., Delley, P.A., Schmidt, A., and M.N Hall. 1998. Cell wall integrity modulates RHO1 activity via the exchange factor ROM2. EMBO J **17:** 2235–2245.

Block, C., and A. Wittinghofer. 1995. Switching to Rac and Rho. Structure **3:**1281–1284.

Boguski, M. S., and F. McCormick. 1993. Proteins regulating Ras and its relatives. Nature **366:**643–654.

Bourne, H. R., D. A. Sanders, and F. McCormick. 1991. The GTPase superfamily: conserved structure and molecular mechanism. Nature **349:**117–127.

Boyce, K. J., M. J. Hynes, and A. Andrianopoulos. 2003. Control of morphogenesis and actin localization by the *Penicillium marneffei RAC* homolog. J. Cell Sci. **116:** 1249-1260.

Cabib, E., J. Drgonova and T. Drgon. 1998. Role of small G proteins in yeast cell polarization and wall biosynthesis. Annu. Rev. Biochem. **67:** pp. 307–333.

Cabib, E., Dong-Hyun Roh, M. Schmidt, Luciana B. Crotti and A. Varma. 2001. The Yeast Cell Wall and Septum as Paradigms of Cell Growth and Morphogenesis. The Journal of Biological Chemistry **276:** 19679-19682.

Carlisle, P. L., Banerjee, M., A. C. Lazzell, J Monteagudo, L. Lopez-Ribot, and D. Kadosh. 2009. Expression levels of a filament-specific transcriptional regulator are sufficient to determine *Candida albicans* morphology and virulence. Proc. Natl. Acad. Sci. USA **106:** 599–604

Chen C, Ha YS, Min JY, Memmott SD, MB. Dickman. 2006. Cdc42 is required for proper growth and development in the fungal pathogen Colletotrichum trifolii. Eukaryot. Cell **5:**155-66.

Chuang, T.-H., K. M. Hahn, J.-D. Lee, D. E. Danley, and G. M. Bokoch. 1997. The small GTPase Cdc42 initiates an apoptotic signaling pathway in Jurkat T lymphocytes. Mol. Biol. Cell **8:**1687–1698

Cooper, C. R., Jr., and P. J. Szaniszlo. 1993. Evidence for two cell division cycle (CDC) genes that govern yeast bud emergence in the pathogenic fungus *Wangiella dermatitidis*. Infect. Immun. **61:** 2069-2081

Coso, O. A., M. Chiariello, J.-C. Yu, H. Teramoto, P. Crespo, N. Xu, T. Miki, and J. S. Gutkind. 1995. The small GTP-binding proteins Rac1 and Cdc42 regulate the activity of the JNK/SAPK signaling pathway. Cell **81:**1137-1146

Dadachova E, RA. Bryan, X. Huang, T. Moadel, AD. Schweitzer, P. Aisen, Nosanchuk JD & A Casadevall. 2007. Ionizing radiation changes the electronic properties of melanin and enhances the growth of melanized fungi. PLoS ONE **5:** e457

Delley, P. A., and M. N. Hall. 1999. Cell wall stress depolarizes cell growth via hyperactivation of RHO1. J. Cell. Biol. **147:**163–174.

Delmer D P, J P Pear, A Andrawis, D M Stalker.1995. Genes encoding small GTP-binding proteins analogous to mammalian rac are preferentially expressed in developing cotton fibers. Mol Gen Genet. **248**:43–51.

Dixon, D.M., P.J. Szaniszlo and A. Polak. 1991. Dihydroxynaphthaline (DHN) melanin and its relationship with virulence in the early stages of phaeohyphomycosis. In: G.T. Cole and H.C. Hoch (ed.), The fungal spore and disease initiation in plants and animals, Plenum Publishing Corporation, New York. 297-318.

Douglas, C. M., J. A. D'Ippolito, G. J. Shei, M. Meinz, J. Onishi, J. A. Marrinan, W. Li, G. K. Abruzzo, A. Flattery, K. Bartizal, A. Mitchell, and M. B. Kurtz. 1997. Identification of the *FKS1* gene of *Candida albicans* as the essential target of 1,3-b-D-glucan synthase inhibitors. Antimicrob. Agents Chemother. **41:**2471–2479.

Drgonova J, T. Drgon, K. Tanaka, R. Kollar, GC. Chen, RA. Ford, CS. Chan, Y. Takai, E. Cabib. 1996. Rho1p, a yeast protein at the interfac betweencell polarization and morphogenesis. Science **272:** 277-9

Dong, Y., D. Pruyne, and A, Bretscher. 2003. Formin dependent actin assembly is regulated by distinct modes of Rho signaling in yeast. J Cell Biol **161:** 1081–1092.

Eitzen, G., N. Thorngren, and W. Wickner. 2001. Rho1p and Cdc42p act after Ypt7p to regulate vacuole docking. EMBO J **20:** 5650–5656.

Evangelista, M., K. Blundell, M.S Longtine, Chow, C.J., N. Adames, J.R. Pringle. 1997. Bni1p, a yeast formin linking Cdc42p and the actin cytoskeleton during polarized morphogenesis. Science **276:** 118–122.

Feng, B., X Wang, M. Hauser, S. Kaufmann, S. Jentsch, G. Haase, J. M.Becker, and P. J. Szaniszlo. 2001. Molecular cloning and characterization of *WdPKS1*, a gene involved in dihydroxynaphthalene melanin biosynthesis and virulence in *Wangiella (Exophiala) dermatitidis*. Infect Immun. **69:** 1781-1794.

G.H. Fleet. 1991. Cell walls In: The Yeasts, 2nd edn., Vol. 4 (Rose A.H. and Harrison, J.S., Eds.), pp. 199–277. Academic Press, New York.

Fowler, T., R. M. Berka, and M. Ward. 1990. Regulation of the glaA gene of *Aspergillus niger.* Curr. Genet. **18:** 537-545

Geis, P.A. and P.J. Szaniszlo. 1984. Carotenoid pigments of the dematiaceous fungus

Wangiella dermatitidis. Mycologia **76:** 268-273.
Gao XD, JP Caviston, SE Tcheperegine, E Bi. 2004. Pxl1p, a paxillin-like protein in Saccharomyces cerevisiae, may coordinate Cdc42p and Rho1p functions during polarized growth. Mol Biol Cell.**15:** 3977–3985.

Gladfelter, A. S., I. Bose, T. R. Zyla, E. S.G. Bardes, and D.J. Lew. 2002. Septin ring assembly involves cycles of GTP loading and hydrolysis by Cdc42p. J Cell Biol. **156:** 315-26

Guo, W., F. Tamanoi, and P. Novick. 2001. Spatial regulation of the exocyst complex by Rho1 GTPase. Nat Cell Biol. **3:** 353–360.

Guest, GM, X. Lin, M. Momany. 2004. Aspergillus nidulans RhoA is involved in polar growth, branching, and cell wall synthesis. Fungal Genet Biol. **41:**13-22.

Hall, A. 1998. Rho GTPases and the actin cytoskeleton. Science **279:**509–514.

Hancock, J. F., A. I. Magee, J. E. Childs, and C. J. Marshall. 1989. All ras proteins are polyisoprenylated but only some are palmitoylated. Cell **57:**1167–1177.

Harrison, J.C., Bardes, E.S.G., Y. Ohya, D Lew. 2001. A role for the Pkc1p/Mapk1p kinase cascade in the morphogenesis checkpoint. Nat. Cell Biol. **3:** 417–420.

Harii, Y., J. E. Beeler, K. Sakaguchi, M. Tachibana, and T. Miki. 1994. A novel oncogene, ost, encodes a guanine nucleotide exchange factor that potentially links Rho and Rac signalling pathways. EMBO J. **13:**4776–4786

Hurtado, C. A., J. M. Beckerich, C. Gaillardin, and R. A. Rachubinski. 2000. A *rac* homolog is required for induction of hyphal growth in the dimorphic yeast *Yarrowia lipolytica*. J. Bacteriol. **182:**2376-2386

Imamura, H., K. Tanaka, T. Hihara, M. Umikawa, T. Kamei, K. Takahashi, *et al.* 1997. Bni1p and Bnr1p: downstream targets of the Rho family small G-proteins which interact with profilin and regulate actin cytoskeleton in *Saccharomyces cerevisiae*. EMBO J **16:** 2745–2755.

Inoue, S. B., N. Takewaki, T. Takasuka, T. Mio, M. Adachi, Y. Fujii, C. Miyamoto, M. Arisawa, Y. Furuichi, and T. Watanabe. 1995. Characterization and gene cloning of β-1,3-D-glucan synthase from *Saccharomyces cerevisiae.* Eur. J. Biochem. **231:**845–854.

Johnson, D.I. 1999. Cdc42: an essential Rho-type GTPase controlling eukaryotic cell polarity. Microbiol Mol Biol Rev **63:** 54–105.

Kane, S. M., and R. Roth. 1974. Carbohydrate metabolism during ascospore development in yeast. J. Bacteriol. **118:**8–14.

Kang, M.S., P.J. Szaniszlo, V. Notario, and E. Cabib. 1986. The effect of papulocandin B on ß-1,3-glucan synthetases: a possible relationship between inhibition and enzyme conformation. Carbohyd. Res. **149:** 13-21.

Kang, M. S., and E. Cabib. 1986. Regulation of fungal cell wall growth: a guanine nucleotide-binding proteinaceous component required for activity of (1-3)-b-D-glucan synthase. Proc. Natl. Acad. Sci. USA **83:**5808–5812.

Kathleen, L., Gould and Viesturs Simanis. 1997. The control of septum formation in fission yeast**.** Genes Dev. **11:** 2939-2951

Kelly R, Register E, Hsu MJ, Kurtz M, and Nielsen J. 1996. Isolation of a gene involved in 1,3-*β*-glucan synthesis in *Aspergillus nidulans* and purification of the corresponding protein. J Bacteriol **178**: 4381–4391.

Khosravi-Far, R., M. Chrzanowska-Wodnicka, P. A. Solski, E. Alessandra, K. Burridge, and C. J. Der. 1994. Dbl and Vav mediate transformation via mitogen-activated protein kinase pathways that are distinct from those activated by oncogenic Ras. Mol. Cell. Biol. **14:**6848–6857.

Kwon-Chung, K.J., and J.E.Bennet. 1992. Medical mycology, p.866. lea and Febiger, Philadephia, Pa.

Kollar, R., B.B. Reinhold, E. Petrakova, H.J. Yeh, G. Ashwell, J. Drgonova, J.C. Kapteyn, F.M. Klis and E. Cabib.1997. Architecture of the yeast cell wall. Beta(1→6)-glucan interconnects mannoprotein, β-1,3-glucan, and chitin. J. Biol. Chem. **272:** pp. 17762–17775.

Kondoh, O., Tachibana, Y., Ohya, Y., Arisawa, M., and Watanabe, T. 1997. Cloning of the *RHO1* gene from *Candida albicans* and its regulation of beta-1,3-glucan synthesis. J Bacteriol **179:** 7734–7741.

Krainer, E., R.E. Stark, F. Naider, K. Alagramam and J.M. Becker. 1994. Direct observation of cell wall glucans in whole cells of *Saccharomyces cerevisiae* by magic-angle spinning ^{13}C-NMR. Biopolymers **34:** pp. 1627–1635.

Kreger, D.R. and M. Kopecka. 1975. On the nature and formation of the fibrillar nets produced by protoplasts of *Saccharomyces cerevisiae* in liquid media: an electronmicroscopic, X-ray diffraction and chemical study. J. Gen. Microbiol. **92:** pp. 207–220.

Langfelder, K., M. Streibel, B. Jahn, G. Haase, and A.A.Brakhage. 2003. Biosythesis of fungal melanins and their importance for human pathogenic fungi. Fungal. Gen. Biol. **38:** 143-158

Levin, D.E. 2005. Cell wall integrity signaling in *Saccharomyces cerevisiae*. Microbiol Mol Biol Rev **69:** 262–291

L. M. Barton and R. A. Prade. 2008. Inducible RNA Interference of *brlA*β in *Aspergillus nidulans*. Eukaryotic Cell **7:** 2004-2007.

Li, Z., Mendoza, L., Z. Wang, H. Liu, C. Park, S. Kauffman, J. M. Becker, and P. J. Szaniszlo. 2006. WdChs1p, a class II chitin synthase, is more responsible than WdChs2p (Class I) for normal yeast reproductive growth in the polymorphic, pathogenic fungus *Wangiella (Exophiala) dermatitidis*. Arch Microbiol **185:** 316-329.

Lin FC, R. M. Brown, R. R. Drake, B. E. Haley. 1990. Identification of the uridine 5_-diphosphoglucose (UDP-Glc) binding subunit of cellulose synthase in *Acetobacter xylinum* using the photoaffinity probe 5-azido-UDP-Glc. J Biol Chem **265**:4782–4784

Liu, H., T.R. Cottrell, L.M. Pierini, W.E. Goldman, and T.L Doering. 2002. RNA interference in the pathogenic fungus *Cryptococcus neoformans*. Genetics **160:** 463–470

Liu, H., S. Kauffman, J. M. Becker, and P. J. Szaniszlo. 2004. *Wangiella (Exophiala) dermatitidis* WdChs5p, a class V chitin synthase, is essential for sustained cell growth at temperature of infection. Eukaryot Cell **3:** 40-51

Liu H, D. Abramczyk, C.R. Jr Cooper, L. Zheng, C. Park, P.J. Szaniszlo. 2008. Molecular cloning and characterization of *WdTUP1*, a gene that encodes a potential transcriptional repressor important for yeast-hyphal transitions in *Wangiella (Exophiala) dermatitidis*. Fungal Genet Biol, **45**:646-56.

Madhani, H.D., and G.R. Fink. 1998. The control of filamentous differentiation and virulence in fungi. Trends Cell Biol. **8:** 348–353

Manners, D.J., A.J. Masson and J.C. Patterson. 1973. The structure of a *β*-1,3-D-glucan from yeast cell walls. Biochem. J. **135:** pp. 19–30

Mahlert, M., L. Leveleki, A. Hlubek, B. Sandrock, and M. **Buker.** 2006. Rac1 and Cdc42 regulate hyphal growth and cytokinesis in the dimorphic fungus Ustilago maydis. Mol. Microbiol. **59:** 567-578

Martinez-Rocha, A.L., Roncero, M.I.G., Lopez-Ramirez, A., Marine, M., Guarro, J., G. Martinez-Cadena, and A Di Pietro. 2008. Rho1 has distinct functions in morphogenesis, cell wall biosynthesis and virulence of *Fusarium oxysporum*. Cell. Microbiol. **10:** 1339–1351

Matsumoto, T. L. Ajello, P. J. Szaniszlo, and T. J. Walsh. 1994. Developments in hyalohyphomycosis and phaeohyphomycosis. J. Vet. Med. Mycol. **32** (Suppl.l)**:** 329-349

Mcintosh, N. D.P., R. J. Rennard, S. M. Karuppayil., and P. J. Szaniszlo. 1995. Abstr. 95th Gen. Meet. Am. Soc. Microbiol. abstr. **30:** p.92.

M. Leon, R Sentandreu, J. Zueco. 2002; A single *FKS* homologue in *Yarrowia lipolytica* is essential for viability Yeast **19:** 1003–1014

Miller, P. J., and D. I. Johnson. 1994. Cdc42p GTPase is involved in controlling polarized cell growth in *Schizosaccharomyces pombe*. Mol. Cell. Biol. **14:**1075-1083

Minden, A., A. Lin, F.-X. Claret, A. Abo, and M. Karin. 1995. Selective activation of the JNK signaling cascade and c-Jun transcriptional activity by the small GTPases Rac and Cdc42Hs. Cell **81:**1147–1157.

Mio, T., M. Adachi Shimizu, Y. Tachibana, H. Tabuchi, S. B. Inoue, T. Yabe, T. Yamada Okabe, M. Arisawa, T. Watanabe, and H. Yamada Okabe. 1997. Cloning of the *Candida albicans* homolog of *Saccharomyces cerevisiae GSC1/ FKS1* and its involvement in 1,3-b-D-glucan synthesis. J. Bacteriol. **179:**4096–4105

Montijn, R. C., P.V. Wolven, S. de Hoog, and F.M. Klis. 1997. b-Glycosylated proteins in the cell wall of the black yeast *Exophiala* (*Wangiella*) *dermatitidi*s. Microbiology. **143**:1673-1680

Mol, P. C., H. M. Park, J. T. Mullins, and E. Cabib. 1994. A GTP-binding protein regulates the activity of (1,3)-b-glucan synthase, an enzyme directly involved in yeast cell wall morphogenesis. J. Biol. Chem. **269:**31267–31274

Munro CA, K. Winter, A. Buchan, K. Henry, J. M. Becker, A. J. Brown, C. E. Bulawa, N. A. Gow. 2001. Chs1 of Candida albicans is an essential chitin synthase required for synthesis of the septum and for cell integrity. Mol Microbiology **39:**1414-26

Muzzarelli, R., C. Jeuniaux and G. W. Gooday (ed.). 1986. Chitin in nature and technology. Plenum press, NY. J. Gen. Microbiology **99:** 1-11.

Müller, A., H. Ensley, H. Pretus, R. McNamee, E. Jones, E. McLaughlin, W. Chandley, W. Browder, D. Lowman and D. Williams. 1997. The application of various protic acids in the extraction of β-1,3-glucan from *Saccharomyces cerevisiae*. Carbohydr. Res. **299:** pp. 203–208.

Mazur, P., N. Morin. W. Baginsky. M. El-sherbeini, J. A. Clemas, J. B. Nielsen, F. Foor. 1995. Differential Expression and Function of Two Homologous Subunits of Yeast 1,3-b-D-Glucan Synthase. Molecular Cell biology **10:** p. 5671–5681

Nakano, K., and I. Mabuchil. 1995. Isolation and sequencing of two cDNA clones encoding Rho proteins from the fission yeast *Schizosaccharomyces pombe*. Gene. **155:** 119-122.

Narumiya, S. 1996. The small GTPase Rho: Cellular functions and signal transduction. J. Biochem. **120:** 215–228

Nakano, K., R. Arai, I. Mabuchi. 1997. The small GTP-binding protein Rho1 is a multifunctional protein that regulates actin localization, cell polarity, and septum formation in the fission yeast *Schizosaccharomyces pombe*. Genes Cells **2:** 679–694.

Nobes, C. D., and A. Hall. 1995. Rho, Rac, and Cdc42 GTPases regulate the assembly **Nobes CD, and A. Hall. 1995.** Rho, rac, and cdc42 GTPases regulate the assembly of multimolecular focal complexes associated with actin stress fibers, lamellipodia, and filopodia. Cell **81:**53-62

Qadota, H., C.P. Python, S.B. Inoue. 1996. Identification of yeast Rho1p GTPase as a regulatory subunit of 1,3-β-glucan synthase. Science **272:** 279–281

Qiu, R.-G., J. Chen, D. Kirn, F. McCormick, and M. Symons. 1995. An essential role for Rac in Ras transformation. Nature **374:**457–459.

Perfect, J. R. 1996. Fungal virulence genes as targets for antifungal chemotherapy. Antimicrobial. Agents Chemother. **40:**1577-1583

Pereira, M., M. S. S. Felipe, M. M. Brigido, C. M. A. Soares, and M. O. Azevedo. 2000. Molecular cloning and characterization of a glucan synthase gene from the human pathogenic fungus *Paracoccidioides brasiliensis*. Yeast **16:**451–462.

Ram, A. Personal communication.

Rappleye, A. Chad, T. J. Engle, and W. E. Goldman. 2004. RNA interference in *Histoplasma capsulatum* demonstrates a role for a-(1,3)-glucan in virulence**.** Molecular Microbiology **53:** 153–165

Rees, D.A., E.R. Morris, D. Thom, and J.K. Madden. 1982. Shapes and interactions of carbohydrate chains. In: The Polysaccharides, Vol. I (Aspinall, G.O., Ed.), pp. 196–290. Academic Press, New York.

Rida, P.C., and U. Surana. 2005. Cdc42-dependent localization of polarisome component Spa2 to the incipient bud site is independent of the GDP/GTP exchange factor Cdc24. Eur J Cell Biol **84:** 939–949.

Ridley, A. J., H. F. Paterson, C. Johnston, D. Diekmann, and A. Hall. 1992.The small GTP-binding protein rac regulates growth factor-induced membrane ruffling. Cell **70:**401–410

Ridley, A. J. 1994. Membrane ruffling and signal transduction. Bioessays.**16:**321–327.

Ridley, A. J. 1995. Rho-related proteins: actin cytoskeleton and cell cycle. Curr. Opin. Genet. Dev. **5:**24

Ridley, A. J., P. M. Comoglio, and A. Hall. 1995. Regulation of scatter factor/hepatocyte growth factor responses by Ras, Rac, and Rho in MDCK cells. Mol. Cell. Biol. **15:**1110–1122

Romano, N., and G. Macino. 1992. Quelling: transient inactivation of gene expression in *Neurospora crassa* by transformation with homologous sequences. Mol Microbiol **6:**3343–3353.

Roberts, R. L., and P. J. Szanizlo. 1978. Temerature-sensitive multicellular

muntants of *Wangiella dermatitidis*. J. Bacteriol. **135:** 622-632

Sandrine Etienne-Manneville 2002. Rho GTPases in cell biology**.** Nature **420:** 629-35

Saka, A., M. Abe, H. Okano, M. Minemura, H. Qadota, T. Utsugi, A. Mino, K. Tanaka, Y. Takai, and Y. Ohya. 2001. Complementing yeast *rho1* mutation groups with distinct functional defects. J Biol Chem **276:** 46165–46171.

Sarkar T. J., D. A. Widdick, E. A. Espeso, M. Orejas, J. Mungroo, M. A. Penalva, H. N. Arst. 1995. The *Aspergillus* PacC zinc ®nger transcription factor mediates regulation of both acid- and alkalineexpressed genes by ambient pH. EMBO J **14:**779-790.

Schmidt, A., and M. N. Hall. 1998. Signaling to the actin cytoskeleton. Annu Rev Cell Dev Biol **14:** 305–338

Schmidt, A., M. Bickle, T. Beck, M.N. Hall. 1997. The yeast phosphatidylinositol kinase homolog *TOR2* activates *RHO1* and *RHO2* via the exchange factor *ROM2*. Cell **88:** 531–542.

Scheffer, J., C. Chen, P. Heidrich, M.B. Dickman, and P. Tudzynski. 2005. A CDC42 Homologue in *Claviceps purpurea* is involved in vegetative differentiation and is essential for pathogenicity. Eukaryot Cell **4:** 1228–1238.

Smith, S.E., C. Csank, G. Reyes, M.A. Ghannoum and V. Berlin. 2002. *Candida albicans* RHO1 is required for cell viability in vitro and in vivo. *FEMS Yeast Res.* **2:** 103–111.

Szaniszlo, P.J., P.A. Geis, C.W. Jacobs, C.R. Cooper, Jr., and J.L. Harris. 1983. Cell wall changes associated with yeast-to-multicellular form conversion in *Wangiella dermatitids*. p. 239-244. *In* D. Schlessinger (ed.), Microbiology-*1983* ASM, Washington, D. C.

Szaniszlo, P.J., M.S. Kang, E. Cabib. 1985. Stimulation of (1→3)glucan synthetase of various fungi by nucleoside triphosphates: generalized regulatory mechanism for cell wall biosynthesis J. Bacteriol. **161:** 1188

Szaniszlo, P. J. 2002. Molecular genetic studies of the model dematiaceous pathogen Wangiella dermatitidis.Int J Med Microbiol. **292:**381-90. Review.

Szaniszlo, P. J. 2006. Virulence factors in black molds with emphasis on melanin,

chitin and *Wangiella* as a molecularly tractable model, p.407-428. In: J. Heitman, S. G. Filler, J. E. Edwards and A. P. Mitchell (ed). Molecular Principles of Fungal Pathogenesis. ASM Press, Washington, D.C.

Szaniszlo, P. J. 2001. WdChs2p, a class I chitin synthase, together with WdChs3p (class III) contributes to virulence in *Wangiella (Exophiala) dermatitidis*. Infect Immun. **69:** 7517-7526.

Szaniszlo, P. J., M. Mendoza and S.M. Karuppayil. 1993. Clues about chromoblastomycotic and other dematiaceous pathogens based on *Wangiella* as a model. In: H.V. Bossche, D. Kerridge, and F. Odds (ed), Dimorphic Fungi in Biology and Medicine, Plenum Publishing Corporation , New York. 241-255.

Symons, M. 1995. The Rac and Rho pathways as a source of drug targets for Ras-mediated malignancies. Curr. Opin. Biotechnol. **6:**668–674.

Tapon, N., and A. Hall. 1997. Rho, Rac and Cdc42 GTPases regulate the organization of the actin cytoskeleton. Curr. Opin. Cell. Biol. **9:**86–92.

Thompson, J. R., C. M. Douglas, W. Li, C. K. Jue, B. Pramanik, X. Yuan, T. H. Rude, D. L. Toffaletti, J. R. Perfect, and M. B. Kurtz. 1999. A glucan synthase FKS1 homolog in *Cryptococcus neoformans* is single copy and encodes an essential function. J. Bacteriol. **181:**444–453.

Van Aelst, L., and C. D'Souza-Schorey. 1997. Rho GTPases and signaling networks. Genes Dev. **11:**2295–2322.

Vallim, M. A., C. B. Nichols, L. Fernandes, K. L. Cramer, and J. A. Alspaugh. 2005. A Rac homolog functions downstream of Ras1 to control hyphal differentiation and high-temperature growth in the pathogenic fungus *Cryptococcus neoformans*. Eukaryot. Cell. **4:**1066-78.

Virag, A., P. L. Maurice, H. Si and S. D. Harris. 2007. Regulation of hyphal morphogenesis by *cdc42* and *rac1* homologues in *Aspergillus nidulans.* Molecular Microbiology **66:** 1579–1596

Wang, Z., L. Zheng, H. Liu, Q. Wang, M. Hauser, S. Kauffman, J. M. Becker, M. Ward, L. J. Wilson, and K. H. Kodama. 1993. Use of Aspergillus overproducing mutants, cured for integrated plasmid, to overproduce heterologous protein. Appl. Microbiol. Biotechnol. **39:** 738-743

Wang, Q., and P. J. Szaniszlo. 2007. WdStuAp, an APSES Transcription Factor, Is a Regulator of Yeast-Hyphal Transitions in *Wangiella (Exophiala) dermatitidis*. Eukaryot. Cell, **6:** 1595 - 1605.

Wiggin, G.R., J.P. Fawcett, and T. Pawson. 2005. Polarity proteins in axon specification and synaptogenesis. Dev Cell **8:** 803–816

Ye X, Feng B, P. J. Szaniszlo. 1999. A color-selectable and site-specific integrative transformation system for gene expression studies in the dematiaceous fungus *Wangiella (Exophiala) dermatitidis*. Curr Genet. **36:**241-7.

Ye X, P. J. Szaniszlo. 2000. Expression of a constitutively active Cdc42 homologue promotes development of sclerotic bodies but represses hyphal growth in the zoopathogenic fungus *Wangiella (Exophiala) dermatitidis*. J Bacteriol. **182:** 4941-50

Young, S. H., and R. R. Jacobs. 1998. Sodium hydroxide-induced conformational change in schizophyllan detected by the fluorescence dye, aniline blue. Carbohydr. Res. **310:** pp. 91–99

Ha, Young-sil., S.F. Covert, and M. Momany. 2006. FsFKS1, the 1,3-_-Glucan Synthase from the Caspofungin-Resistant Fungus *Fusarium solani*. EUKARYOTIC CELL **5:** 1036–1042

Zhao, C., U.S. Jung, P. Garrett-Engele, T. Roe, M.S. Cyert, D.E. Levin. 1998. Temperature-induced expression of yeast *FKS2* is under the dual control of protein kinase C and calcineurin. Mol Cell Biol **18:** 1013–1022

Zohn, I. M., S. L. Campbell, R. Khosravi-Far, K. L. Rossman, and C. J. Der. 1998. Rho family proteins and Ras transformation: the RHOad less traveled gets congested. Oncogene **17:**1415–1438

Vita

Penfei Guo was born in Jieshou, Anhui province, P. R. China on September 14th, 1976, the son of Yukuan Guo and Yanqin Zhang. He graduated from College of Life Sciences of Nankai University (Tianjin), P.R.China, in July 1997 with a B.S in Life. He entered the Graduate Program in Microbiology of Nankai University in September 1998 and received the degree of Master of Science in Microbiology in 2001. He entered the Graduate School of the University of Texas at Austin in August 2002 as a graduate student in the Molecular Genetics and Microbiology Graduate Program.

Permanent address: #2 Fukang Road

Tianjin, 300071

P. R. China

This dissertation was typed by the author.